Washington University in St. Louis
Washington University Open Scholarship

All Theses and Dissertations (ETDs)

1-1-2012

Joint Functions of METT-10 and Dynein in the Caenorhabditis elegans Germ Line

Maia Dorsett
Washington University in St. Louis

Follow this and additional works at: https://openscholarship.wustl.edu/etd

Recommended Citation
Dorsett, Maia, "Joint Functions of METT-10 and Dynein in the Caenorhabditis elegans Germ Line" (2012). *All Theses and Dissertations (ETDs)*. 571.
https://openscholarship.wustl.edu/etd/571

This Dissertation is brought to you for free and open access by Washington University Open Scholarship. It has been accepted for inclusion in All Theses and Dissertations (ETDs) by an authorized administrator of Washington University Open Scholarship. For more information, please contact digital@wumail.wustl.edu.

WASHINGTON UNIVERSITY IN ST. LOUIS

Division of Biology and Biomedical Sciences

Molecular Genetics and Genomics

Dissertation Examination Committee:
Tim Schedl, Chair
Douglas Chalker
John Cooper
James Havranek
Michael Nonet
James Skeath

Joint Functions of METT-10 and Dynein in the Caenorhabditis elegans Germ Line

by

Maia Dorsett

A dissertation presented to the
Graduate School of Arts and Sciences
of Washington University in
partial fulfillment of the
requirements for the degree
of Doctor of Philosophy

May 2012

Saint Louis, Missouri

ABSTRACT OF THE DISSERTATION

Joint Functions of METT-10 and Dynein in the *Caenorhabditis elegans* Germ Line

by

Maia Dorsett

Doctor of Philosophy in Biology and Biomedical Sciences

(Molecular Genetics and Genomics)

Washington University in St. Louis, 2012

Professor Tim Schedl, Chairperson

During normal development as well as in diseased states such as cancer, extracellular "niches" often provide cues to proximal cells and activate intracellular pathways. Activation of such signaling pathways in turn instructs cellular proliferation and differentiation. In the *C.elegans* gonad, GLP-1/Notch signaling instructs germ line stem cells to self renew through mitotic cell division. As germ cells progressively move out of the niche, they differentiate by entering meiosis and eventually form gametes. Using this model system, I uncovered a cooperative role for the METT-10 putative methyltransferase and the dynein motor complex in regulating the balance between germ cell proliferation and differentiation. I demonstrate that Dynein Light Chain-1 (DLC-1), and its partner, Dynein Heavy Chain-1, inhibit the proliferative cell fate, in part through regulation of METT-10 levels and nuclear accumulation. I further show that the methyltransferase domain of METT-10 is required for normal inhibition of germ cell proliferation, and that DLC-1

and METT-10 act antagonistically to activation of the GLP-1 Notch pathway, which plays conserved roles in stem cell fate specification. Moreover, I find that regulation of germ cell proliferative fate is only one of multiple joint functions of METT-10 and the dynein motor complex, and propose that they function together in multiple cellular contexts, including mitotic cell division. The finding that METT-10 and dynein inhibit germ cell proliferative fate, despite promoting mitotic cell division of those cells that do proliferate, highlights a genetic difference between the specification of proliferative fate and its execution.

ACKNOWLEDGEMENTS

I have a lot of people to thank.

First, I would like to thank my advisor, Tim Schedl, for a project that, though challenging, was never boring, and for the independence to let me follow where it took me.

I thank all the administrative staff –Melanie Puhar, Brian Sullivan, Andrew Richards, Christy Durbin, Rita Scott, and Alice Gleason - who were always there to answer my questions, help me get my paperwork in order, order things, and get things fixed.

I would like to thank the members of my thesis committee for their suggestions, discussion, and support. I'd especially like to thank Doug Chalker who served as my chair and has a unique talent for always suggesting just the right experiment, and Mike Nonet for his consistent willingness to answer my questions, share reagents, and even look at my worms.

I was fortunate to share my time in the Schedl lab with a wonderful group of people. I would like to especially thank Paul Fox, my bay mate, for his excellent music collection, scientific discussions, sharing of reagents, and for being so easy to get along with even when I was not. It is hard for me to even put in to words my appreciation for Swathi Arur, who taught me so many important things, the most valuable of which have very little to do with science and so much to do with life. Swathi is a teacher, a cheerleader, a confidant, and an irreplaceable friend.

I thank my previous mentor, Tom Cline, for teaching me a love of classical genetics that will be with me always.

I thank my family because it is hard to succeed at work without support at home. I thank my mom for teaching me molecular biology, helping me with experiments, babysitting my kids, and always being there when I need her and never failing to let me know how much she cares. I thank my dad, who is not only a great friend, but has always served as an example of the type of scientist that I aspire to be. I am so lucky to have had his help in so many aspects of my thesis work – from discussion, writing, and even the experiments – and in so many aspects of my life in general. I thank my big brother, Yair, for his help in writing, for his scientific enthusiasm, and most of all for his friendship. I thank my sister-in-law, Yanjiao, for the sense of wholeness that she brings to our family, and my in-laws – Roben and David – for accepting me, loving me, and supporting me.

There are too many things to thank my husband, Justin, for – so I will pick just the most important. I thank Justin for being supportive, understanding, encouraging, and tolerant - on the good days and the bad. I thank him for being such a great dad. I cannot appreciate him more.

I thank my sons – Eitan and Aaron - because through them I have realized what life is really all about, and with them I have shared and will share the best moments of my life.

Finally, I thank my sources of financial support – the MSTP training grant awarded to Washington University and NIH grant GM63310 awarded to Tim Schedl.

DEDICATION

I dedicate this thesis with love to my grandmother

Hasia Misulovin

because she has overcome more and given more than anyone I know

מוקדש

לסבתי האהובה

חסיה מיסולובין

שעברה הרבה בחייה אבל תרמה לאחרים הרבה

יותר

TABLE OF CONTENTS

LIST OF TABLES

Chapter 2

Chapter 3

LIST OF FIGURES

Chapter 1

Chapter 2

Chapter 3

Chapter 4

Chapter 1 (Introduction):

The *C.elegans* Germ Line as a Model for Stem Cell Biology

A recurring theme of development and disease is the proper specification of cell fates or lack thereof. Of the many developmental decisions that fall under the umbrella of cell fate specification, the regulated balance between cell proliferation and differentiation plays a fundamental role in tissue development and maintenance. A specialized cell type, the stem cell, is the cornerstone of regulated proliferation and differentiation, for it has the unique ability to both self-renew through proliferation and to give rise to daughter cells that differentiate (Lin, 1997; Morrison *et al*., 1997). While it is these fundamental characteristics that make stem cells alike, the genetics and cell biology of stem cell fate and proliferation can differ according to organism, tissue, and developmental context. A comprehensive understanding of the diversity of paradigms regulating stem cell fate, maintenance, and proliferation will enhance our fundamental views of what "stemness" entails, and its misregulation in disease states such as cancer.

Current and contrasting models of stem cell self-renewal

Most models of stem cell self-renewal fall into three predominant paradigms: (1) asymmetric division, wherein one daughter cell is specified to remain a stem cell and the other daughter cell differentiates, (2) symmetric division in which the stem cell divides to give rise to two daughter stem cells or two daughter cells that will differentiate, and (3) population-level self-renewal wherein the collective behavior of cells provides a steady source of proliferating cells that can differentiate at some frequency (Lin, 1997). These paradigms are not organism-specific or tissue-specific,

as multiple paradigms can operate within a single organism and in the same tissue-type between organisms.

Two excellent examples of the asymmetric division paradigm come from studies in *Drosophila*, although this paradigm is also characterized in mammalian tissues, including neural and hematopoietic stem cells (Takano *et al*., 2004; Beckmann *et al*., 2007; Doe, 2008). Asymmetric division, which leads to the formation of one stem cell and a daughter cell which differentiates, can be mediated by intrinsic and extrinsic factors (Figure 1).

An example of the role of intrinsic factors in guiding asymmetric division comes from studies of the *Drosophila* neuroblast (NB), which divides asymmetrically to self-renew a NB and give rise to a Ganglion Mother Cell (GMC) that differentiates (reviewed in (Doe, 2008). Proteins that are asymmetrically segregated between the future NB and GMC play a significant role in determining cell fates. One example of such a protein is the pro-differentiation factor Numb. Numb is segregated into the future GMC and functions as an inhibitor of Notch signaling which promotes the self-renewal fate (Uemura *et al*., 1989; Guo *et al*., 1996; Lu *et al*., 1998; Ohshiro *et al*., 2000). Factors that are segregated into the future NB include aPKC, which among other things, functions to inhibit proper localization of Numb (Smith *et al*., 2007).

Extrinsic factors guiding stem cell self-renewal are often provided by the niche micro-environment (Walker *et al*., 2009). While such extrinsic factors are probably essential for the establishment and/or maintenance of all stem cells, the division of germ line stem cells (GSCs) in *Drosophila* provides a particularly elegant

example of how extrinsic factors can determine stem cell fate. In the male, GSCs reside at the apical tip of the testes surrounding a somatic hub, and divide to self-renew a GSC and to give rise to a gonialblast that will differentiate (Dansereau and Lasko, 2008). To remain a GSC, a cell must remain in contact with the hub, which secretes the short range signaling molecule and JAK/STAT ligand Unpaired (Upd) (Yamashita *et al*., 2003; Dansereau and Lasko, 2008). Activation of the JAK/STAT signaling pathway maintains GSC fate. Because contact with the hub (which serves as the stem cell niche) is essential for maintenance of GSC fate, asymmetric division is achieved by orienting the mitotic spindle at a right angle to the GSC contact with the hub (Yamashita *et al*., 2003). After cell division, one cell maintains hub contact and remains a GSC, while the other lacks hub contact and becomes a gonialblast.

In contrast to the strictly asymmetric division observed for male *Drosophila* GSCs, mammalian spermatogonial stem cells (SSCs) are proposed to undergo symmetric cell division, although there is significant debate on this matter (Lin, 1997; Oatley and Brinster, 2008). Under the symmetric model, SSCs exist in a niche that is primarily made up of Sertoli cells (Oatley and Brinster, 2008). Undifferentiated type A spermatogonia (A_s cells) act as stem cells, and can divide to give rise to either additional two A_s cells that separate or to two A_{pr} cells that remain as an interconnected pair and differentiate (Lin, 1997).

The third paradigm, population-level self-renewal, is most clearly illustrated by *C. elegans* germ cell development (Lin, 1997). The adult *C. elegans* hermaphrodite gonad exists as two U-shaped gonad arms that meet at a common

uterus (Figure 2). Each gonad functions as an assembly line with distal to proximal polarity with respect to the uterus. At the distal region near the somatic distal tip cell (DTC), extending approximately 18-20 cell diameters and encompassing 200-250 cells, are the proliferating germ cells, including the germ line stem cells (Hubbard, 2007). Proliferation of this distal cell population provides a continuous flux of germ cells that pushes germ cells away from the distal niche and promotes their entry into meiosis. At a staggered region called the "transition zone" corresponding to leptotene/zygotene of meiosis I, germ cells definitively enter meiosis as evidenced by expression of meiotic markers (Hansen *et al*., 2004a). These germ cells then proceed through the stages of meiotic development to give rise to differentiated gametes or die by physiological apoptosis (Hubbard, 2007; Jaramillo-Lambert *et al*., 2007). Hermaphrodites first produce sperm at the 4th larval stage, and then switch to oocyte production in the adult, and a continuously mated hermaphrodite can lay as many as ~1400 progeny in a lifetime (Kimble and Ward, 1988).

On the gross morphological level, the renewal of *C. elegans* germ line stem cells resembles the renewal of male *Drosophila* GSCs, wherein the DTC takes the place of the *Drosophila* hub. Similarly to the *Drosophila* hub, the DTC functions as a stem cell niche. In fact, the DTC is necessary and sufficient for germ line proliferation and maintenance: ectopic DTCs lead to additional proliferative zones (and ectopic germ lines) while early distal tip cell ablation leads to germ line loss (Kimble and White, 1981; Feng *et al*., 1999). The DTC functions as a stem cell niche by expressing the membrane-bound Notch ligand LAG-2 and extends out cytoplasmic

processes that enable it to directly contact cells located 8-10 cell diameters away from the distal end (Kimble and Crittenden, 2007). Binding of LAG-2 to the GLP-1/Notch receptor in the distal-most germ cells results in activation of the GLP-1/Notch signaling pathway in the germ cells and specification of proliferative fate. Loss-of-function mutations in the GLP-1 receptor cause premature meiotic entry of all germ cells, while GLP-1 hyperactivation causes germ cell overproliferation and germ line tumor formation (Austin and Kimble, 1987; Berry *et al*., 1997; Pepper *et al*., 2003).

While *C. elegans* germ line development may resemble *Drosophila* GSC self-renewal on the gross morphological level, there are significant differences. First, there is no consistent spindle orientation among mitotically dividing *C.elegans* germ cells, and thus there is no evidence for regulated asymmetric division (Crittenden *et al*., 2006). In addition, while the distal tip cell has processes that extend approximately 8-9 diameters away from the distal end, the proliferative zone extends anywhere from 19-26 cell diameters, suggesting that cells can proliferate in the absence of direct contact with the niche cell (Hansen *et al*., 2004a; Crittenden *et al*., 2006). Thus, it is thought that differentiation may be a consequence of a *progressive* displacement away from the niche (Morrison and Kimble, 2006), and the signaling pathways that enable such a transition are the object of intense research, including the thesis work presented here.

On the surface, there are significant differences among the paradigms of stem cell self-renewal. However, whether similar underlying mechanisms operate to ensure balanced stem cell self-renewal remains an open question. Like many

biological examples, from developmental patterning to genome regulation, common molecular strategies can underlie seemingly disparate outcomes; often, such examples teach us what is most fundamental to the execution of a particular biological process. The apparent uniqueness of the *C. elegans* strategy for germ line maintenance thus makes it a prime candidate for expanding our understanding of stem cell self-renewal and the pathways that limit it.

Genetic pathways underlying stem cell self-renewal and cancer

A genetic network ensures the switch from proliferative to meiotic fates in the *C. elegans* germ line (Figure 2; Hansen and Schedl, 2006; Kimble and Crittenden, 2007). As stated earlier, the primary signal instructing germ cells to proliferate is activation of the GLP-1/Notch signaling pathway in the germ cells themselves through interaction with the somatic distal tip cell expressing the Notch ligand, LAG-2. Binding of LAG-2 to GLP-1 receptor results in a series of cleavage events that release the intracellular portion of GLP-1. GLP-1(INTRA) translocates to the nucleus where it complexes with LAG-3, and acts as a co-activator for the LAG-1 transcription factor to promote the transcription of target genes that promote the proliferative fate (reviewed in Fiuza and Arias, 2007). Most of these target genes remain unknown, although there is evidence that the PUF protein, FBF-2, is a transcriptional target of LAG-1 and functions to promote germ line stem cell proliferation and/or maintenance (Lamont *et al*., 2004).

There are two Notch receptors in the worm, *lin-12* and *glp-1*. Although the proteins are functionally equivalent, *lin-12* function is limited to the soma and embryo, and is best characterized in the vulva, while *glp-1* functions in the germ line and embryo (Fitzgerald *et al*., 1993). Germ line proliferation is roughly proportional to the extent of GLP-1/Notch signaling. Weak *glp-1* gain-of-function mutations result in less penetrant and smaller tumors, while partial losses of *glp-1* function result in smaller germ lines (P.M. Fox, unpublished data; Qiao *et al*., 1995; Kerins, 2006). Moreover, the finding that cells continue to proliferate for at least 10 cell diameters beyond the reaches of the distal tip cell means that Notch signaling persists outside of the DTC niche and is dampened with relatively standardized timing. Thus, regulation of the strength and endurance of the *glp-1* signal ensures a proper balance between germ line proliferation and differentiation. In many systems, the Notch molecule is regulated at the level of expression, surface availability, intracellular trafficking, and stability (Fortini, 2009; Fortini and Bilder, 2009). In the *C.elegans* germ line specifically, several proteins have been propose to regulate Notch activity. These include a number of the *sel (*suppressor enhancer of *lin-12*) genes, most notably, *sel-10*, an E3-ubiquitin ligase that regulates Notch levels (Sundaram and Greenwald, 1993; Lai, 2002) and the proteasomal component, *pas-5* (Macdonald et al., 2008).

GLP-1 signaling inhibits at least three genetic pathways that promote meiotic entry and/or inhibit proliferation (Figure 2; Hansen *et al*., 2004a). Two of these pathways are characterized by the genes *gld-1* and *gld-2*; *gld-1* encodes a K-

homology RNA binding domain containing protein and functions as a translational repressor, while *gld-2* encodes a poly-A polymerase and functions, in part, to promote GLD-1 levels (Jones and Schedl, 1995; Lee and Schedl, 2001; Wang *et al*., 2002; Hansen *et al*., 2004b). *gld-1* and *gld-2* single mutants exhibit a significant amount of meiotic entry and various meiotic defects (Francis *et al*., 1995; Kadyk and Kimble, 1998). However, simultaneous disruption of *gld-1* and *gld-2* leads to the formation of large germ line tumors with minimal meiotic entry (Kadyk and Kimble, 1998; Hansen *et al*., 2004a). Moreover, these tumors occur in the absence of *glp-1* activity, demonstrating that one of the primary roles of *glp-1* signaling is to inhibit the function of *gld-1* and *gld-2*. The fact that some meiotic entry is observed in *gld-1 gld-2* double mutants demonstrates that at least one other pathway operates in parallel to *gld-1* and *gld-2* to promote meiotic entry (Hansen *et al*., 2004a). Several other genes, namely *gld-3* and the PUF protein *nos-3*, also promote meiotic entry and inhibit proliferation downstream of *glp-1*. These proteins, like *gld-2*, function in part to promote GLD-1 levels (Eckmann *et al*., 2004; Hansen *et al*., 2004b). GLD-1, in turn, represses translation of a number of target genes, including *glp-1* itself (Marin and Evans, 2003).

One of the key questions in stem cell biology is whether similar genetic mechanisms underlie the diversity of paradigms for stem cell self-renewal. Several lines of evidence suggest that homologous factors regulate stem cell fate and proliferation across paradigms. These factors include the PUF (Pumilio and FBF) protein family of translational regulators, piwi proteins, and the Notch signaling

pathway (Wong *et al*., 2005). The Notch signaling pathway plays a particularly pervasive role in stem cell regulation. In addition to promoting *C. elegans* germ cell proliferative fate, *Notch* signaling promotes the adoption of the NB stem cell fate in *Drosophila* (Doe, 2008) and the maintenance of stem cell fate in several mammalian cell and tissue types, including melanoblasts, neuroblasts, hematopoietic precursors, and the intestine (Pinnix and Herlyn, 2007; Doe, 2008). In most cases, Notch is activated in the stem cell itself, but the stem cell can also act as the ligand expressing signaling cell in order to promote its own maintenance. For example, female *Drosophila* germ line stem cells express the Notch ligands Delta and Serrate and signal to the niche. One function of the signal is to maintain the population of niche cells, which in turn, maintains germ line stem cell fate (Dansereau and Lasko, 2008).

Notch plays two qualitatively different roles in promoting stem cell proliferation. Notch signaling specifies stem cell fate and promotes proliferation *per se* through regulation of cell cycle progression mechanisms. Both these roles can be co-opted by a number of cancers. One example of the role of Notch activation in cancer is the inception and growth of T-acute lymphoblastic leukemia (T-ALL) (Roy *et al*., 2007). Activating mutations in *Notch1* are found in 55-60% of all cases of T-ALL. Notch likely promotes T-cell proliferation through upregulation of *c-myc* and downregulation of *p53*. In addition, *Notch1* plays early roles in T-cell development and fate specification, and it is thought that its leukemiogenic activity is a distortion of its regular developmental functions.

On a broader scale, increasing evidence suggests that *Notch* activation may promote cancer through inappropriate specification of stem cell fate. The "cancer stem cell hypothesis" proposes that many tumors are comprised of heterogenous population of cells that includes "cancer stem cells" – that is, cells that have the ability to self-renew and give rise to other cell types within the tumor (Visvader and Lindeman, 2008). It is thought that cancer stem cells play key roles in tumor initiation, metastasis, and significantly, resistance to conventional treatments targeting only rapidly amplifying cell populations. In some breast and brain cancers, it is proposed that aberrant *Notch* signaling promotes the self-renewal fate of cancer stem cells (Farnie and Clarke, 2007; Garzia *et al*., 2009; Korkaya and Wicha, 2009). Whether *Notch* activation affects cell fate or cell proliferation in a particular cancer is likely to be an important clinical consideration.

Finally, there are several situations where *Notch* acts to inhibit stem cell proliferation and self-renewal. For example, in mammalian skin, *Notch1* acts as a tumor suppressor, as deletions lead to basal cell carcinoma (Roy *et al*., 2007), and *Notch* inhibits stem cell fate in the *Drosophila* midgut (Micchelli and Perrimon, 2006).

Stem cell self-renewal and cell proliferation

Stem cell proliferation and self-renewal are separable though interrelated processes. The term "proliferation" refers to *cell division*, while "self-renewal" refers to the specification of *stem cell fate*. In the asymmetric paradigm, where each division

leads to the renewal of the stem cell and an addition of a cell that will differentiate, cell division is separable from cell fate specification, and there are genetic factors that have been shown to specifically affect one process or the other (Doe, 2008). This is also true for symmetric cell division, where daughter cells must choose between "stem cell" and "differentiated" cell fates.

The difference between proliferation and self-renewal is less clear when considering the paradigm of population level self-renewal in the *C. elegans* germ line, in part because what distinguishes the "stem-cell like" from "differentiated" cell populations is their method of cell division. The distal proliferative zone is often referred to as the "mitotic zone" and the process of differentiation as the "mitosis/meiosis switch" (Kimble and Crittenden, 2007). Thus, the relationship between cell fate and cell division in the *C. elegans* germ line remains a relatively open question.

One unanswered question is whether failures in one type of cell division or the other result in a fate change, or whether cell fates are specified prior to and independently of the ability of cells to execute mitosis or meiosis. Some mutations (in the RNA regulators *gld-1* and *puf-8*) that prevent the normal meiotic progression cause a return to mitosis (Francis *et al*., 1995; Subramaniam and Seydoux, 2003), suggesting that a failure in meiotic progression can lead to a reversal in cell fate, although it is unclear whether ectopically proliferating cells share the stem cell character of the distal population. However, there are numerous mutations that disrupt meiosis, including early meiotic steps, that do not cause a return to mitosis,

suggesting that only specific progression defects can reverse cell fate (MacQueen and Villeneuve, 2001; MacQueen *et al*., 2002; Martinez-Perez and Villeneuve, 2005; Lee *et al*., 2007; Goodyer *et al*., 2008). Furthermore, some genetic perturbations that cause mitotic cell cycle arrest do not cause bulk meiotic entry. These include germ line RNAi of the Cdk1 homolog, *ncc-1* (S. Arur, unpublished data) and mutations in *glp-4* (Beanan and Strome, 1992). However, it is possible that these factors are also required for meiosis as well. Moreover, it is unknown if *C.elegans* germ cells can enter meiosis only at particular cell cycle stage, and how cell cycle progression may bear on competence for meiotic entry (Hubbard, 2007).

Because the term "proliferation" has been used to refer to both cell division and fate choice in the *C.elegans* germ line, perhaps it is most appropriate to define "proliferative fate" as a decision to mitotically divide, and "proliferation *per se*" as the act of mitotic division. Indeed, one of the main contributions of the thesis work presented here is to demonstrate that two factors required for a normal mitotic cell cycle, METT-10 and dynein, inhibit the specification of germ cell proliferative fate, demonstrating that proliferative fate is genetically separable from the act of mitotic cell division itself.

REFERENCES

Austin, J., and Kimble, J. (1987). glp-1 is required in the germ line for regulation of the decision between mitosis and meiosis in C. elegans. Cell *51*, 589-599.

Beanan, M.J., and Strome, S. (1992). Characterization of a germ-line proliferation mutation in C. elegans. Development *116*, 755-766.

Beckmann, J., Scheitza, S., Wernet, P., Fischer, J.C., and Giebel, B. (2007). Asymmetric cell division within the human hematopoietic stem and progenitor cell compartment: identification of asymmetrically segregating proteins. Blood *109*, 5494-5501.

Berry, L.W., Westlund, B., and Schedl, T. (1997). Germ-line tumor formation caused by activation of glp-1, a Caenorhabditis elegans member of the Notch family of receptors. Development *124*, 925-936.

Crittenden, S.L., Leonhard, K.A., Byrd, D.T., and Kimble, J. (2006). Cellular analyses of the mitotic region in the Caenorhabditis elegans adult germ line. Mol Biol Cell *17*, 3051-3061.

Dansereau, D.A., and Lasko, P. (2008). The development of germ line stem cells in Drosophila. Methods Mol Biol *450*, 3-26.

Doe, C.Q. (2008). Neural stem cells: balancing self-renewal with differentiation. Development *135*, 1575-1587.

Eckmann, C.R., Crittenden, S.L., Suh, N., and Kimble, J. (2004). GLD-3 and control of the mitosis/meiosis decision in the germ line of Caenorhabditis elegans. Genetics *168*, 147-160.

Farnie, G., and Clarke, R.B. (2007). Mammary stem cells and breast cancer--role of Notch signalling. Stem Cell Rev *3*, 169-175.

Feng, H., Zhong, W., Punkosdy, G., Gu, S., Zhou, L., Seabolt, E.K., and Kipreos, E.T. (1999). CUL-2 is required for the G1-to-S-phase transition and mitotic chromosome condensation in Caenorhabditis elegans. Nat Cell Biol *1*, 486-492.

Fitzgerald, K., Wilkinson, H.A., and Greenwald, I. (1993). glp-1 can substitute for lin-12 in specifying cell fate decisions in Caenorhabditis elegans. Development *119*, 1019-1027.

Fiuza, U.M., and Arias, A.M. (2007). Cell and molecular biology of Notch. J Endocrinol *194*, 459-474.

Fortini, M.E. (2009). Notch signaling: the core pathway and its posttranslational regulation. Dev Cell *16*, 633-647.

Fortini, M.E., and Bilder, D. (2009). Endocytic regulation of Notch signaling. Curr Opin Genet Dev.

Francis, R., Barton, M.K., Kimble, J., and Schedl, T. (1995). gld-1, a tumor suppressor gene required for oocyte development in Caenorhabditis elegans. Genetics *139*, 579-606.

Garzia, L., Andolfo, I., Cusanelli, E., Marino, N., Petrosino, G., De Martino, D., Esposito, V., Galeone, A., Navas, L., Esposito, S., Gargiulo, S., Fattet, S., Donofrio, V., Cinalli, G., Brunetti, A., Vecchio, L.D., Northcott, P.A., Delattre, O., Taylor, M.D., Iolascon, A., and Zollo, M. (2009). MicroRNA-199b-5p impairs cancer stem cells through negative regulation of HES1 in medulloblastoma. PLoS ONE *4*, e4998.

Goodyer, W., Kaitna, S., Couteau, F., Ward, J.D., Boulton, S.J., and Zetka, M. (2008). HTP-3 links DSB formation with homolog pairing and crossing over during C. elegans meiosis. Dev Cell *14*, 263-274.

Guo, M., Jan, L.Y., and Jan, Y.N. (1996). Control of daughter cell fates during asymmetric division: interaction of Numb and Notch. Neuron *17*, 27-41.

Hansen, D., Hubbard, E.J., and Schedl, T. (2004a). Multi-pathway control of the proliferation versus meiotic development decision in the Caenorhabditis elegans germ line. Dev Biol *268*, 342-357.

Hansen, D., and Schedl, T. (2006). The regulatory network controlling the proliferation-meiotic entry decision in the Caenorhabditis elegans germ line. Curr Top Dev Biol *76*, 185-215.

Hansen, D., Wilson-Berry, L., Dang, T., and Schedl, T. (2004b). Control of the proliferation versus meiotic development decision in the C. elegans germ line through regulation of GLD-1 protein accumulation. Development *131*, 93-104.

Hubbard, E.J. (2007). Caenorhabditis elegans germ line: a model for stem cell biology. Dev Dyn *236*, 3343-3357.

Jaramillo-Lambert, A., Ellefson, M., Villeneuve, A.M., and Engebrecht, J. (2007). Differential timing of S phases, X chromosome replication, and meiotic prophase in the C. elegans germ line. Dev Biol *308*, 206-221.

Jones, A.R., and Schedl, T. (1995). Mutations in gld-1, a female germ cell-specific tumor suppressor gene in Caenorhabditis elegans, affect a conserved domain also found in Src-associated protein Sam68. Genes Dev *9*, 1491-1504.

Kadyk, L.C., and Kimble, J. (1998). Genetic regulation of entry into meiosis in Caenorhabditis elegans. Development *125*, 1803-1813.

Kerins, J. (2006). PRP-17 and the pre-mRNA splicing pathway are preferentially required for the proliferation versus meiotic development decision and germ line sex determination in *Caenorhabditis elegans*., Washington University Saint Louis, MO.

Kimble, J., and Crittenden, S.L. (2007). Controls of germ line stem cells, entry into meiosis, and the sperm/oocyte decision in Caenorhabditis elegans. Annu Rev Cell Dev Biol *23*, 405-433.

Kimble, J., and Ward, S. (1988). Germ-line development and fertilization. In: The nematode *Caenorhabditis elegans*., Cold Spring Harbor, NY: Cold Spring Harbor Laboratory Press.

Kimble, J.E., and White, J.G. (1981). On the control of germ cell development in Caenorhabditis elegans. Dev Biol *81*, 208-219.

Korkaya, H., and Wicha, M.S. (2009). HER-2, notch, and breast cancer stem cells: targeting an axis of evil. Clin Cancer Res *15*, 1845-1847.

Lai, E.C. (2002). Protein degradation: four E3s for the notch pathway. Curr Biol *12*, R74-78.

Lamont, L.B., Crittenden, S.L., Bernstein, D., Wickens, M., and Kimble, J. (2004). FBF-1 and FBF-2 regulate the size of the mitotic region in the C. elegans germ line. Dev Cell *7*, 697-707.

Lee, M.H., Ohmachi, M., Arur, S., Nayak, S., Francis, R., Church, D., Lambie, E., and Schedl, T. (2007). Multiple functions and dynamic activation of MPK-1

extracellular signal-regulated kinase signaling in Caenorhabditis elegans germ line development. Genetics *177*, 2039-2062.

Lee, M.H., and Schedl, T. (2001). Identification of in vivo mRNA targets of GLD-1, a maxi-KH motif containing protein required for C. elegans germ cell development. Genes Dev *15*, 2408-2420.

Lin, H. (1997). The tao of stem cells in the germ line. Annu Rev Genet *31*, 455-491.

Lu, B., Rothenberg, M., Jan, L.Y., and Jan, Y.N. (1998). Partner of Numb colocalizes with Numb during mitosis and directs Numb asymmetric localization in Drosophila neural and muscle progenitors. Cell *95*, 225-235.

Macdonald, L.D., Knox, A., and Hansen, D. (2008). Proteasomal regulation of the proliferation vs. meiotic entry decision in the Caenorhabditis elegans germ line. Genetics *180*, 905-920.

MacQueen, A.J., Colaiacovo, M.P., McDonald, K., and Villeneuve, A.M. (2002). Synapsis-dependent and -independent mechanisms stabilize homolog pairing during meiotic prophase in C. elegans. Genes Dev *16*, 2428-2442.

MacQueen, A.J., and Villeneuve, A.M. (2001). Nuclear reorganization and homologous chromosome pairing during meiotic prophase require C. elegans chk-2. Genes Dev *15*, 1674-1687.

Marin, V.A., and Evans, T.C. (2003). Translational repression of a C. elegans Notch mRNA by the STAR/KH domain protein GLD-1. Development *130*, 2623-2632.

Martinez-Perez, E., and Villeneuve, A.M. (2005). HTP-1-dependent constraints coordinate homolog pairing and synapsis and promote chiasma formation during C. elegans meiosis. Genes Dev *19*, 2727-2743.

Micchelli, C.A., and Perrimon, N. (2006). Evidence that stem cells reside in the adult Drosophila midgut epithelium. Nature *439*, 475-479.

Morrison, S.J., and Kimble, J. (2006). Asymmetric and symmetric stem-cell divisions in development and cancer. Nature *441*, 1068-1074.

Morrison, S.J., Shah, N.M., and Anderson, D.J. (1997). Regulatory mechanisms in stem cell biology. Cell *88*, 287-298.

Oatley, J.M., and Brinster, R.L. (2008). Regulation of spermatogonial stem cell self-renewal in mammals. Annu Rev Cell Dev Biol *24*, 263-286.

Ohshiro, T., Yagami, T., Zhang, C., and Matsuzaki, F. (2000). Role of cortical tumour-suppressor proteins in asymmetric division of Drosophila neuroblast. Nature *408*, 593-596.

Pepper, A.S., Killian, D.J., and Hubbard, E.J. (2003). Genetic analysis of Caenorhabditis elegans glp-1 mutants suggests receptor interaction or competition. Genetics *163*, 115-132.

Pinnix, C.C., and Herlyn, M. (2007). The many faces of Notch signaling in skin-derived cells. Pigment Cell Res *20*, 458-465.

Qiao, L., Lissemore, J.L., Shu, P., Smardon, A., Gelber, M.B., and Maine, E.M. (1995). Enhancers of glp-1, a gene required for cell-signaling in Caenorhabditis

elegans, define a set of genes required for germ line development. Genetics *141*, 551-569.

Roy, M., Pear, W.S., and Aster, J.C. (2007). The multifaceted role of Notch in cancer. Curr Opin Genet Dev *17*, 52-59.

Smith, C.A., Lau, K.M., Rahmani, Z., Dho, S.E., Brothers, G., She, Y.M., Berry, D.M., Bonneil, E., Thibault, P., Schweisguth, F., Le Borgne, R., and McGlade, C.J. (2007). aPKC-mediated phosphorylation regulates asymmetric membrane localization of the cell fate determinant Numb. EMBO J *26*, 468-480.

Subramaniam, K., and Seydoux, G. (2003). Dedifferentiation of primary spermatocytes into germ cell tumors in C. elegans lacking the pumilio-like protein PUF-8. Curr Biol *13*, 134-139.

Sundaram, M., and Greenwald, I. (1993). Suppressors of a lin-12 hypomorph define genes that interact with both lin-12 and glp-1 in Caenorhabditis elegans. Genetics *135*, 765-783.

Takano, H., Ema, H., Sudo, K., and Nakauchi, H. (2004). Asymmetric division and lineage commitment at the level of hematopoietic stem cells: inference from differentiation in daughter cell and granddaughter cell pairs. J Exp Med *199*, 295-302.

Uemura, T., Shepherd, S., Ackerman, L., Jan, L.Y., and Jan, Y.N. (1989). numb, a gene required in determination of cell fate during sensory organ formation in Drosophila embryos. Cell *58*, 349-360.

Visvader, J.E., and Lindeman, G.J. (2008). Cancer stem cells in solid tumours: accumulating evidence and unresolved questions. Nat Rev Cancer *8*, 755-768.

Walker, M.R., Patel, K.K., and Stappenbeck, T.S. (2009). The stem cell niche. J Pathol *217*, 169-180.

Wang, L., Eckmann, C.R., Kadyk, L.C., Wickens, M., and Kimble, J. (2002). A regulatory cytoplasmic poly(A) polymerase in Caenorhabditis elegans. Nature *419*, 312-316.

Wong, M.D., Jin, Z., and Xie, T. (2005). Molecular mechanisms of germ line stem cell regulation. Annu Rev Genet *39*, 173-195.

Yamashita, Y.M., Jones, D.L., and Fuller, M.T. (2003). Orientation of asymmetric stem cell division by the APC tumor suppressor and centrosome. Science *301*, 1547-1550.

Figure 1. Models of Asymmetric and Symmetric Stem Cell Division. Cells that will adopt the "stem cell fate" are shown in green, cells that will differentiate are shown in red. (A-B) Asymmetric division of stem cells is mediated by intrinsic and extrinsic factors. (A) In the *Drosophila* NB, the asymmetric localization of cell fate determinants relative to spindle orientation is essential for the adoption of differential cell fates. (B) Male germ line stem cells maintain their "stem cell fate" through contact with the somatic cell hub, which expresses the short-range signaling molecule Unpaired. Asymmetric division is achieved by orienting the mitotic spindle perpendicular to cell contact with the hub, ensuring that only one cell maintains hub contact. (C) It is thought that mammalian male germ line stem cells undergo either symmetric division to either expand the stem cell population or to give rise to two (connected) cells that will differentiate.

Figure 1

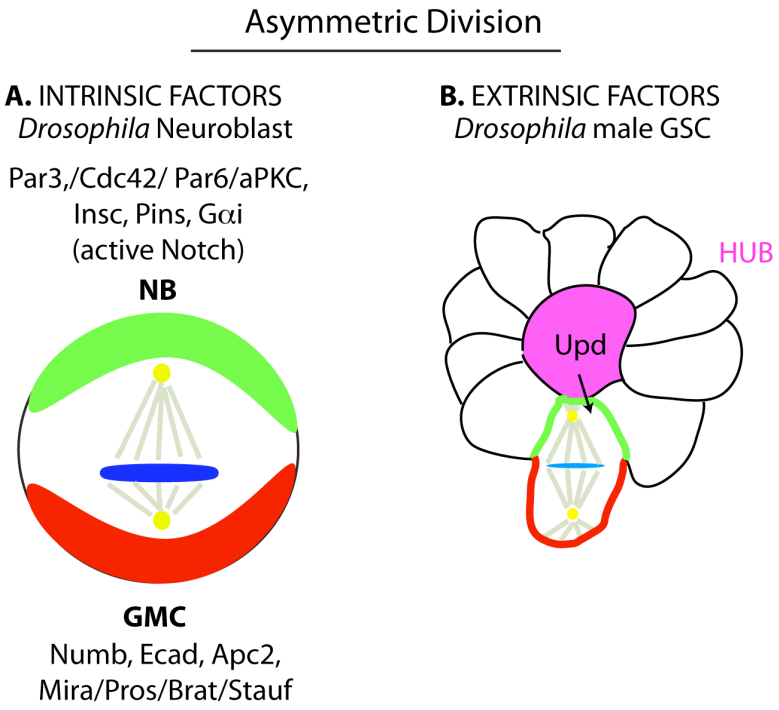
Asymmetric Division
A. INTRINSIC FACTORS
Drosophila Neuroblast
Par3,/Cdc42/ Par6/aPKC,
Insc, Pins, Gαi
(active Notch)
NB
GMC
Numb, Ecad, Apc2,
Mira/Pros/Brat/Stauf
B. EXTRINSIC FACTORS
Drosophila male GSC
HUB
Upd
Symmetric Division
C. Mammalian Spermatogonial Stem Cell
SSC (As)
SSC (As)
SSC (As)
SSC (As)
Apr
Apr

Figure 2. Physical and genetic architecture of the proliferation versus meiotic entry decision in the *C. elegans* germ line. The *C.elegans* adult hermaphrodite has two U-shaped gonad arms that meet at a common uterus. Each arm is organized with a distal to proximal polarity. At the distal region of the germ line, in contact with the somatic distal tip cell **(1)**, are the proliferating germ cells **(2)**. Proliferation of these cells results in a net flux of germ cells away from the niche provided by the DTC, and meiotic entry at a region called the transition zone **(3)**. Germ cells that proceed through an extended meiotic prophase **(4)** to eventual give rise to sperm **(5)** at the L4 larval stage and oocytes **(6)** in adulthood. **(A)** Binding of the LAG-2 ligand (expressed by the DTC) to the GLP-1 Notch receptor in the distal-most germ cells activates the GLP-1/Notch signaling pathway and promotes the proliferative or stem cell fate. One function of the GLP-1 signaling pathway is to repress the activity of genetic pathways that promote entry into meiosis and inhibits the proliferative fate **(B).**

Figure 2

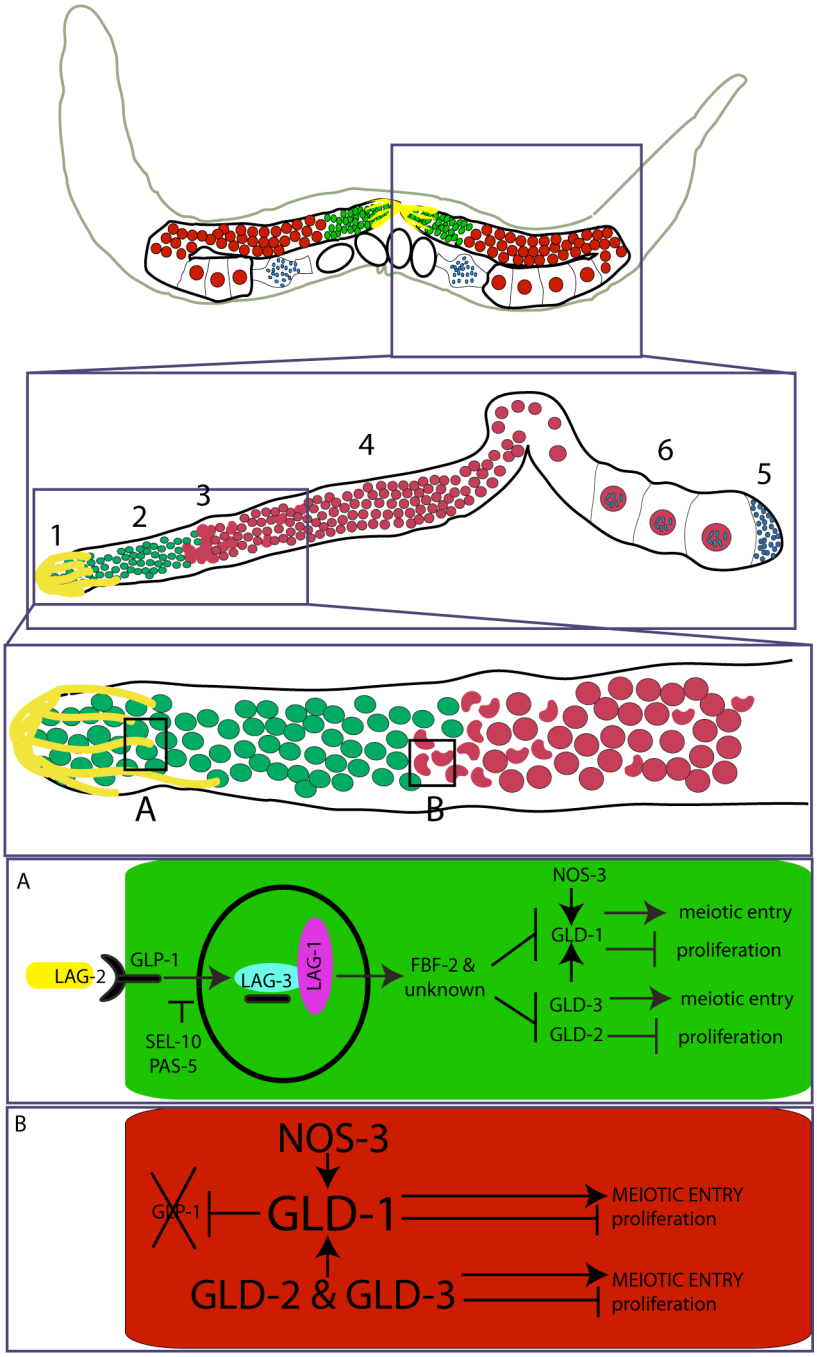
1
2
3
4
5
6
A
B
A
LAG-2
GLP-1
LAG-3
LAG-1
SEL-10
PAS-5
FBF-2 &
unknown
NOS-3
GLD-1
meiotic entry
proliferation
GLD-3
GLD-2
meiotic entry
proliferation
B
NOS-3
GLP-1
GLD-1
MEIOTIC ENTRY
proliferation
GLD-2 & GLD-3
MEIOTIC ENTRY
proliferation

Chapter 2:

METT-10, A Putative Methyltransferase, Inhibits Germ Cell Proliferative Fate in *Caenorhabditis elegans*

INTRODUCTION

From early development to later life, tissues are formed and maintained by stem cell populations. Stem cells have the unique ability to give rise to both differentiated cell types and self-renewing daughters, and must decide between maintaining self-renewing capability and differentiating. A balance between cell proliferation and differentiation is critical for normal tissue development and the avoidance of disease. For instance, uncontrolled self-renewal is a hallmark of cancer (Krivtsov *et al*., 2006), while a failure to maintain proliferation is often equally detrimental (Kauffman *et al*., 2003).

The *Caenorhabditis elegans* germline offers an excellent model system to study factors regulating this balance. *C. elegans* germ cells begin from germline precursors set aside early in life (Sulston *et al*., 1983). Following initiation of post-embryonic development, germline stem cells are specified to maintain a proliferative fate and undergo mitotic cell division, or to differentiate into gametes, whereby they enter a meiotic developmental program (Hansen and Schedl, 2006; Kimble and Crittenden, 2007). This decision is spatially regulated within the gonad. Proliferating germ cells reside in the distal end and enter meiosis more proximally at a region of the germline called the "transition zone", which corresponds to leptotene/zygotene of meiosis I (Figure 1A). Currently, there is no evidence for asymmetric division within the proliferative zone, and it is thought that differentiation may be the consequence of progressive displacement away from the niche (Morrison and Kimble, 2006).

The signal for continued proliferation of germ cell precursors is provided by activation of the Notch signaling pathway in distal germ cells (Austin and Kimble, 1987; Berry *et al*., 1997). The ligand LAG-2, a member of the conserved family of Delta/Serrate proteins, is expressed by a somatic cell called the distal tip cell, effectively creating a "niche" (Henderson *et al*., 1994). Binding of LAG-2 to GLP-1 (one of two *C. elegans* Notch receptors) likely results in cleavage of the intracellular domain of GLP-1 and its subsequent translocation to the nucleus (Mumm and Kopan, 2000). Upon translocation to the nucleus, GLP-1 (INTRA) complexes with other proteins, such as the DNA-binding transcription factor LAG-1, to activate transcription of target genes which promote the proliferative fate (Lamont *et al*., 2004; Wilson and Kovall, 2006). This role of GLP-1 in promoting the choice of proliferative fate was elucidated primarily by genetic analysis. Loss of *glp-1* function results in the premature differentiation and meiotic entry of all germ cells (Austin and Kimble, 1987), while constitutive activation of *glp-1* causes germline tumors (Berry *et al*., 1997).

Although *glp-1* signaling is a central component controlling the specification of germ cell proliferative fate, the mechanism of this important cellular decision is far from understood. A complete picture of the components that transduce or inhibit the *glp-1* signal, govern the maintenance of proliferative cells, and ensure their proper differentiation and entry into meiosis is essential for understanding cell fate decisions including aberrant cell fate decisions leading to human cancers (Weng *et al*., 2004; Koch and Radtke, 2007).

To further characterize the specification of germ cell proliferative fate, we characterized a novel tumorous allele of the *mett-10* gene isolated in a forward genetic screen for factors that disrupt the balance between germ cell proliferation and differentiation (Francis *et al*., 1995a). We demonstrate that METT-10, a conserved putative methyltransferase, inhibits germ cell proliferative fate in *C. elegans*, possibly through inhibition of the pro-proliferative functions of the *glp-1/Notch* signaling pathway.

RESULTS

A *mett-10* allele with a tumorous phenotype

To identify genes regulating the transition between proliferative and meiotic fates, we carried out a screen for recessive tumorous mutants exhibiting ectopic or excessive proliferation (Francis *et al*., 1995a). We isolated an allele of *mett-10*, the worm ortholog of the METT10D putative methyltransferase of vertebrates (see below); *mett-10(oz36)* exhibits a cold-sensitive and partially penetrant tumorous phenotype (Table 1). The tumorous phenotype is variable and includes both regions of ectopic proliferation near the "loop" region of the germline normally occupied by cells in meiotic pachytene, as well as what is typically called the "late-onset tumorous" phenotype, in which the distal proliferative zone progressively increases in length as the animals age. These phenotypes indicate an imbalance of proliferation over differentiation similar to *glp-1/Notch* gain-of-function mutations (Berry *et al*.,

1997; Pepper *et al*., 2003), and are distinct from tumors that arise from a return to proliferation from meiotic development (Francis *et al*., 1995a; Subramaniam and Seydoux, 2003) or that result from disrupting the function of multiple factors acting downstream of *glp-1* to promote meiotic entry (Kadyk and Kimble, 1998; Eckmann *et al*., 2004; Hansen *et al*., 2004a).

We confirmed that the cells suspected to be ectopic proliferating cells are cycling by testing for incorporation of the nucleotide analog, EdU, which labels cells in S-phase of the cell cycle (Salic and Mitchison, 2008). In wild type germlines, a 3 hour pulse of EdU labels most cells in the proliferative zone, but not in the adjacent meiotic region (Figure 1B). The suspected ectopic proliferating cells in the *mett-10(oz36)* mutant label with EdU within a 3 hour period, demonstrating that they are cycling (Figure 1C). Because EdU labels cells both in mitotic as well as meiotic S-phase, we further characterized these cells by staining for additional mitotic and meiotic markers. Ectopic phospho-histone-3 (pH3) nuclei were observed in *mett-10(oz36)* mutants, consistent with ectopic mitosis (Figure 1D-E). Furthermore, these cells were negative for the meiotic marker, GLD-1 (Hansen *et al*., 2004b). Together, these data suggest that the *mett-10(oz36)* mutation causes the proliferation of germ cells which should otherwise have entered meiosis. Because the *C.elegans* germline stem cells have not been unequivocally identified, we cannot definitively attribute our phenotype to overproliferation of the germline stem cells themselves, rather than a potential transient amplifying population. However, the degree of tumor formation seen in older animals, coupled with the similarity of the overproliferative phenotype

to that of *glp-1/Notch* gain-of-function mutants suggests that *mett-10(oz36)* may affect stem cell fate specification.

We cloned *mett-10* by genetic mapping, cosmid rescue, and sequencing of candidate genes. Several lines of evidence indicate that the gene affected by the *oz36* mutation is ZK1128.2, the ortholog of human Methyltransferase-10 Domain Containing protein (METT10D) (Figure 2A). First, the mutation responsible for the tumorous phenotype genetically maps to a genomic region containing ZK1128.2 (data not shown). Second, a transgene containing the ZK1128.2 coding region rescues the *mett-10(oz36)* mutant phenotype (Table 1). Finally, sequencing of the *oz36* allele, as well as other mutations in the same complementation group (see below), all reveal molecular lesions within the ZK1128.2 coding region (Figure 2B).

The N-terminal domain of human METT10D was crystallized in complex with S-adenosyl methionine (SAM), the substrate used by SAM-dependent methyltransferases to catalyze the transfer of a methyl group to a wide variety of substrates, including protein, DNA, RNA, small molecules and lipids (Martin and McMillan, 2002; Wu *et al*., To be published.). Based on sequence conservation and secondary structure prediction, *C.elegans* METT-10 is predicted to bind SAM (Figure 2A). Furthermore, both human and *C.elegans* METT-10 contain a full "SAM-dependent methyltransferase fold", including conserved protein motifs known to be responsible for the catalysis of the methyl-transfer (Figure 2A; Malone *et al*., 1995). With only two known exceptions, proteins containing the SAM-dependent methyltransferase fold act as methyltransferases (see Discussion). Thus, it is highly

likely that METT-10 acts as a methyltransferase in *C. elegans,* although the biochemical nature of the substrate is unknown at this time.

Loss of *mett-10* function results in multiple temperature-sensitive phenotypes

The *oz36* mutation creates a premature stop codon that truncates the protein shortly after the putative methyltransferase domain. While the *mett-10(oz36)* mutant is tumorous at lower temperatures (Table 1), at 25˚C it behaves as a loss-of-function and fails to complement a deficiency (*nDf40*). At this non-permissive temperature, *mett-10(oz36)* animals are sterile (Ste) or maternal-effect lethal (Mel), with multiple somatic phenotypes including slow growth (Gro), a protruding vulva (Pvl), and distension of the intestinal lumen (data not shown, Table 2, Figure 3B,E).

We identified two additional *mett-10* alleles by testing uncloned Ste/Pvl mutants mapping to the same genetic region for complementation of *mett-10(oz36)* at 25˚C (Figure 2B). *mett-10(g38)* was first identified as *let-42* in previous screens for maternal effect lethal mutations (Cassada *et al*., 1981). *mett-10(oj32)* was isolated in a screen for temperature sensitive sterile and uncoordinated mutants and was originally named *stu-18* (O'Connell *et al*., 1998). Based on sequence conservation between *C. elegans* METT-10 and Human METT10D, the *oj32* mutation (G110R) disrupts a conserved glycine that binds to S-adenosyl methionine, the substrate used by SAM-dependent methyltransferases, and thus should compromise enzymatic activity (Figure 2, Malone *et al*., 1995).

Two deletion alleles were obtained from the Japanese National Bioresource Project (*tm2697*) and the *C. elegans* gene knockout consortium (*ok2204*) (Figure 2B). The *tm2697* deletion is an internal in-frame deletion C-terminal to the core of the conserved methyltransferase domain. The *ok2204* deletion removes the entire methyltransferase domain, and we believe that it is essentially a null allele.

Like *mett-10(oz36)*, all other *mett-10* alleles exhibit a temperature sensitive Ste/Mel/Pvl phenotype (Table 2, Figure 3C,F). Germline sterility in *mett-10* loss-of-function mutants appears to be a result of abnormalities in gonad morphology and defects in germ cell meiotic development. At 25˚C, 30% of *mett-10(ok2204)* germlines have at least one extra protrusion in this distal gonad (Figure 4A-B). Moreover, many germlines contain pachytene cells in the proximal-most region of the germline, normally occupied by diakinetic oocytes (data not shown). In situations where proximal *mett-10(ok2204)* germ cells progress from pachytene to diplotene, there is often a disruption of normal linear oocyte organization (Figure 4E-F).

In addition to abnormalities in their meiotic development, and unlike *mett-10(oz36)* germline tumors, *mett-10(ok2204)* germ cells appear to have difficulty in progressing through the mitotic cell cycle. At all temperatures, the proliferative zone of *mett-10(ok2204)* germlines contain abnormally large, diffuse nuclei (Figure 4B,D). Because this nuclear morphology is associated with cell cycle arrest (Gartner *et al*., 2000; Moser *et al*., 2009), we tested if these cells were actively cycling by labeling with EdU and co-staining for phospho-histone-3. We found that these large cells do not incorporate EdU during a time period sufficient to label essentially all

proliferative zone nuclei in wild type germlines and are not pH3 –positive (Figure 4C-D). Together, these data suggest that these large nuclei arrest at some point other than M-phase of the cycle, and thus, that METT-10 may normally promote mitotic cell cycle progression. Overall, *mett-10* loss-of-function germlines are quite small at 25˚C, suggesting that METT-10 may contribute to the execution of proliferation *per se*.

In additional to the developmental defects described above, we observed that *mett-10* mutants exhibit defects in susceptibility to RNA interference (RNAi) at all temperatures. To better characterize this phenotype, we tested multiple *mett-10* alleles for their susceptibility to dsRNA directed against the somatic gene, *unc-22*, and the germ line gene, *gld-1*. We found that mutations in *mett-10* have strong effects on germ line RNAi, but relatively mild effects on the soma (Figure 5), suggesting that METT-10 normally functions to promote the RNA interference pathway in the germ line. Significantly, *mett-10* RNAi defects are not suppressed by a mutation in *eri-1*, a nuclease that acts downstream to the "core" RNAi machinery to degrade siRNAs generated by exogenous RNAi, suggesting that METT-10 may function in the generation of functional siRNAs (Figure 5 and Kennedy *et al*., 2004).

Consistent with their loss-of-function nature, *mett-10* somatic and germline defects are suppressed by a wild-type *mett-10* transgene (Table 2, data not shown) and, with the exception of maternal effect embryonic lethality and RNAi-resistance, *mett-10* phenotypes are maternally rescued (Table 2). Significantly, while all alleles

exhibit the Ste/Mel/Pvl phenotype with variable penetrance at 25˚C, in contrast to *mett-10(oz36)*, none are tumorous under any temperature condition (Table 3).

mett-10(oz36) likely produces a "poisonous" product

Since *mett-10(oz36)* is the only allele that is tumorous on its own, we thought it possible that the mutation might confer a novel activity unrelated to the normal *mett-10(+)* function. However, the evidence indicates that this is not the case. If *mett-10(oz36)* is tumorous because it has acquired a new function, then the tumorous phenotype should be unmodified by a wild type copy of *mett-10*. However, the tumorous phenotype of *mett-10 (oz36*) is recessive and is also completely suppressed by a wild type transgene (Table 1).

Genetic experiments indicate that *mett-10(oz36)* likely encodes a product that poisons processes in which *mett-10(+)* normally participates. If *mett-10(oz36)* encodes a poisonous product, the tumorous phenotype should depend on the dosage of *mett-10(oz36)*. To increase the effective dose of *mett-10(oz36)*, we took advantage of the fact that the *oz36* mutation is a premature stop codon and that the transcript should be degraded by nonsense-mediated decay (NMD). Disruption of NMD should therefore result in increased production of a 'poisonous product' (Hodgkin *et al*., 1989; Page *et al*., 1999). We observed that genetic disruption of NMD by the *smg-2(e2008)* mutation significantly enhances the overproliferation phenotype of *mett-10(oz36)* to 98% penetrance (Table 1). NMD-disruption also enhances the degree of tumor formation in the mutants, with much larger tumors forming in *smg-2(e2008);*

mett-10(oz36) animals than in *mett-10(oz36)* animals alone (Figure 6B-C). Interestingly, even in an NMD-defective background, *mett-10(oz36)* is recessive, indicating that wild type METT-10 fully suppresses the tumorous phenotype (Table 1). This suggests that the tumorous phenotype of *mett-10(oz36)* mutants may be caused by the simultaneous loss of METT-10 function, and the poisoning of another protein by METT-10(oz36). Supporting this idea, heteroallelic *mett-10(oz36)/mett-10(g38)* mutants exhibit a partially penetrant tumorous phenotype that is more severe than *mett-10(oz36)/mett-10 (+)* and less severe than *mett-10(oz36)* homozygotes in an NMD-defective background (Table 1).

NMD-disruption also enhances maternal-effect embryonic lethality in the *mett-10(oz36)* mutant, as the few progeny laid by *smg-2(e2008); mett-10(oz36)* mothers at 15˚C or 20˚C die late in embryogenesis or shortly after hatching with a variety of abnormalities (Figure 3G-I). This suggests that *mett-10(oz36)* expression may also disrupt some aspect of embryonic development.

METT-10 inhibits germ cell proliferative fate

A straightforward interpretation of the *mett-10(oz36)* tumorous phenotype is that wild type METT-10 inhibits specification of germ cell proliferative fate. However, because the *mett-10(oz36)* allele forms a product that poisons other processes, it was also possible that it may indirectly affect proliferative fate specification. To address this possibility, we tested if *mett-10* loss-of-function alleles were also compromised for the proliferative/meiotic fate decision. Because none of

these alleles are tumorous on their own, we tested their ability to enhance a genetic background sensitized for the tumorous phenotype by an elevation of *glp-1/Notch* activity [*glp-1(oz264)*](Kerins, 2006). We found that *mett-10* alleles significantly enhance the *glp-1(oz264)* tumorous phenotype at 20˚C (Table 3), demonstrating that METT-10 normally either inhibits germ cell proliferative fate or promotes meiotic entry.

Our conclusion that METT-10 normally acts to inhibit germ cell proliferation and/or promote meiotic entry is further supported by our finding that *mett-10* loss-of-function alleles can partially suppress the premature meiotic entry phenotype of a temperature-sensitive *glp-1* loss-of-function mutant [*glp-1(bn18)*] (Kodoyianni *et al*., 1992; Qiao *et al*., 1995). Adult *glp-1 (bn18)* animals raised at 20˚C and shifted to 25˚C for six hours have minimal proliferative zones and an absence of nuclei in M-phase (as evidenced by an absence of phospho-histone-3 (pH3)-positive nuclei) because removal of *glp-1/Notch* signaling induces all germ cells to enter meiosis (Figure 7E,F,J; P. Fox and T. Schedl, unpublished data; Kodoyianni *et al*., 1992; Qiao *et al*., 1995). However, we observed pH3-positive nuclei, albeit reduced in number, in *glp-1(bn18) mett-10(g38)* double mutants after a six hour shift, despite equivalent numbers of pH3-positive nuclei in *glp-1(bn18)* and *glp-1(bn18) mett-10(g38)* unshifted controls (Figure 7G,H,J). The reduction in overall proliferative zone size and number of pH3-positive nuclei in *glp-1(bn18) mett-10(g38)* germlines upon temperature-shift suggests that germ cells are still induced to enter meiosis upon removal of *glp-1* signaling, although with different temporal dynamics; in support of

this, longer shifts of *glp-1(bn18) mett-10(g38)* animals result in the meiotic entry of all germ cells (Figure 7I).

Given the central role of *glp-1/Notch* signaling in the specification of germ cell proliferative fate, we sought to determine if METT-10 normally acts downstream of, upstream of, or in parallel to *glp-1* to inhibit germ cell proliferative fate. Several lines of evidence indicate that it is unlikely that GLP-1 normally acts to inhibit METT-10. The first makes use of the fact that METT-10(oz36) acts similarly to a dominant negative protein, in that increased expression of the mutant protein drives the overproliferation phenotype towards the *mett-10* loss-of-function direction. Thus, if GLP-1 acts upstream of METT-10, we would not expect the *mett-10(oz36)* tumorous phenotype to be dependent on *glp-1* activity. However, we find that tumor formation in the *mett-10(oz36)* background is exquisitely dependent on *glp-1* signaling; *glp-1(bn18)* fully suppresses the *smg-2(e2008); mett-10(oz36)* tumorous (but not the embryonic lethality) phenotype at the permissive temperature of 20˚C (Table 1, Figure 6C-E), suggesting that METT-10 may negatively regulate *glp-1* signaling to inhibit the specification of proliferative fate.

The idea that METT-10 acts upstream of or in parallel to *glp-1* signaling to inhibit germ cell proliferation is further supported by our analysis of genetic interactions between *mett-10* and the genetic pathways that function downstream of *glp-1* to redundantly promote meiotic entry. These pathways are defined by the genes *gld-1* and *gld-2*. In animals that have lost either *gld-1* or *gld-2*, germ cells enter meiosis, but do not undergo normal meiotic progression (Francis *et al*., 1995b; Kadyk

and Kimble, 1998). Germ cells that have lost both *gld-1* and *gld-2* fail to enter meiosis, resulting in germline tumors that are independent of *glp-1* activity (Kadyk and Kimble, 1998; Hansen *et al*., 2004a). We made double mutants between *mett-10(oz36)* and null alleles of *gld-1, gld-2*, and *gld-3* (which acts in the *gld-2* pathway) (Eckmann *et al*., 2004). Since *gld-1(q485)* hermaprodites have germline tumors that are due to a return to mitosis, while males are unaffected (Francis *et al*., 1995a), we analyzed *gld-1(q485); mett-10(oz36)* males and found that *mett-10(oz36)* does not act redundantly with *gld-1* to promote meiotic entry (Table 4). Furthermore, we found that while *gld-2(q497)* enhanced the *mett-10(oz36)* tumorous phenotype, this was completely suppressible by a reduction in *glp-1* activity introduced either by the *glp-1* null allele, *glp-1(q175)*, or even the temperature-sensitive *glp-1* hypomorph, *glp-1(bn18)*, raised at the permissive temperature of 20˚C (Figure 8, Table 4). Results similar to those for *gld-2* were observed for *gld-3* (Table 4).

METT-10 is a nuclear protein expressed in many cell types

To localize the METT-10 protein *in vivo*, we expressed a GFP-tagged version of METT-10 under control of the endogenous promoter (see Methods) as an extrachromosomal array. We found that METT-10::GFP is a nuclear protein expressed in many of the same tissues where *mett-10* disruption causes phenotypic abnormalities, including the intestine, vulva, and cells of the somatic gonad including the distal tip cell, gonadal sheath cells, and spermatheca (Figure 9A-E).

To visualize METT-10 expression in the germline, where extrachromosomal arrays are often silenced relative to somatic copies (although *mett-10::gfp* is weakly expressed in the germline from an array), we generated an integrated version of *pmett-10:mett-10::gfp*. METT-10::GFP expression rescues all *mett-10* mutant phenotypes (Tables 1-3). The observed germline localization of METT-10 is consistent with its role in inhibition of germ cell proliferative fate; METT-10::GFP protein levels are low in the distal proliferative zone and increase as cells enter meiosis, although some proliferative nuclei are positive (Figure 10). METT-10::GFP persists throughout meiotic prophase as a predominantly nuclear protein that does not colocalize with DNA (Figures 9F & 11).

The germ line expression pattern of METT-10 is altered in both *glp-1* loss-of-function and gain-of-function mutant backgrounds. In line with our previous observation that METT-10 accumulates as germ cells enter meiosis, we find that in shifted *glp-1(bn18)* animals in which almost all germ cells have entered meiosis, nuclear METT-10 is uniformly detected in distally located meiotic nuclei (Figure 10). However, there is also an increase in METT-10 in distal nuclei when we shift the *glp-1* gain-of-function mutant, *glp-1(ar202)*, to 25˚C to induce tumor formation, although patches expressing low METT-10 levels can be found (Figure 10). It is likely that this represents an expansion of the normally small proliferative zone population that expresses METT-10 and that may require its function for normal cell cycle progression. Our finding that METT-10 expression does not inversely correlate with

levels of GLP-1 activity further supports our hypothesis that METT-10 functions upstream of or in parallel to GLP-1 to antagonize its pro-proliferative functions.

METT-10 acts in the germline to inhibit germ cell proliferative fate

Since METT-10 is expressed in both the germline and the soma, including cells of the somatic gonad that can affect germ cell fate (McCarter *et al*., 1997; Killian and Hubbard, 2004; Voutev *et al*., 2006), we used mosaic analysis to determine whether METT-10 acts in the soma or the germline to inhibit germ cell proliferative fate. We carried out mosaic analysis by taking advantage of the fact that in *C. elegans,* injected DNA forms extrachromosomal arrays that are imperfectly transmitted during cell division (Yochem and Herman, 2005). To form marked extrachromosomal arrays carrying wild type *mett-10*, we co-injected a rescuing *mett-10 (+)* construct with a construct carrying the *sur-5::GFP* cell autonomous marker that is expressed in the nuclei of almost all somatic cells (Yochem *et al*., 1998). We found that, even with loss in the somatic gonad, the presence of the *sur-5::GFP; mett-10(+)* array in the germline (detected by transmission of the array to progeny) fully suppresses the tumorous phenotype of the *smg-2(e2008); mett-10(oz36)* double mutant (Figure 12). Conversely, expression of *mett-10 (+)* in cells of the somatic gonad did not suppress the *smg-2 (e2008); mett-10(oz36)* tumorous phenotype in the event of germline loss (Figure 12) . We conclude that METT-10 acts in the germline to inhibit the specification of proliferative fate.

DISCUSSION

Unlike the post-mitotic soma, the adult *C. elegans* germline is a dynamic system; germ cells proliferate through mitotic cell division to maintain their population, and at some frequency, switch to meiosis to produce gametes (Crittenden *et al*., 2003; Hansen and Schedl, 2006; Kimble and Crittenden, 2007). The temporal and spatial dynamics of this decision, as well as the conservation of the Notch pathway that governs germ cell proliferation, makes it an excellent system to study the genetic architecture governing stem cell proliferation and fate specification. Here we identify a role for the previously uncharacterized, though highly conserved, METT-10 putative methyltransferase in inhibiting the choice of proliferative fate in the *C. elegans* germline. In addition to its role in proliferative fate specification, we find that METT-10 is essential for normal germ line RNAi sensitivity, development of the vulva, somatic gonad, and embryo, and contributes to the progression of germ cells through both mitosis and meiosis. The role of METT-10 in promoting mitotic cell cycle progression, while inhibiting the specification of proliferative fate, delineates a genetic difference between the developmental decision of proliferate *fate* specification and the process of cell proliferation *per se*.

METT-10 acts as an inhibitor of germ cell proliferative fate in *C. elegans*

Likely by way of stem cell fate specification, germ cell proliferation is promoted by the conserved *glp-1/Notch* signaling pathway (Crittenden *et al*., 2003; Hansen and Schedl, 2006; Kimble and Crittenden, 2007). One approach to identify

regulators of the germ cell proliferation is to study mutations that phenocopy the germ cell overproliferation phenotype observed in Notch gain-of-function mutants (Berry *et al*., 1997; Pepper *et al*., 2003). *mett-10(oz36)*, which leads to the formation of late-onset tumors, phenocopies the phenotype of *glp-1* hyperactivation. Interestingly, while we can demonstrate that METT-10 normally plays a role in regulating germ cell proliferative fate (see below), *mett-10(oz36)* is a unique *mett-10* allele in that it is the only allele that is ever tumorous on its own.

Because *mett-10(oz36)* has, with respect to germline proliferation, a phenotype more severe than the null, *mett-10(oz36)* must have additional properties beyond simple loss of METT-10 function that contribute to the tumorous phenotype. Our genetic analysis indicates that *mett-10(oz36)* not only results in a loss of normal METT-10 function, but also produces a protein that functionally poisons or interferes with an unknown factor(s) to cause germline tumors; thus, the overproliferation observed in *mett-10(oz36)* mutants is likely a synergistic phenotype that results from simultaneous loss of *mett-10* function and the function of at least one other unknown factor. Our analysis here makes multiple predictions that will be helpful for the identification of such a factor(s), including not only that disrupting its function should enhance overproliferation of *mett-10* simple loss-of-function alleles, but also that it may physically interact with METT-10(oz36). The fact that it took this special allele to recapitulate the *glp-1/Notch* gain-of-function phenotype highlights the redundancy governing *glp-1* signal inhibition and germ cell fate specification and suggests that *glp-1* occupies a unique "constriction point" in this complex genetic network. This is

further supported by the identification of many negative regulators of *Notch* signaling that act at multiple steps in the signal transduction process, as well as the redundancy between the downstream pathways controlling meiotic entry (Sundaram and Greenwald, 1993; Hubbard *et al*., 1997; Crittenden *et al*., 2003; Hansen and Schedl, 2006; Macdonald *et al*., 2008).

Although it took a unique allele to identify the role of *mett-10* in inhibition of germ cell proliferative fate, genetic analysis indicates that METT-10 normally functions in this process. We find that *mett-10* loss-of-function alleles can enhance the tumorous phenotype of *glp-1* gain-of-function mutations, while suppressing premature meiotic entry upon reduction of *glp-1* signaling.

How does METT-10 inhibit germ cell proliferation? Our observation that METT-10 accumulates in nuclei as germ cells enter meiosis suggests that METT-10 may function in the nucleus to promote a switch from proliferative to meiotic fates. One possibility is that it inhibits the pro-proliferative functions of active *glp-1/Notch* signaling, since *mett-10*-associated overproliferation phenotypes resemble *glp-1* hyperactivation and are exquisitely dependent on *glp-1* activity. Moreover, genetic pathway analysis suggests that *mett-10* does not function in any of the characterized meiotic entry pathways that act downstream of *glp-1* signaling. While these data suggest that METT-10 may negatively regulate *glp-1/Notch* signaling, it is still possible that it acts in parallel to GLP-1. Moreover, we cannot say whether METT-10 inhibits *Notch* signaling in general, as we were unable to detect clear

genetic interactions with alleles of *lin-12*, the other *C. elegans* Notch receptor (Methods).

Molecularly, it is likely that METT-10 functions as a methyltransferase, and methylation is probably important for its function in proliferative fate specification. METT-10 contains a well-conserved SAM-dependent methyltransferase fold, which has been shown to bind SAM in the human protein (Wu *et al*., To be published.). The *mett-10(oj32)* mutation, which disrupts a key SAM-binding residue, also disrupts the balance between germ cell proliferation versus meiotic entry when examined in a weak *glp-1* gain-of-function genetic background. Almost all of the many characterized proteins that contain a SAM-dependent methyltransferase fold function as methyltransferases (Martin and McMillan, 2002). The two notable exceptions include putrescine aminopropyltransferase (PAPT), which binds a decarboxylated form of SAM (and not SAM itself) to catalyze the transfer of an amino-propyl group, rather than a methylgroup, during spermidine synthesis (Korolev *et al*., 2002), and Dnmt2, which contains a full methyltransferase fold, binds SAM, but lacks detectable DNA methyltransferase activity (Dong *et al*., 2001). Although methyltransferases can methylate protein, nucleic acid, small molecules, and lipids, in the absence of close homologs with known functions and target specificity, the biochemical nature of their target substrates cannot be easily predicted from protein or sequence structure (Martin and McMillan, 2002). Thus, it is currently unclear what METT-10 methylates if it functions as a methyltransferase.

Defects in proliferative fate specification are unlikely to be a downstream consequence of the *mett-10(-)* RNAi defect

At all temperatures, *mett-10* mutants are germ line RNAi resistant. However, the role of METT-10 in RNAi is unlikely to be directly responsible for its phenotype with regard to germ cell proliferation. There is no correlation between degree of RNAi-defect and degree of overproliferation for *mett-10* alleles. In addition, RNAi-mediated depletion of the *C. elegans* DICER homolog, *dcr-1*, does not enhance the tumorous phenotype of the *glp-1* gain-of-function allele, *glp-1(oz264)* (data not shown). Finally, *ego-1*, an RNA-dependent RNA polymerase the contributes to germline RNAi, acts in the opposite direction to *mett-10* with respect to germ cell proliferation; *ego-1* was isolated as an enhancer of premature meiotic entry phenotype of *glp-1* loss-of-function, and strong *ego-1* alleles exhibit premature meiotic entry (Vought *et al*., 2005). Thus, it is unlikely that a general RNA interference defect is responsible for the imbalance of proliferation over differentiation in *mett-10* mutants, although it is possible that the same biochemical or cellular functions of *mett-10* underlie both phenotypes.

Loss of METT-10 function results in a diverse set of developmental phenotypes

In addition to inhibiting proliferative fate in the distal germline, *mett-10* functions in multiple developmental contexts. The phenotype of *mett-10* loss-of-function mutants, including abnormal morphology of the vulva and gonad, as well as multiple defects in germ cell and embryonic development, are a testament to the

potential diversity of *mett-10* functions and targets. Interestingly, many of the defects observed in these mutants, specifically those involving vulval morphogenesis and apparent defects in mitotic progression of germ cells, are associated with defects in cell division. Multiple screens for cell division mutants have been based on this observation, including the one that lead to the identification of the *mett-10(oj32)* allele (O'Connell *et al*., 1998; Fay and Han, 2000). This potential role for *mett-10* in enabling cell division, coupled with its developmental role as an inhibitor of proliferative fate, highlights the importance of distinguishing the specification of developmental cell fates from the cellular mechanisms that ensure their proper execution.

MATERIALS AND METHODS

General worm culture and genetics

Standard procedures for culture and genetic manipulation of *C. elegans* strains were followed (Brenner, 1974). To generate and screen for tumorous mutants, N2 Bristol animals were mutagenized with 50mM EMS, and a dissecting microscope was used to screen an aged F2 generation for tumorous animals (Francis *et al*., 1995a). For analysis of temperature sensitive phenotypes, hermaphrodites were allowed to lay eggs overnight at 20˚C, were removed, and the plates were shifted to 25˚C for the life of the F1 generation and phenotypes were scored at 1 day past the L4 stage at 25˚C. All experiments analyzed only hermaphrodite germlines with the exception of the

enhancement of *gld-1(q485)*, in which male germlines were analyzed. However, germline tumors were observed in rare, spontaneous *smg-2(e2008); mett-10(oz36)* males, indicating that the effect of the *oz36* mutation is not sex-specific.

Complementation testing between *mett-10(oz36)* and other *mett-10* alleles was done by crossing potential *mett-10* alleles to the hT2[qIs48]gfp balancer, and then crossing *gfp(+)* males to an *unc-32(e189) mett-10(oz36)* strain. Non-green, non-unc hermaprodite progeny were picked to a new plate and shifted to 25°C. To examine the interaction between *mett-10* and *lin-12*, we built double mutants between the *lin-12(n379)* gain-of-function and *mett-10(g38)* or *mett-10(oz36)*. No enhancement of the multi-vulval phenotype of *lin-12(n379)* was observed, although *mett-10(-)lin-12(n379)* animals lacking maternal gene product were very sick, grew slowly, and had few progeny. *mett-10* alleles obtained from the knockout consortium and NBP-Japan were cleaned up by outcrossing to N2 Bristol 3X or recombining the markers *unc-32* and *dpy-18* on and off the third chromosome. Strain constructions were verified by single worm PCR and sequencing of alleles.

Alleles used in this study by chromosome:

I: *smg-2(e2008), gld-1(q485), gld-2(q497)*

II: *gld-3(q730)*

III: *lin-12(n379), glp-1(oz264), glp-1(bn18), glp-1(q175), unc-32(e189), unc-36(e251), mett-10(oz36), mett-10(g38), mett-10(tm2697), mett-10(ok2204), mett-10(oj32), unc-119(ed3), dpy-18(e364), nDf40*

IV: *eri-1(mg366)*

Integrated Transgenes: *ozIs7[pmett-10:mett-10::gfp; unc-119(+)]* [chromosome I]
Extrachromosomal arrays: *ozEx66 [pmett-10:mett-10::gfp; unc-119(+)]*, *ozEx63[pmett-10:mett-10;sur-5::gfp; unc-119(+)]*

RNA interference and Western Blot Analysis

Clones for feeding RNAi against *unc-22* and *gld-1* were generated by PCR amplification and cloning of 1kb exonic sequences into the pPD128.36 double T7 promoter vector. Clones were sequenced to verify identity, and transformed into the *E. coli* host HT115(DE3). Feeding RNAi was performed at 20˚C as previously described (Lee *et al.*, 2007). Gravid adults were placed on RNAi plates and allowed to lay overnight before removal. F1 L4 hermaphrodites were transferred onto fresh RNAi plates, allowed to age for 24 hours, and then scored quantitatively for either degree of paralysis (*unc-22*) by dissecting microscope or for phenotypes associated with *gld-1* dysfunction, including small oocytes and germ line tumors by DIC microscopy. To quantitate degree of GLD-1 knockdown, 100 animals were washed, boiled in 2X SDS sample buffer, and loaded onto an SDS-page gel. After transfer, GLD-1 was detected by using a Rabbit anti-GLD-1 antibody at 1:1000, while the LMN-1 control was detected using guinea pig anti-Celamin at 1:10,000.

Mapping of SAM-binding residues on *C. elegans* METT-10

Because of their structural nature and relatively low sequence conservation, the mapping of previously characterized methyltransferase motifs (reviewed in

(Malone *et al*., 1995) onto *C. elegans* METT-10 was done primarily by aligning the *C. elegans* protein to human METT10D, a portion of which was crystallized in complex with S-adenosyl methionine (SAM) by the Structural Genomics Consortium [Structure (PDB 2H00) which can be found at: http://www.rcsb.org/pdb/explore.do?structureId=2H00]. This was aided by secondary structure prediction using Jpred3 [http://www.compbio.dundee.ac.uk/~www-jpred/]. As many methyltransferase motifs are defined by their interaction with SAM, we examined the METT-10-SAM interaction interface using RSCB ligand Explorer (available as a link through the above website), which also served to define which residues are predicted to be essential for SAM-binding.

Immunohistochemistry

Germline dissection, fixation, and staining was carried out as previously described (Lee *et al*., 2007). Antibodies used were: monoclonal mouse anti-GFP (mAb3E6) from Invitrogen (Cat# A-11120), Rabbit anti-GLD-1 (Jones *et al*., 1996), Rabbit anti-phosphohistone-3 (Upstate, Cat#06-570), guinea pig anti-Celamin (gift from J. Liu, Cornell), and donkey anti-mouse Alexa 594, goat anti-rabbit Alexa 488, goat anti-rabbit Alexa 594, and goat anti-guinea pig-Alexa-488 obtained from Molecular Probes (Invitrogen, CA). For EdU labeling and co-staining with antibodies, we used a protocol modified from that of Sarah Crittenden (University of Wisconsin-Madison, personal communication). To make EdU plates, a small culture

of MG1693 *E. coli* (thymidine deficient bacteria, available from the *E.coli* stock center) were grown overnight at 37˚C, and diluted 1/50 the next day in a solution of 1 % glucose, 1.25 μg/ml thiamine, 0.5μM thymidine, 1mM $MgSO_4$, and 20μM EdU in M9 minimal media. This was grown at 37˚C for 24 hours in the dark, before being spun down, resuspended in a small volume of M9 and plated on 60mm M9 plates. For labeling and staining of proliferative cells, worms were picked on to EdU, washed off in PBS, dissected, and fixed for < 5 minutes in 3% paraformaldehyde/ /0.1 M K_2HPO_4 (pH 7.2) at room temperature. Germlines were taken through the normal antibody staining protocol, including DAPI-staining, followed by the Click-IT EdU reaction, performed according to the manufacturer's instructions (Molecular Probes, Cat#A10027).

Image capture and processing

Fluoresence micrographs were taken on a Zeiss compound microscope using AxioPlan 2.0 imaging software and Hamamatsu camera. Each dissected and stained gonad was captured as a montage, with overlapping cell boundaries. The montages were then assembled in Adobe Photoshop CS3 and processed identically. The boundary of each montage was processed using a feather tool of 20 pixels for each image.

Confocal images were captured on a Perkin Elmer Ultraview Confocal Microscope using a z-step of 1 micron. Where stated, multiple slices were assembled into an extended focus image using Volocity image analysis software.

Construction of transgenes and generation of transgenics

To create the initial METT-10::GFP construct, the entire METT-10 genomic region, including 1.6 kb upstream and 1.9 kb downstream of the METT-10 coding region was amplified as two PCR products meeting at the translational stop using KOD DNA polymerase (Novagen, Cat # 71086), using the following primers: [5' region: ATTA- NotI- GCGTCGTAGCCTGTGTTCAATTCC (F) and ATTA-BamHI-TCGGCATATTAAATTTTTCAAATACTGCACTAG (R)] and [3' region: ATTA-BamHI-TAAATAGCATAATTTTATTTATTCAATATTTATACC (F) and ATTA-NotI- GGATACTGTATGTACAACTGATCTCTGAGC (R)]. This 5.5 kb region includes parts, but not all, of the adjacent genes. These fragments were digested with BamHI and NotI and ligated in a three-part ligation with NotI digested-pMM016 (Praitis *et al*., 2001), a plasmid containing the *unc-119*+ transformation marker, to create pMM016(*mett-10*+). GFP(ivs):FLAG was amplified from (pPD115.70, gift of Andrew Fire) and cloned into pMM016(*mett-10*+) using the BamHI site. Proper orientation was determined by PCR, and the entirety of the *mett-10* region was sequenced to confirm integrity. To create low-copy integrated transgenic lines, the microparticle bombardment method was used (Praitis *et al*., 2001).

Mosaic analysis

To generate arrays for mosaic analysis, pMM016 [*mett-10+*] was co-injected with pTG96 [*sur-5::gfp]* (gift of Min Han's lab) at concentrations of 20ng/ul and 80ng/ul, respectively. These arrays were crossed into *smg-2(e2008); mett-10(oz36)* worms. Green animals were cloned individually at the L4 stage. After 2.5 days, plates were screened for animals with green embryos or progeny to determine if the array had passed through the germline. Animals were segregated based on germline transmission, germlines were dissected, fixed briefly for 10' in 3% paraformaldehyde to preserve GFP fluorescence, DAPI stained, and mounted for scoring of germline phenotype and GFP distribution.

ACKNOWLEDGEMENTS

The work described in this chapter includes that of Tim Schedl, who isolated the *mett-10(oz36)* mutant and Bethany Westlund, who identified *g38* as a *mett-10* allele, cloned *mett-10*, and carried out initial phenotypic analysis and epistasis with *glp-1*. This majority of chapter will be published in *Genetics* as the following citation: Maia Dorsett, Bethany Westlund, and Tim Schedl. METT-10, a putative methyltransferase, inhibits germ cell proliferative fate in *Caenorhabditis elegans*.

I'd like to thank the *Caenorhabditis* Genetics Center, the Japanese National Bioresource Project, the *C. elegans* gene knockout consortium, and Randall Cassada for strains, and the Structural Genomics Consortium for making the crystal structure of human METT10D freely accessible. I thank Momoyo Hanazawa for constructing the *glp-1(oz264) mett-10(g38)* strain, and Jim Collins for help with injections for mosaic analysis. I extend my sincerest thanks to Swathi Arur, Dale Dorsett, Kevin O'Connell, Jim Skeath, Paul Fox, Justin Fay, and Mike Nonet for experimental suggestions, provisions of reagents, or comments on this manuscript.

REFERENCES

Austin, J., and Kimble, J. (1987). glp-1 is required in the germ line for regulation of the decision between mitosis and meiosis in C. elegans. Cell *51*, 589-599.

Berry, L.W., Westlund, B., and Schedl, T. (1997). Germ-line tumor formation caused by activation of glp-1, a Caenorhabditis elegans member of the Notch family of receptors. Development *124*, 925-936.

Brenner, S. (1974). The genetics of Caenorhabditis elegans. Genetics *77*, 71-94.

Cassada, R., Isnenghi, E., Culotti, M., and von Ehrenstein, G. (1981). Genetic analysis of temperature-sensitive embryogenesis mutants in Caenorhabditis elegans. Dev Biol *84*, 193-205.

Crittenden, S.L., Eckmann, C.R., Wang, L., Bernstein, D.S., Wickens, M., and Kimble, J. (2003). Regulation of the mitosis/meiosis decision in the Caenorhabditis elegans germline. Philos Trans R Soc Lond B Biol Sci *358*, 1359-1362.

Dong, A., Yoder, J.A., Zhang, X., Zhou, L., Bestor, T.H., and Cheng, X. (2001). Structure of human DNMT2, an enigmatic DNA methyltransferase homolog that displays denaturant-resistant binding to DNA. Nucleic Acids Res *29*, 439-448.

Eckmann, C.R., Crittenden, S.L., Suh, N., and Kimble, J. (2004). GLD-3 and control of the mitosis/meiosis decision in the germline of Caenorhabditis elegans. Genetics *168*, 147-160.

Fay, D.S., and Han, M. (2000). Mutations in cye-1, a Caenorhabditis elegans cyclin E homolog, reveal coordination between cell-cycle control and vulval development. Development *127*, 4049-4060.

Francis, R., Barton, M.K., Kimble, J., and Schedl, T. (1995a). gld-1, a tumor suppressor gene required for oocyte development in Caenorhabditis elegans. Genetics *139*, 579-606.

Francis, R., Maine, E., and Schedl, T. (1995b). Analysis of the multiple roles of gld-1 in germline development: interactions with the sex determination cascade and the glp-1 signaling pathway. Genetics *139*, 607-630.

Gartner, A., Milstein, S., Ahmed, S., Hodgkin, J., and Hengartner, M.O. (2000). A conserved checkpoint pathway mediates DNA damage--induced apoptosis and cell cycle arrest in C. elegans. Mol Cell *5*, 435-443.

Hansen, D., Hubbard, E.J., and Schedl, T. (2004a). Multi-pathway control of the proliferation versus meiotic development decision in the Caenorhabditis elegans germline. Dev Biol *268*, 342-357.

Hansen, D., and Schedl, T. (2006). The regulatory network controlling the proliferation-meiotic entry decision in the Caenorhabditis elegans germ line. Curr Top Dev Biol *76*, 185-215.

Hansen, D., Wilson-Berry, L., Dang, T., and Schedl, T. (2004b). Control of the proliferation versus meiotic development decision in the C. elegans germline through regulation of GLD-1 protein accumulation. Development *131*, 93-104.

Henderson, S.T., Gao, D., Lambie, E.J., and Kimble, J. (1994). lag-2 may encode a signaling ligand for the GLP-1 and LIN-12 receptors of C. elegans. Development *120*, 2913-2924.

Hodgkin, J., Papp, A., Pulak, R., Ambros, V., and Anderson, P. (1989). A new kind of informational suppression in the nematode Caenorhabditis elegans. Genetics *123*, 301-313.

Hubbard, E.J., Wu, G., Kitajewski, J., and Greenwald, I. (1997). sel-10, a negative regulator of lin-12 activity in Caenorhabditis elegans, encodes a member of the CDC4 family of proteins. Genes Dev *11*, 3182-3193.

Jones, A.R., Francis, R., and Schedl, T. (1996). GLD-1, a cytoplasmic protein essential for oocyte differentiation, shows stage- and sex-specific expression during Caenorhabditis elegans germline development. Dev Biol *180*, 165-183.

Kadyk, L.C., and Kimble, J. (1998). Genetic regulation of entry into meiosis in Caenorhabditis elegans. Development *125*, 1803-1813.

Kauffman, T., Tran, J., and DiNardo, S. (2003). Mutations in Nop60B, the Drosophila homolog of human dyskeratosis congenita 1, affect the maintenance of the germ-line stem cell lineage during spermatogenesis. Dev Biol *253*, 189-199.

Kennedy, S., Wang, D., and Ruvkun, G. (2004). A conserved siRNA-degrading RNase negatively regulates RNA interference in C. elegans. Nature *427*, 645-649.

Kerins, J. (2006). PRP-17 and the pre-mRNA splicing pathway are preferentially required for the proliferation versus meiotic development decision and germline sex determination in *Caenorhabditis elegans.*, Washington University Saint Louis, MO.

Killian, D.J., and Hubbard, E.J. (2004). C. elegans pro-1 activity is required for soma/germline interactions that influence proliferation and differentiation in the germ line. Development *131*, 1267-1278.

Kimble, J., and Crittenden, S.L. (2007). Controls of germline stem cells, entry into meiosis, and the sperm/oocyte decision in Caenorhabditis elegans. Annu Rev Cell Dev Biol *23*, 405-433.

Koch, U., and Radtke, F. (2007). Notch and cancer: a double-edged sword. Cell Mol Life Sci *64*, 2746-2762.

Kodoyianni, V., Maine, E.M., and Kimble, J. (1992). Molecular basis of loss-of-function mutations in the glp-1 gene of Caenorhabditis elegans. Mol Biol Cell *3*, 1199-1213.

Korolev, S., Ikeguchi, Y., Skarina, T., Beasley, S., Arrowsmith, C., Edwards, A., Joachimiak, A., Pegg, A.E., and Savchenko, A. (2002). The crystal structure of spermidine synthase with a multisubstrate adduct inhibitor. Nat Struct Biol *9*, 27-31.

Krivtsov, A.V., Twomey, D., Feng, Z., Stubbs, M.C., Wang, Y., Faber, J., Levine, J.E., Wang, J., Hahn, W.C., Gilliland, D.G., Golub, T.R., and Armstrong, S.A. (2006). Transformation from committed progenitor to leukaemia stem cell initiated by MLL-AF9. Nature *442*, 818-822.

Lamont, L.B., Crittenden, S.L., Bernstein, D., Wickens, M., and Kimble, J. (2004). FBF-1 and FBF-2 regulate the size of the mitotic region in the C. elegans germline. Dev Cell *7*, 697-707.

Lee, M.H., Ohmachi, M., Arur, S., Nayak, S., Francis, R., Church, D., Lambie, E., and Schedl, T. (2007). Multiple functions and dynamic activation of MPK-1 extracellular signal-regulated kinase signaling in Caenorhabditis elegans germline development. Genetics *177*, 2039-2062.

Macdonald, L.D., Knox, A., and Hansen, D. (2008). Proteasomal regulation of the proliferation vs. meiotic entry decision in the Caenorhabditis elegans germ line. Genetics *180*, 905-920.

Malone, T., Blumenthal, R.M., and Cheng, X. (1995). Structure-guided analysis reveals nine sequence motifs conserved among DNA amino-methyltransferases, and suggests a catalytic mechanism for these enzymes. J Mol Biol *253*, 618-632.

Martin, J.L., and McMillan, F.M. (2002). SAM (dependent) I AM: the S-adenosylmethionine-dependent methyltransferase fold. Curr Opin Struct Biol *12*, 783-793.

McCarter, J., Bartlett, B., Dang, T., and Schedl, T. (1997). Soma-germ cell interactions in Caenorhabditis elegans: multiple events of hermaphrodite germline development require the somatic sheath and spermathecal lineages. Dev Biol *181*, 121-143.

Morrison, S.J., and Kimble, J. (2006). Asymmetric and symmetric stem-cell divisions in development and cancer. Nature *441*, 1068-1074.

Moser, S.C., von Elsner, S., Bussing, I., Alpi, A., Schnabel, R., and Gartner, A. (2009). Functional dissection of Caenorhabditis elegans CLK-2/TEL2 cell cycle defects during embryogenesis and germline development. PLoS Genet *5*, e1000451.

Mumm, J.S., and Kopan, R. (2000). Notch signaling: from the outside in. Dev Biol *228*, 151-165.

O'Connell, K.F., Leys, C.M., and White, J.G. (1998). A genetic screen for temperature-sensitive cell-division mutants of Caenorhabditis elegans. Genetics *149*, 1303-1321.

Page, M.F., Carr, B., Anders, K.R., Grimson, A., and Anderson, P. (1999). SMG-2 is a phosphorylated protein required for mRNA surveillance in Caenorhabditis elegans and related to Upf1p of yeast. Mol Cell Biol *19*, 5943-5951.

Pepper, A.S., Killian, D.J., and Hubbard, E.J. (2003). Genetic analysis of Caenorhabditis elegans glp-1 mutants suggests receptor interaction or competition. Genetics *163*, 115-132.

Praitis, V., Casey, E., Collar, D., and Austin, J. (2001). Creation of low-copy integrated transgenic lines in Caenorhabditis elegans. Genetics *157*, 1217-1226.

Qiao, L., Lissemore, J.L., Shu, P., Smardon, A., Gelber, M.B., and Maine, E.M. (1995). Enhancers of glp-1, a gene required for cell-signaling in Caenorhabditis elegans, define a set of genes required for germline development. Genetics *141*, 551-569.

Salic, A., and Mitchison, T.J. (2008). A chemical method for fast and sensitive detection of DNA synthesis in vivo. Proc Natl Acad Sci U S A *105*, 2415-2420.

Subramaniam, K., and Seydoux, G. (2003). Dedifferentiation of primary spermatocytes into germ cell tumors in C. elegans lacking the pumilio-like protein PUF-8. Curr Biol *13*, 134-139.

Sulston, J.E., Schierenberg, E., White, J.G., and Thomson, J.N. (1983). The embryonic cell lineage of the nematode Caenorhabditis elegans. Dev Biol *100*, 64-119.

Sundaram, M., and Greenwald, I. (1993). Suppressors of a lin-12 hypomorph define genes that interact with both lin-12 and glp-1 in Caenorhabditis elegans. Genetics *135*, 765-783.

Vought, V.E., Ohmachi, M., Lee, M.H., and Maine, E.M. (2005). EGO-1, a putative RNA-directed RNA polymerase, promotes germline proliferation in parallel with GLP-1/notch signaling and regulates the spatial organization of nuclear pore complexes and germline P granules in Caenorhabditis elegans. Genetics *170*, 1121-1132.

Voutev, R., Killian, D.J., Ahn, J.H., and Hubbard, E.J. (2006). Alterations in ribosome biogenesis cause specific defects in C. elegans hermaphrodite gonadogenesis. Dev Biol *298*, 45-58.

Weng, A.P., Ferrando, A.A., Lee, W., Morris, J.P.t., Silverman, L.B., Sanchez-Irizarry, C., Blacklow, S.C., Look, A.T., and Aster, J.C. (2004). Activating mutations of NOTCH1 in human T cell acute lymphoblastic leukemia. Science *306*, 269-271.

Wilson, J.J., and Kovall, R.A. (2006). Crystal structure of the CSL-Notch-Mastermind ternary complex bound to DNA. Cell *124*, 985-996.

Wu, H., Min, J., Zeng, H., Loppnau, P., Weigelt, J., Sundstrom, M., Arrowsmith, C.H., Edwards, A.M., Bochkarev, A., and Plotnikov, A.N. (To be published.). The

Crystal Structure of Human methyltransferase 10 domain containing protein. http://www.rcsb.org/pdb/explore.do?structureId=2H00.

Yochem, J., Gu, T., and Han, M. (1998). A new marker for mosaic analysis in Caenorhabditis elegans indicates a fusion between hyp6 and hyp7, two major components of the hypodermis. Genetics *149*, 1323-1334.

Yochem, J., and Herman, R.K. (2005). Genetic mosaics. WormBook, 1-6.

Table 1*: The mett-10 (oz36)* tumorous phenotype is the result of a poisonous product

Genotype	temp (˚C)	% Tum	n
mett-10(oz36)	15	72	107
mett-10(oz36)	20	41	66
mett-10(oz36)/+	15	0	64
mett-10(oz36)/+	20	0	70
ozIs7[mett-10::GFP]; oz36	15	0	76
ozIs7[mett-10::GFP]; oz36	20	0	80
mett-10(oz36)/mett-10(ok2204)	15	0	32
mett-10(oz36)/nDf40	15	0	44
smg-2(e2008); mett-10(oz36)/+	20	0	54
smg-2(e2008); mett-10(oz36)/mett-10(g38)	20	18	40
smg-2(e2008); mett-10(oz36)	20	98	80
smg-2(e2008); glp-1 (bn18) mett-10(oz36)	15	0	128
smg-2(e2008); glp-1 (bn18) mett-10(oz36)	20	0	98

Full genotypes of the mutant combinations are: *unc-32(e189) mett-10(oz36)/ nDf40 dpy-18(e364), unc-32(e189) mett-10 (oz36)/ mett-10(ok2204) dpy-18(e364), smg-2(e2008); unc-36(e251) mett-10(oz36) / unc-119 (ed3), smg-2(e2008); unc-36(e251) mett-10(oz36)/ unc-32(e189) mett-10(g38).* All animals were m+, i.e. came from mothers carrying a wild type copy of *mett-10*. Animals grown at 15˚C were scored at 3 days past L4 and animals grown at 20˚C were scored at 2 days past L4.

Table 2: Loss of *mett-10* function leads to multiple, temperature sensitive phenotypes sensitive to maternal gene dose.

genotype	m	temp	% Pvl	%Ste	% Mel	n
mett-10(oz36)	no	20	1	4	0	116
mett-10(oz36)	no	25	43	100	N.A.	103
mett-10(oz36)	yes	25	0	3	97	58
mett-10(g38)	no	20	2	7	0	59
mett-10(g38)	no	25	21	89	11	63
mett-10(g38)	yes	25	0	10	90	21
mett-10(tm2697)	no	20	10	19	0	133
mett-10(tm2697)	no	25	88	100	N.A.	142
mett-10(tm2697)	yes	25	0	2	98	60
mett-10(oj32)	no	20	0	18	0	71
mett-10(oj32)	no	25	11	100	N.A.	75
mett-10(oj32)	yes	25	0	0	100	53
mett-10(ok2204)	no	20	12	8	0	52
mett-10(ok2204)	no	25	98	99	N.A.	82
ozIs7[mett-10::GFP];mett-10(ok2204)	no	25	5	0	0	38
mett-10(ok2204)	yes	25	0	0	100	45

m= endogenous maternal gene product; Pvl= Protruding vulva; Ste = Sterile (no embryos present); Mel = maternal effect lethal (lays dead embryos). All animals were scored 1 day past the L4 stage by DIC.

Table 3: *mett-10* inhibits proliferative fate in the *C. elegans* germline

Genotype	temp(˚C)	% Tum	n
glp-1(oz264)	20	1	100
mett-10(ok2204)	15	0	54
mett-10(ok2204)	20	0	68
mett-10(oz36)	15	72	107
mett-10(oz36)	20	41	66
glp-1(oz264) mett-10(oz36)	20	100	72
mett-10(oj32)	15	0	72
mett-10(oj32)	20	0	48
glp-1(oz264) mett-10(oj32)	20	49	96
mett-10(tm2697)	15	0	68
mett-10(tm2697)	20	0	76
glp-1(oz264) mett-10(tm2697)	20	84	112
mett-10(g38)	15	0	78
mett-10(g38)	20	0	56
glp-1(oz264) mett-10(g38)	20	89	47
ozIs7[mett-10::gfp];glp-1(oz264) mett-10(g38)	20	0	56

All animals were m+, i.e. came from mothers carrying a wild type copy of *mett-10*. Animals grown at 15˚C were scored at 3 days past L4 and animals grown at 20˚C were scored at 2 days past L4.
Tumorous (Tum) includes proliferation throughout the germline, although some germ cells in various meiotic stages may be observed.

Table 4: Genetic interactions between *mett-10* and known meiotic entry genes.

genotype	% Tum	n or reference
mett-10(oz36)	41	66
*gld-1(q485)**	0	Francis et. al. (1995a)
*gld-1(q485); mett-10(oz36)**	0	21
gld-2(q497)	2	Kadyk and Kimble (1998)
gld-2(q497); mett-10(ok2204)	0	102
gld-2(q497); mett-10(oz36)	100	98
gld-2(q497); glp-1(bn18) mett-10(oz36)	0	97
*gld-2(q497); glp-1(q175) mett-10(oz36)***	0	44
gld-3(q730)	0	Eckmann et. al. (2004)
gld-3(q730); mett-10(oz36)#*	100$	47
*gld-3(q730); glp-1(q175) mett-10(oz36)***	0	28

*data from male germlines, as *gld-1(q485)* hermaphrodites have proximal proliferation due to a return to mitosis (Francis et.al, 1995a).
**homozygous for *unc-32(e189).*
All data collected at 20˚C from animals with maternal *mett-10* gene product, with the exception of *gld-3* strains (#), which make synthetic proximal proliferation tumors with *mett-10*, and do not exhibit an increase in the length of the distal proliferative zone ($).

Figure 1. *mett-10 (oz36),* a tumorous mutant. (A) A fluorescence micrograph of a dissected, DAPI-stained wild type adult *C. elegans* hermaphrodite germline, with schematic above. In the distal region proliferating germ cells (2) reside in close contact with the somatic distal tip cell (1). At the transition zone (3), germ cells enter meiosis, and proceed through meiotic prophase (4) to give rise to sperm in the L4 stage (6) and oocytes during adulthood (5). (B&C) Fluorescence micrographs of distal germlines labeled for 3 hr with EdU from (B) wild type and (C) *mett-10(oz36)* animals. White arrows mark the distal tip. (D-E) Extended focus projections of distal germlines from (D) wild type and (E) *mett-10(oz36)* animals stained for the M-phase marker phospho-histone-3 (pH3). Yellow dotted lines indicate the approximate boundary of the proliferative and transition zones. All images are from animals raised at 15˚C. Scale bar = 20 microns.

Figure 1

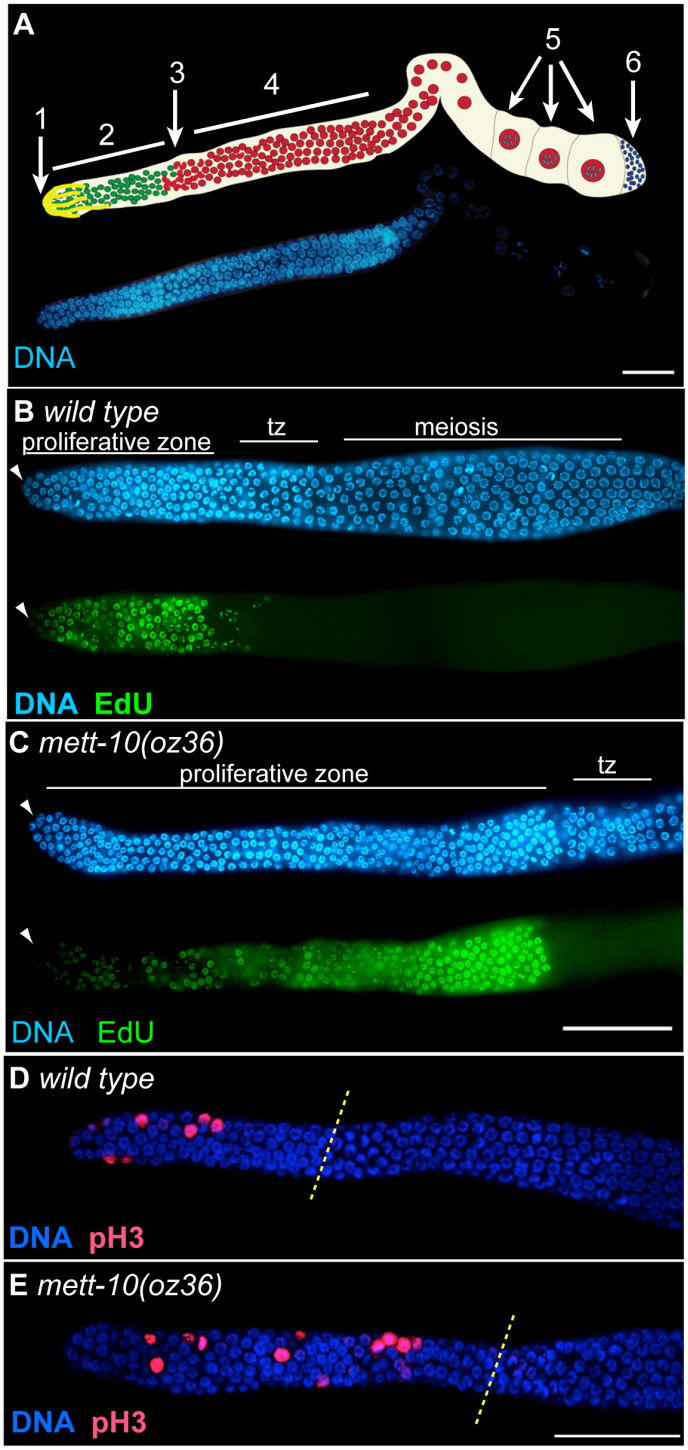
A
1
2
3
4
5
6
DNA
B wild type
proliferative zone
tz
meiosis
DNA EdU
C mett-10(oz36)
proliferative zone
tz
DNA EdU
D wild type
DNA pH3
E mett-10(oz36)
DNA pH3

Figure 2. *C. elegans* METT-10 encodes a putative methyltransferase. (A) Alignment of the methyltransferase-10 domain of *C. elegans* METT-10 (GenBank Acc# NP_499247), *H. sapiens* METT10D (GenBank Acc# NP_076991), and *X. laevis* MGC81116 (GenBank Acc# NP_001085334). The architecture of the methyltransferase domain is shown both by identification of methyltransferase motifs (Malone *et al*., 1995), as well as secondary structure predictions with α-helices in pink and ß-sheets in green (see methods). Motifs I, II, III, IV, V, and X were identified by examination of the Human METT10D N-terminal crystal structure (PDB 2H00), which did not include the region predicted to contain motifs VI and VIII (see Methods). Previous work suggests that Motifs X, I, and III are primarily responsible for binding to S-adenosyl methionine, (SAM) while Motifs IV, VI, and VIII are primarily responsible for enzyme catalysis (Malone *et al*., 1995). Red arrows show location of residues with significant contacts with SAM in the crystal structure of human METT10D. *mett-10(oj32)* mutates the contacting glycine (G110, large red arrow) in Motif I to an Arginine. This residue normal provides direct contact with the methionine group of SAM. The overall structure and ability to bind SAM appears highly conserved between orthologs, with the exception of an insertion of a predicted (*) α–helix between ß4 and a5 in *C. elegans*. Not depicted is the C-terminal half of the METT-10 protein, which may contain the target recognition domain, and is significantly less conserved between orthologs. (B) Domain architecture of METT-10 marked with protein sequence changes caused by *mett-10* alleles. Gray shading highlights the conserved methyltransferase-10 domain.

Figure 2

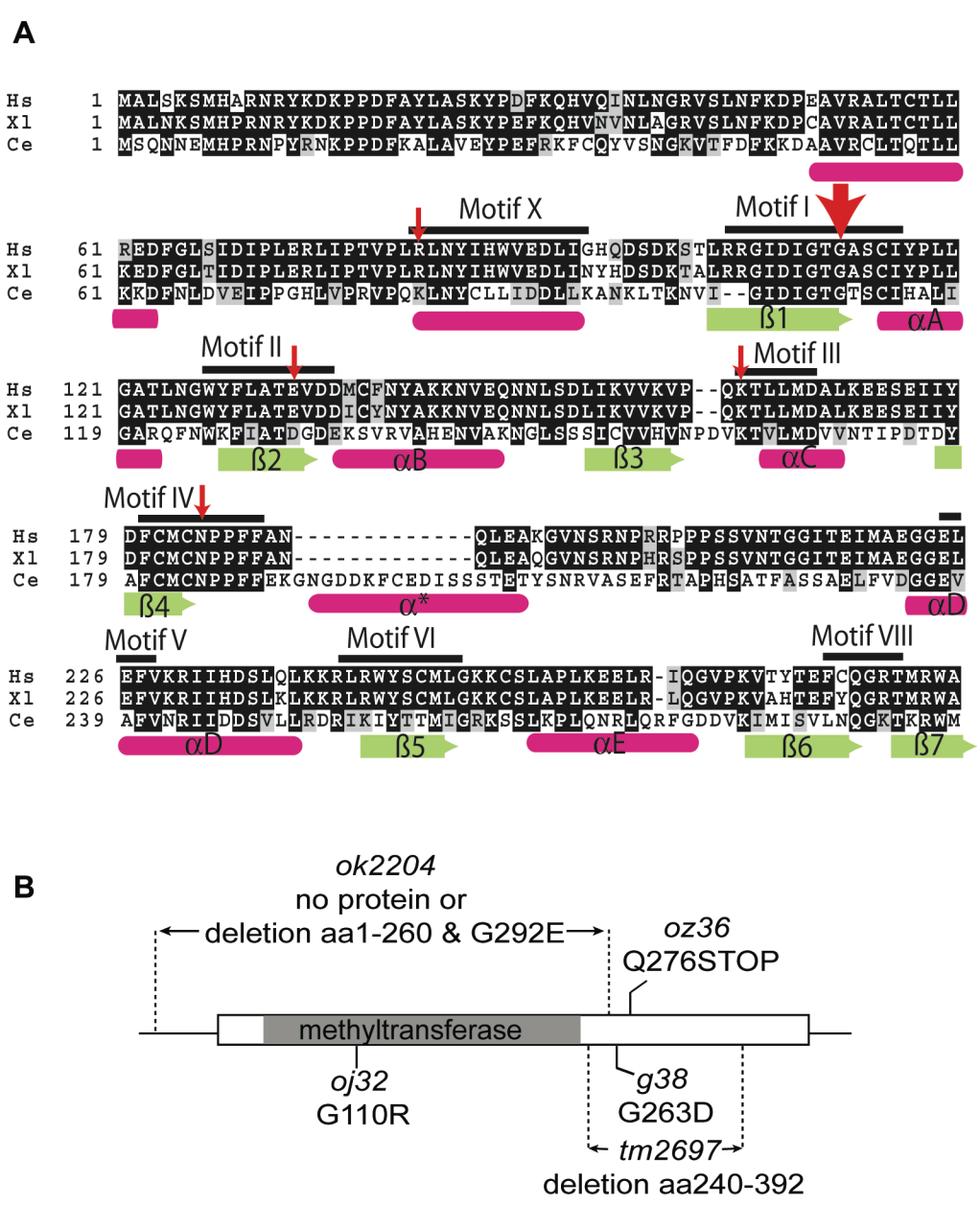
A
Hs 1 MALSKSMHARNRYKDKPPDFAYLASKYPDFKQHVQINLNGRVSLNFKDPEAVRALTCTLL
Xl 1 MALNKSMHPRNRYKDKPPDFAYLASKYPEFKQHVNVNLAGRVSLNFKDPCAVRALTCTLL
Ce 1 MSQNNEMHPRNPYRNKPPDFKALAVEYPEFRKFCQYVSNGKVTFDFKKDAAVRCLTQTLL
Motif X
Motif I
Hs 61 REDFGLSIDIPLERLIPTVPLRLNYIHWVEDLIGHQDSDKSTLRRGIDIGTGASCIYPLL
Xl 61 KEDFGLTIDIPLERLIPTVPLRLNYIHWVEDLINYHDSDKTALRRGIDIGTGASCIYPLL
Ce 61 KKDFNLDVEIPPGHLVPRVPQKLNYCLLIDDLLKANKLTKNVI--GIDIGTGTSCIHALI
ß1
αA
Motif II
Motif III
Hs 121 GATLNGWYFLATEVDDMCFNYAKKNVEQNNLSDLIKVVKVP--QKTLLMDALKEESEIIY
Xl 121 GATLNGWYFLATEVDDICYNYAKKNVEQNNLSDLIKVVKVP--QKTLLMDALKEESEIIY
Ce 119 GARQFNWKFIATDGDEKSVRVAHENVAKNGLSSSICVVHVNPDVKTVLMDVVNTIPDTDY
ß2
αB
ß3
αC
Motif IV
Hs 179 DFCMCNPPFFAN----------QLEAKGVNSRNPRRPPPSSVNTGGITEIMAEGGEL
Xl 179 DFCMCNPPFFAN----------QLEAQGVNSRNPHRSPPSSVNTGGITEIMAEGGEL
Ce 179 AFCMCNPPFFEKGNGDDKFCEDISSSTETYSNRVASEFRTAPHSATFASSAELFVDGGEV
ß4
α*
αD
Motif V
Motif VI
Motif VIII
Hs 226 EFVKRIIHDSLQLKKRLRWYSCMLGKKCSLAPLKEELR-IQGVPKVTYTEFCQGRTMRWA
Xl 226 EFVKRIIHDSLKLKKRLRWYSCMLGKKCSLAPLKEELR-LQGVPKVAHTEFYQGRTMRWA
Ce 239 AFVNRIIDDSVLLRDRIKIYTTMIGRKSSLKPLQNRLQRFGDDVKIMISVLNQGKTKRWM
αD
ß5
αE
ß6
ß7
B
ok2204
no protein or
deletion aa1-260 & G292E
oz36
Q276STOP
methyltransferase
oj32
G110R
g38
G263D
tm2697
deletion aa240-392

Figure 3: Loss of *mett-10* function causes multiple temperature-sensitive somatic defects. Vulva of (A) wild-type (B) *mett-10(oz36)* and (C) *mett-10(ok2204)* animals raised at 25˚C. *mett-10* mutants have the protruding vulva (Pvl) phenotype (arrow). (D) A normal posterior region of intestine in a wild-type animal. White arrows mark the borders of the intestinal lumen. (E) *mett-10(oz36)* and (F) *mett-10(ok2204)* animals raised at 25˚C have distended intestinal lumens containing visible bacteria. (G-H) Phenotypes of progeny of *smg-2(e2008); mett-10(oz36)* animals at 20˚C. (G) Most embryos arrest during late embryonic development with visible vacuoles (black arrows), (H) embryos are often abnormal in size (see small embryo on left), and (I) the progeny that do hatch arrest shortly after with visible abnormalities (e.g. white arrow).

Figure 3

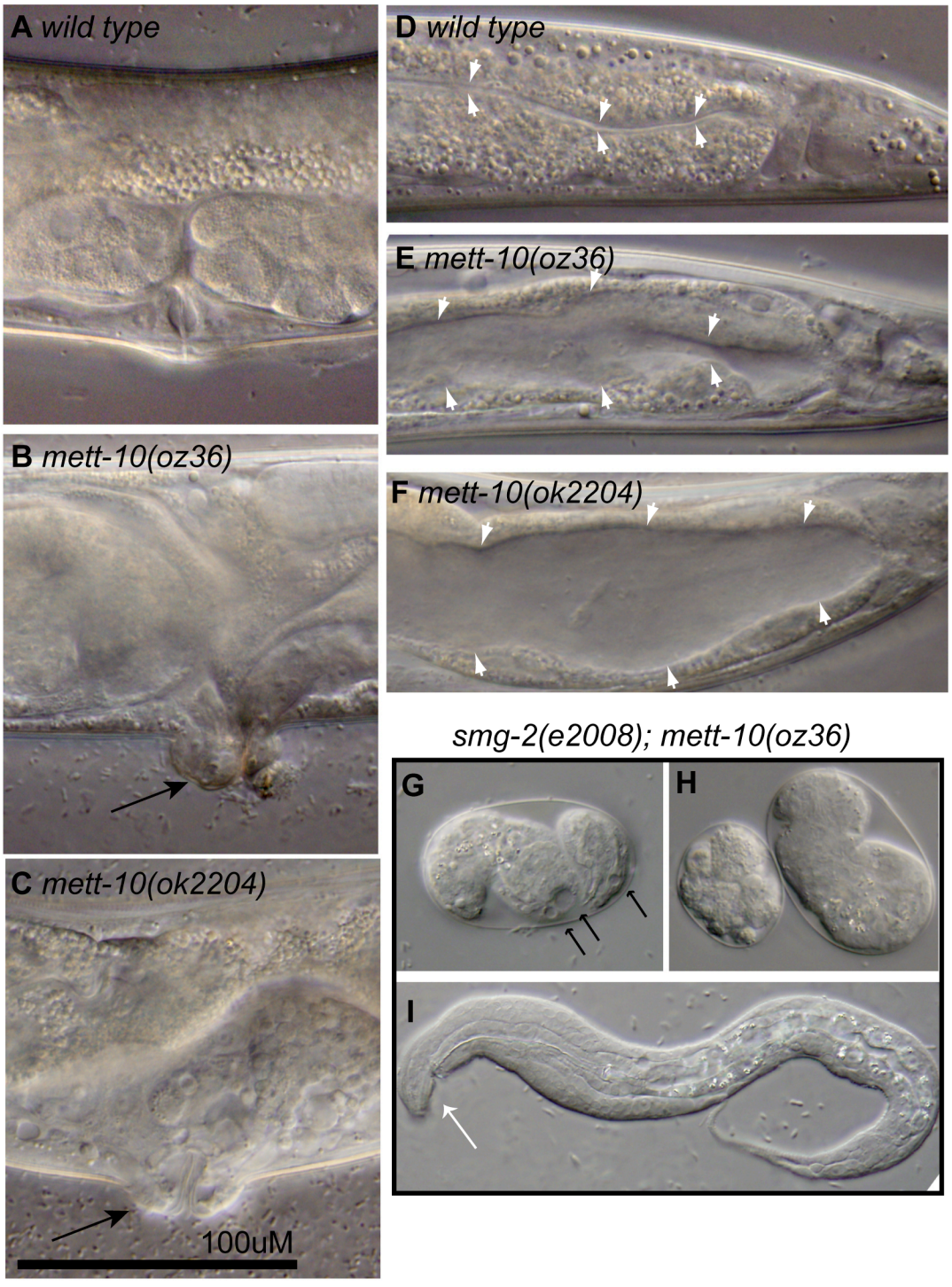
A wild type
B mett-10(oz36)
C mett-10(ok2204)
100uM
D wild type
E mett-10(oz36)
F mett-10(ok2204)
smg-2(e2008); mett-10(oz36)
G
H
I

Figure 4: Germline phenotypes of *mett-10(ok2204)*. (A) A one micron confocal slice of the distal end of a wild type germline stained with the meiotic marker GLD-1. (B) Confocal slices of representative distal germlines from *mett-10(ok2204) m-z-* animals raised at 25˚C and stained with an antibody against GLD-1. Phenotypes range from small distal regions containing abnormally large nuclei (white arrows) to gross morphological abnormalities with multiple gonadal protrusions (larger yellow arrows). Many of the protrusions stain with the meiotic marker GLD-1, suggesting that they are often filled with meiotic cells and do not represent duplications of the distal tip. These gonad abnormalities are not observed for any *mett-10* allele at 15˚C. (C) A confocal slice of a wild type germline labeled with EdU for 4 hours at 15˚C and stained with anti-phosphohistone-3 to mark cells in M-phase. With 4 hours of labeling, essentially all cells within the proliferative zone are labeled. (D) A *mett-10(ok2204)* germline labeled with EdU for 4 hours at 15˚C and stained for phospho-histone-3. Large, diffuse nuclei are visible in the distal region (white arrows); these cells do not label with EdU in this time period and do not appear to be in M-phase (absent for pH3). (E) Fluorescence micrograph of a wild type proximal germline stained with an antibody against lamin to visualize oocyte nuclear positions. Wild type animals produce a single row of oocytes. (F) The proximal germline of a *mett-10(ok2204)* animal shifted from 20˚C to 25˚ for 2 days as an L4. Disorganization of the oocytes and abnormal chromosomal morphology are visible. All scale bars = 20 microns.

Figure 4

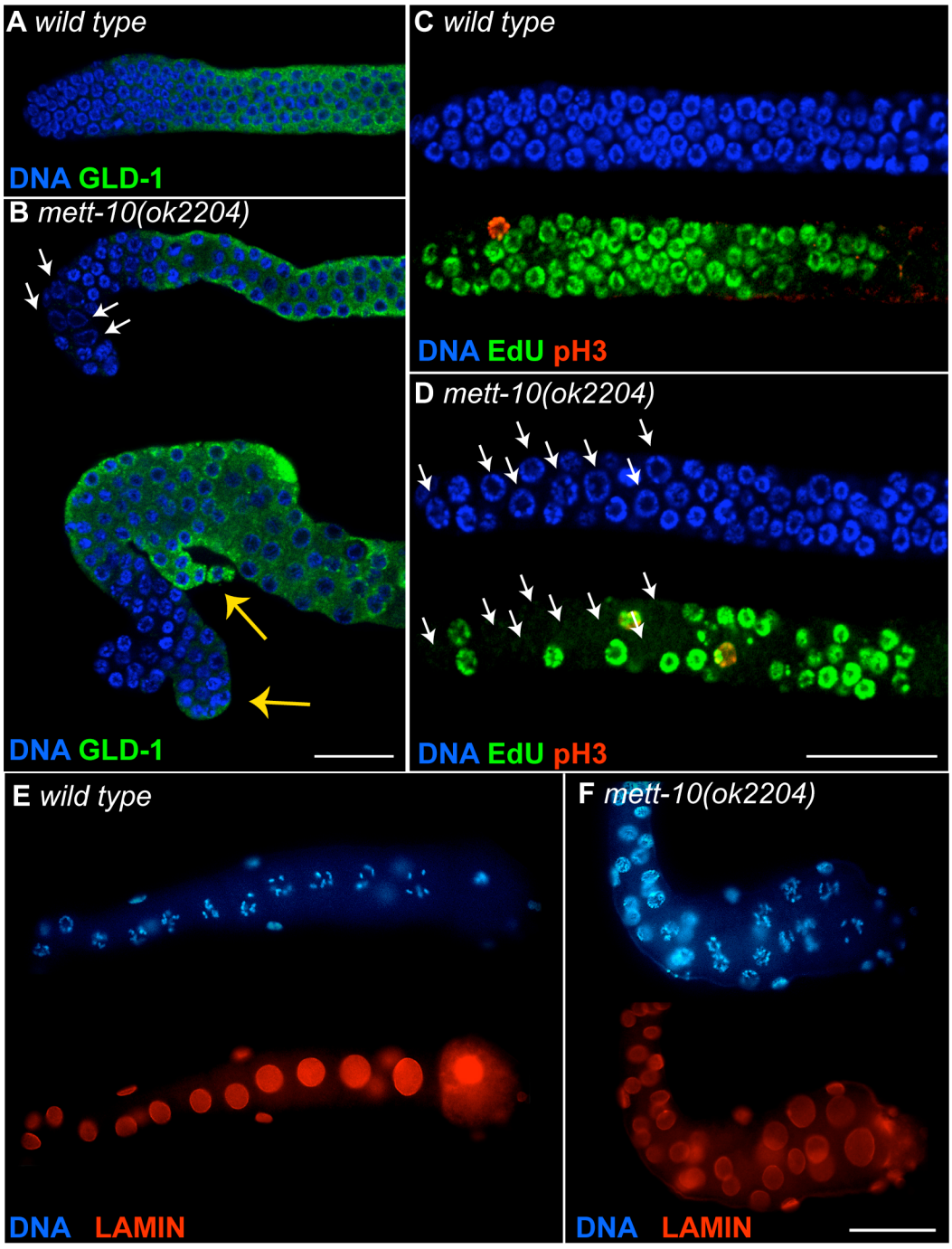
A wild type
DNA GLD-1
B mett-10(ok2204)
DNA GLD-1
C wild type
DNA EdU pH3
D mett-10(ok2204)
DNA EdU pH3
E wild type
DNA LAMIN
F mett-10(ok2204)
DNA LAMIN

Figure 5

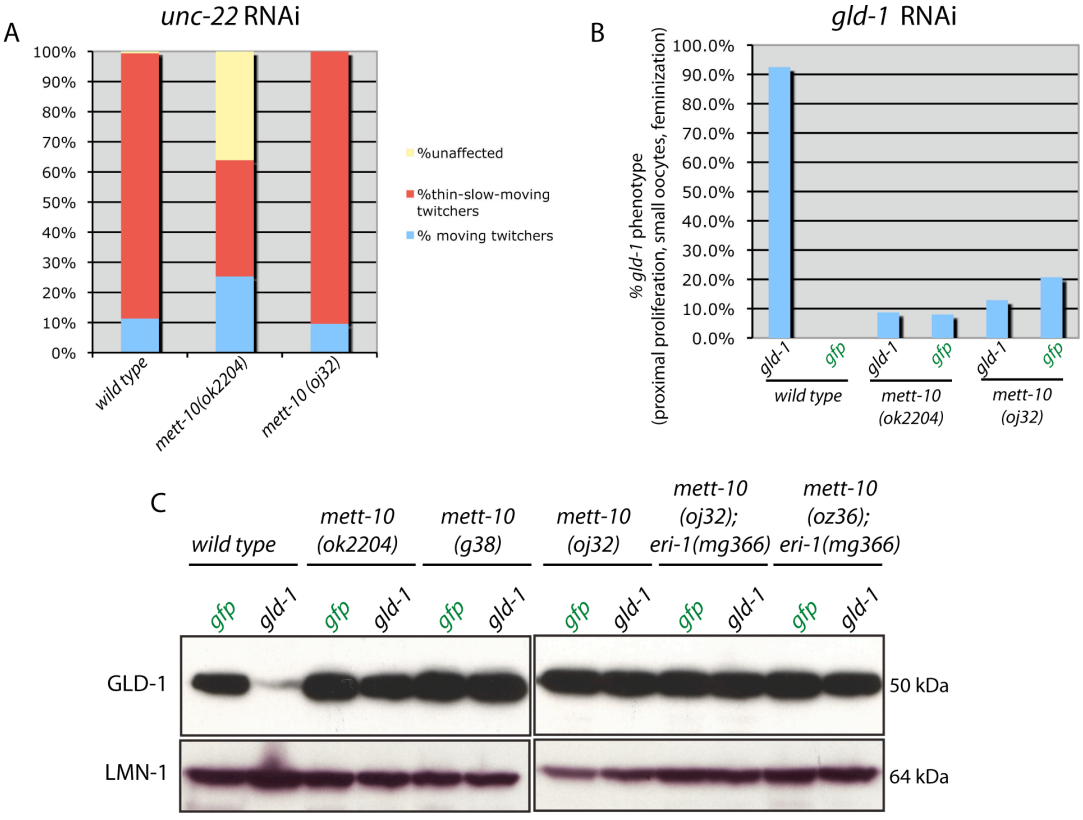

Figure 5: *mett-10* disruption causes germ line RNAi resistance. (A) Effect of feeding RNAi directed against the somatic gene *unc-22*. Strong *unc-22* knockdown causes partial paralysis and the "twitching" phenotype. (B) Effect of feeding RNAi directed against the germ line-specific gene, *gld-1*. (C) Quantitation of degree of GLD-1 knock down with Western analysis. The *eri-1(mg366)* "enhanced RNAi" mutant does not suppress the *mett-10* RNAi resistance phenotype.

Figure 6: *mett-10(oz36)* overproliferation is *glp-1* dependent. Fluoresence micrographs of germlines stained with DAPI to visualize DNA morphology (blue) and for the meiotic marker GLD-1 (green). (A, A') in wild-type hermaphrodites, GLD-1 levels increase as germ cells enter meiosis and decrease as they transition from pachytene to diplotene (Jones *et al*., 1996). (B, B') homozygous *mett-10(oz36)* animals raised at 15˚C exhibit a late-onset tumorous phenotype, as evidenced by an increase in length of the distal proliferative zone and a spatial delay in GLD-1 accumulation. (C, C') Disruption of nonsense-mediated mRNA decay with a mutation in *smg-2* significantly enhances the penetrance (Table 1) and degree of tumor formation of *mett-10(oz36)* at 20˚C resulting in germlines containing proliferating cells throughout. (D, D') At the permissive temperature of 20˚C, *glp-1(bn18)* hypomorphic temperature-sensitive mutants have only slight reductions in distal proliferative zone size. (E, E') *glp-1(bn18)* fully suppresses the tumorous phenotype of *smg-2(e2008); mett-10(oz36)* animals at 20˚C. Scale bar = 20 microns.

Figure 6

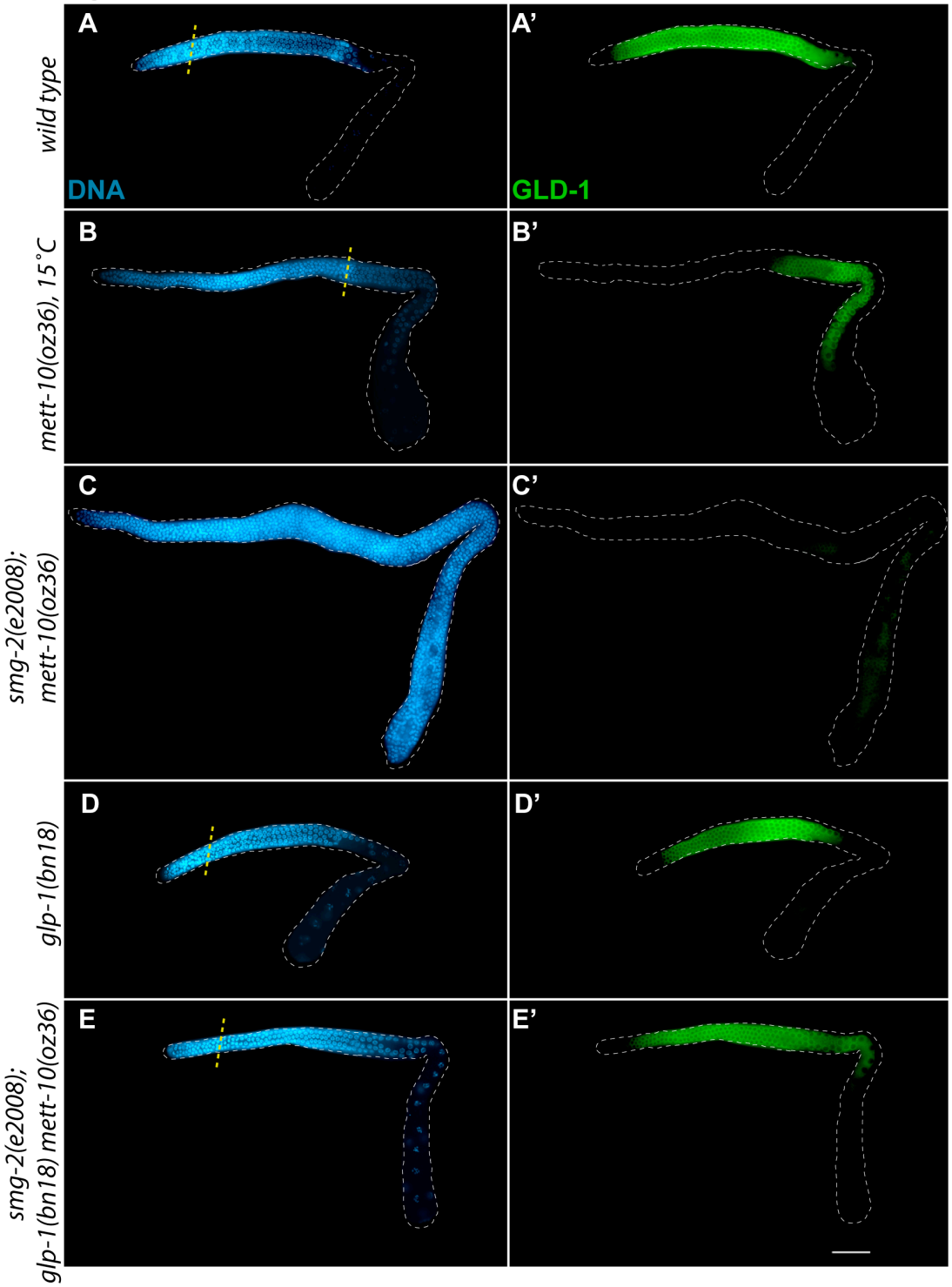
A
A'
wild type
DNA
GLD-1
B
B'
mett-10(oz36), 15˚C
C
C'
smg-2(e2008); mett-10(oz36)
D
D'
glp-1(bn18)
E
E'
smg-2(e2008); glp-1(bn18) mett-10(oz36)

Figure 7. *mett-10(g38)* suppresses the temporal dynamics of premature meiotic entry in *glp-1(bn18).* (A-I) Extended focus projections of distal germ lines stained with DAPI to visualize DNA (blue) and for the M-phase marker phospho-histone-3 (pH3) (red). White dotted lines indicate the approximate boundary between the proliferative and transition zones as defined by DNA morphology. (A-D) wild-type and *mett-10(g38)* animals have similar proliferative zone size and number of pH3-positive nuclei at 20˚C, and exhibit small decreases in the number of pH3-positive nuclei upon a six hour shift to 25˚C. (E-F) Upon a six hour shift to 25˚C, no pH3-positive nuclei can be found in *glp-1(bn18)*. (G-H) After a six hour shift to 25˚C, *glp-1(bn18) mett-10(g38)* germ lines still contain pH3- positive nuclei and retain a longer proliferative zone than *glp-1(bn18)* alone. (I). After an 18 hour shift to 25˚C, no pH3-positive nuclei can be found in *glp-1(bn18) mett-10(g38)* germ lines and nuclear morphology is consistent with all cells entering meiosis with transition zone nuclei located immediately adjacent to the distal tip (white arrow). (J) Quantification of A-H. Scale bar = 20 microns.

Figure 7

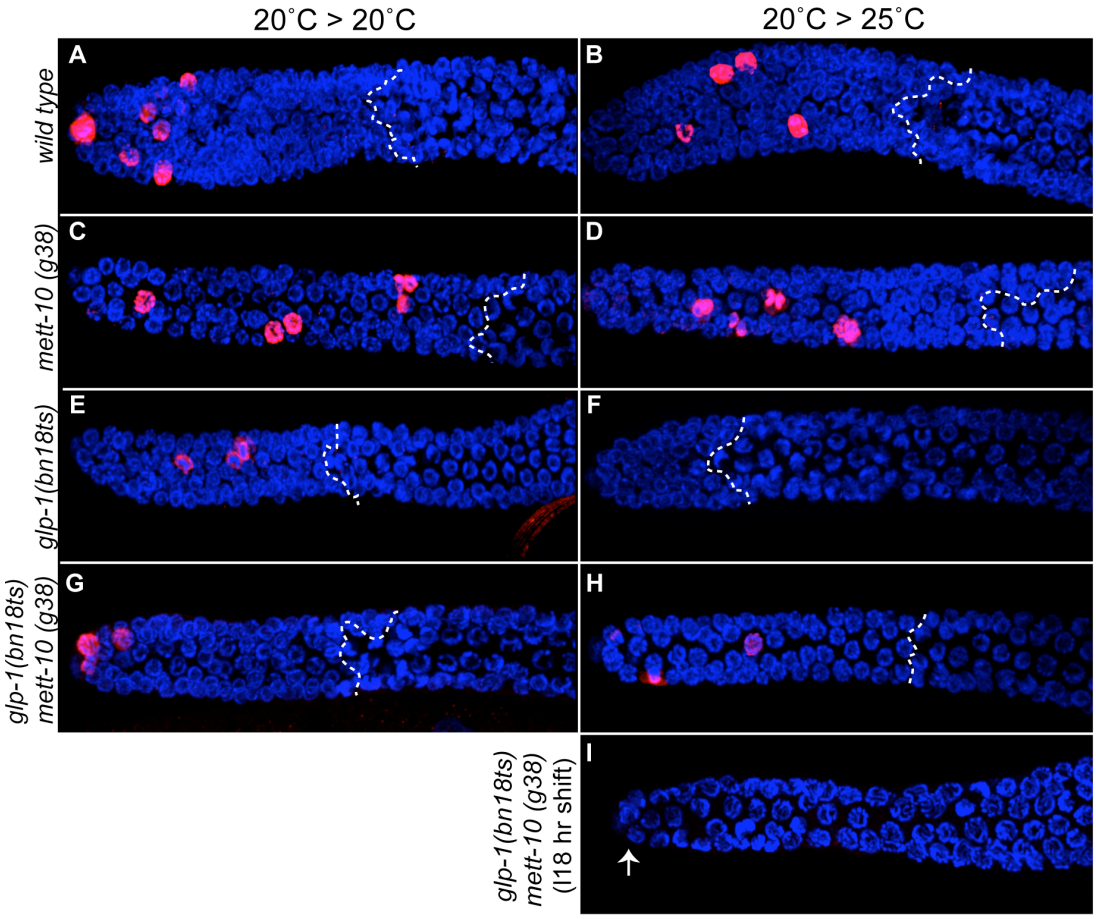
20˚C > 20˚C
20˚C > 25˚C
A
B
wild type
C
D
mett-10 (g38)
E
F
glp-1(bn18ts)
G
H
glp-1(bn18ts)
mett-10 (g38)
I
glp-1(bn18ts)
mett-10 (g38)
(l18 hr shift)
J
pH3-positive nuclei after six hour shift
0
1
2
3
4
5
6
7
8
n=13
n=14
n=13
n=19
n=44
n=37
n=41
n=54
wt 20˚C>20˚C
wt 20˚C>25˚C
mett-10(g38) 20˚C>20˚C
mett-10(g38) 20˚C>25˚C
glp-1(bn18) 20˚C>20˚C
glp-1(bn18) 20˚C>25˚C
glp-1(bn18) mett-10(g38) 20˚C>20˚C
glp-1(bn18) mett-10(g38) 20˚C>25˚C

Figure 8: *glp-1* activity is epistatic to *gld-2(q497); mett-10(oz36)* synthetic tumors. (A) Simultaneous removal of *gld-2* and *mett-10* function does not cause germ line tumors, but animals are sterile consistent with the meiotic defects seen in *gld-2(q497)* mutants alone (Kadyk and Kimble, 1998). (B) The *mett-10(oz36)* allele does form synthetic tumors with the *gld-2* null. (C) *gld-2(q497); mett-10(oz36)* tumors are suppressed by a weak *glp-1* loss-of-function allele, *glp-1(bn18)*.

Figure 8

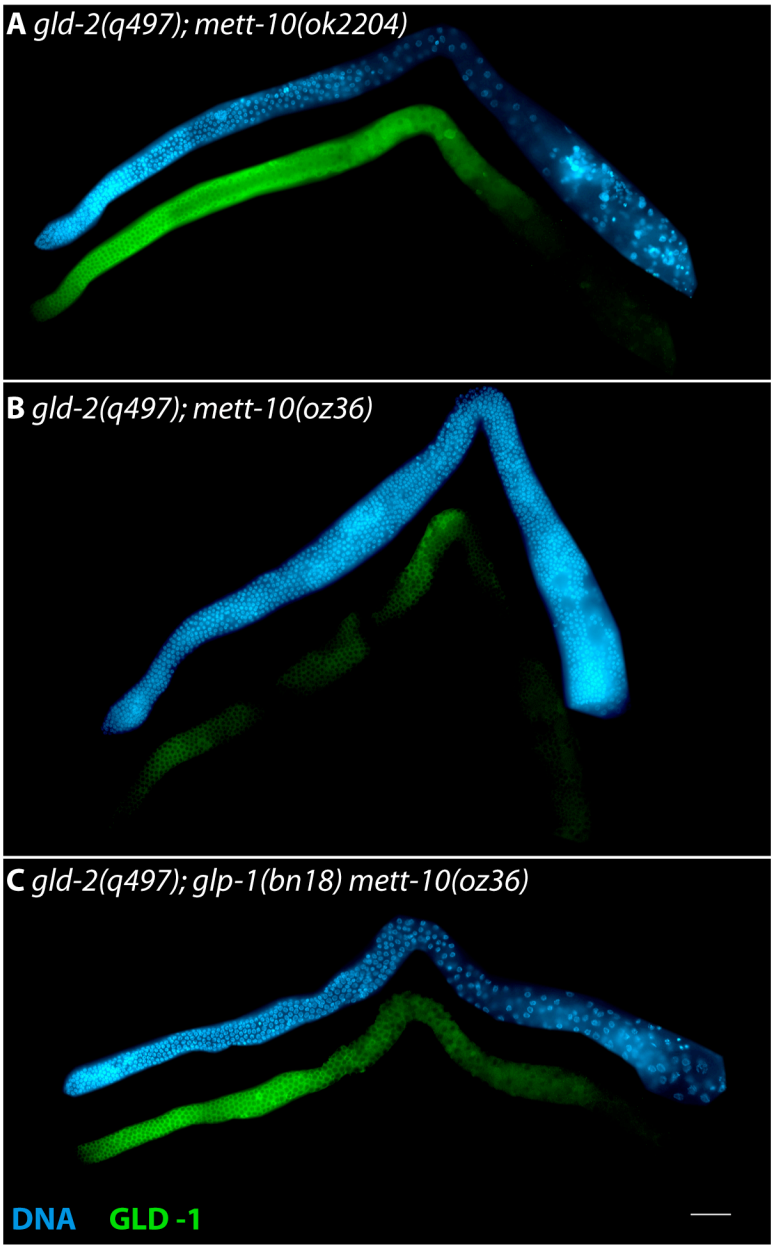
A gld-2(q497); mett-10(ok2204)
B gld-2(q497); mett-10(oz36)
C gld-2(q497); glp-1(bn18) mett-10(oz36)
DNA
GLD -1

Figure 9

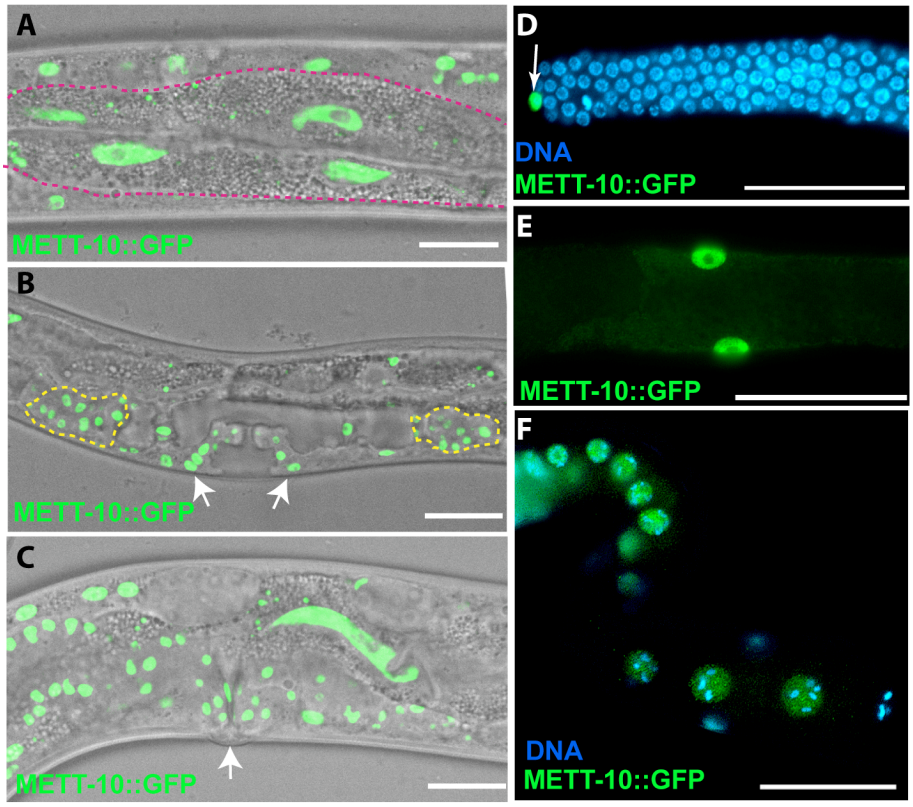

Figure 9. METT-10::GFP is a nuclear protein expressed in multiple cell types. (A-C) Imaging of METT-10::GFP in live animals. (A) METT-10::GFP can be seen in intestinal nuclei (intestine delineated by dashed line), (B) in the developing vulval epithelium (white arrows; seen here at L4 stage), spermatheca (yellow dotted lines) and (C) the adult vulva. (D-G) Fluorescence micrographs of METT-10::GFP expression in the somatic gonad and germ line. METT-10::GFP is expressed in (D) sheath cell nuclei, (E) the distal tip cell (white arrow), and (F) oocyte nuclei. Scale bar = 20 microns.

Figure 10. The pattern of METT-10::GFP accumulation in the distal germ line is altered in *glp-1* mutants. METT-10::GFP in the distal germ line. Proliferating germ cells were labeled with a 3 hr pulse of EdU (red). METT-10::GFP (green) accumulates in nuclei as cells enter meiosis, although some faint staining is also observed in some proliferative nuclei. (B) A 6 hour shift of *glp-1(bn18)* animals to 25˚C results in almost all germ cells entering meiosis, and a concomitant shift in the pattern of METT-10 accumulation. (C) *glp-1(ar202gf)* animals shifted for a day to 25˚C at the L4 stage form germ line tumors. Increased distal METT-10 is also observed in many of these animals, although "low METT-10" patches are also observed (regions encircled by white dotted lines). Scale bar = 20 microns.

Figure 10

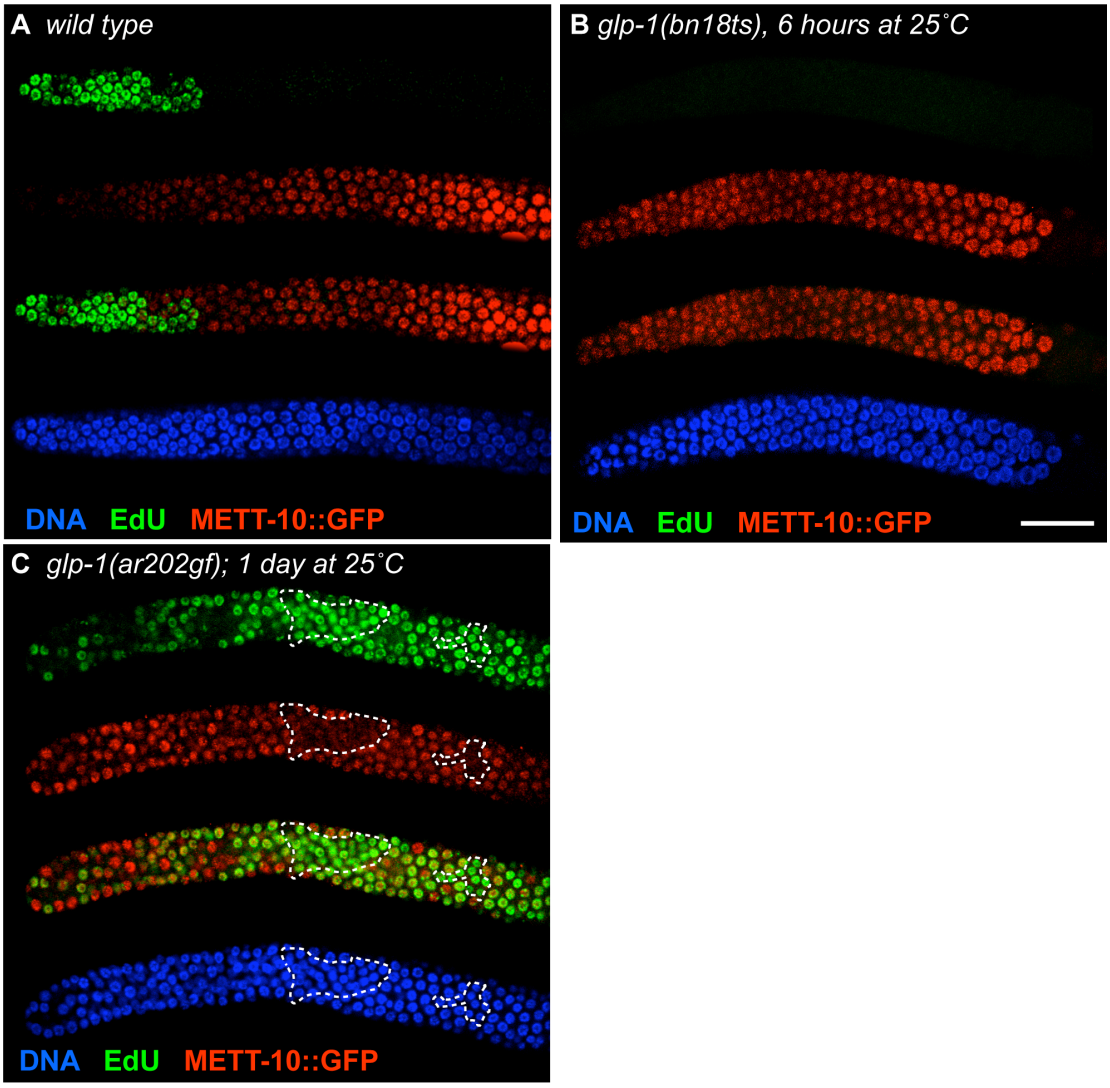
A wild type
DNA EdU METT-10::GFP
B glp-1(bn18ts), 6 hours at 25˚C
DNA EdU METT-10::GFP
C glp-1(ar202gf); 1 day at 25˚C
DNA EdU METT-10::GFP

Figure 11

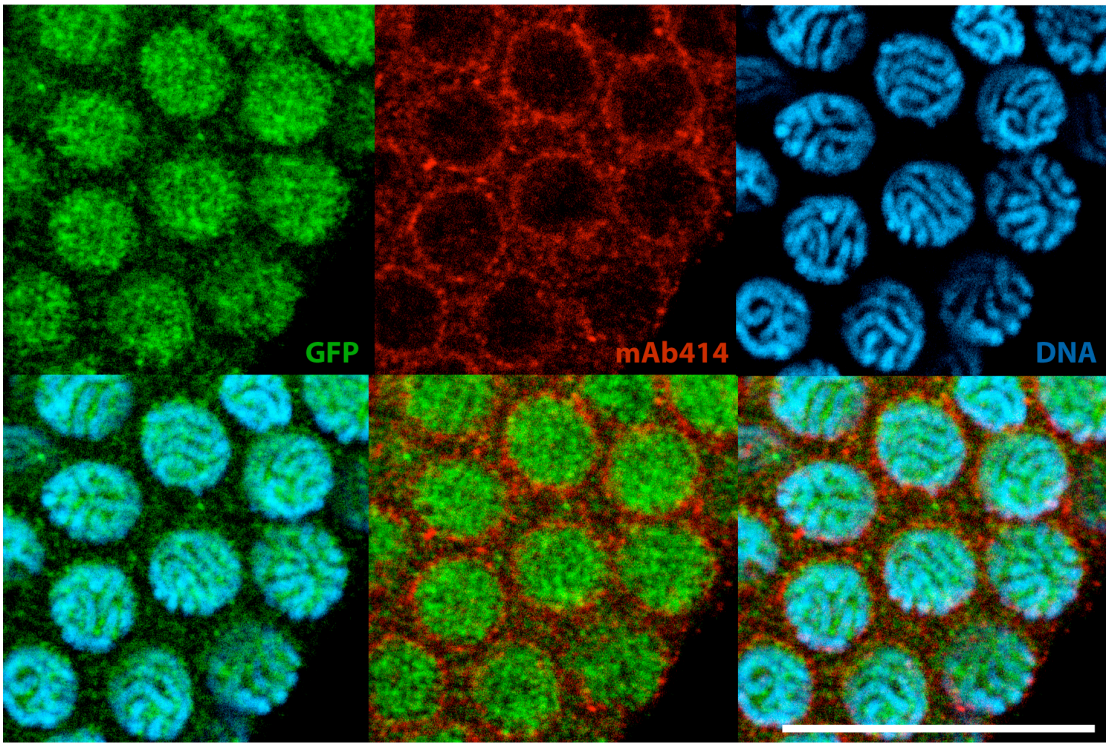

Figure 11: METT-10 is nuclear protein that does not colocalize with DNA. Confocal slices of germ cells in meiotic pachytene expressing METT-10::GFP and stained with mAB414 (which marks the nuclear pore, RED), anti-GFP (GREEN), and DAPI (BLUE) to visualize nuclear morphology. Overlays show that METT-10::GFP localizes predominantly within the nucleus, but does not overlap with the DNA. Scale bar = 20 mi

Figure 12. *mett-10* acts in the germ line to inhibit proliferative fate. To determine the focus of METT-10 action in proliferative fate decisions, we carried out mosaic analysis. A GFP - marked extrachromosomal array *ozEx63* was generated by co-injection of a plasmid containing *sur-5::gfp* (Yochem *et al*., 1998) and a plasmid containing *pmett-10:mett-10(+)*. The array was crossed into the *smg-2 (e2008); mett-10 (oz36)* background. Animals were individually scored for presence of the array in the germ line (presence in progeny), cells of the somatic gonad (gonadal sheath and distal tip cell), and the intestine. Location of array loss within the lineage was inferred by the absence of GFP in all scored tissues descending from a given cell. Germ lines were dissected, DAPI stained, and scored as Tumorous or Not Tumorous. Green circle indicates presence of array, while open circle indicates absence. Loss of the rescuing array in the germ line lineage results in a failure to suppress the fully penetrant tumorous phenotype of the *smg-2 (e2008); mett-10 (oz36)* double mutant, while loss in the somatic gonad is tolerated. One animal had one tumorous germ line and one non-tumorous germ line, both with GFP+ somatic gonads. We infer that this is likely a later loss in one of the germ line precursors Z2 or Z3.

Figure 12

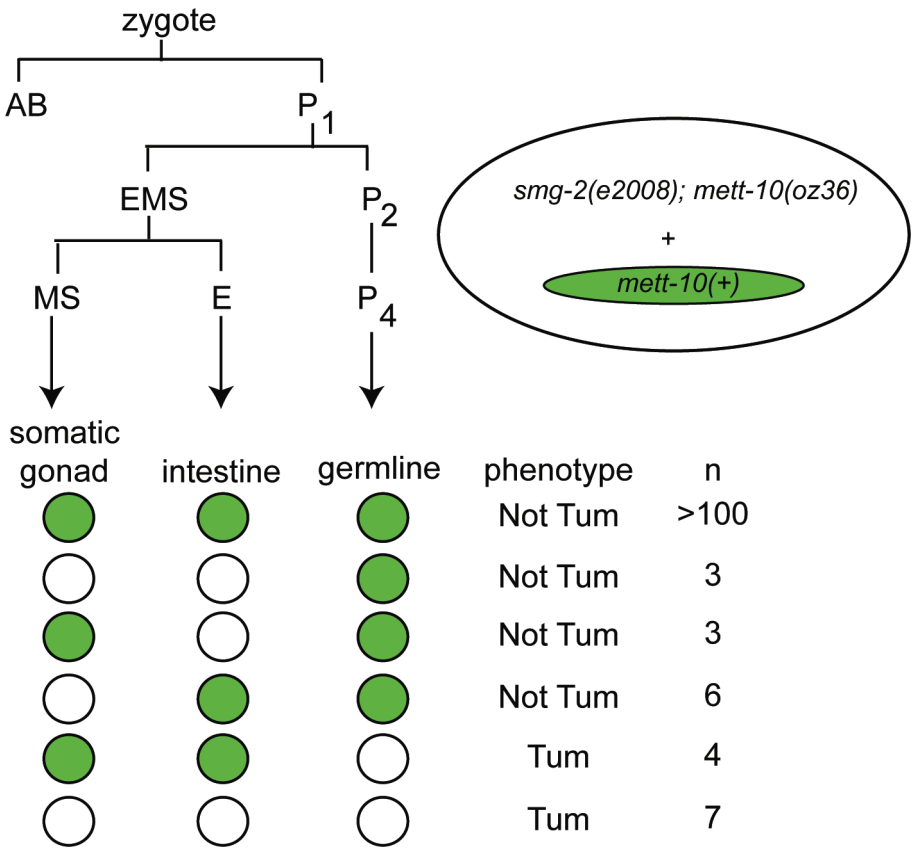
zygote
AB
P1
EMS
P2
MS
E
P4
somatic gonad
intestine
germline
smg-2(e2008); mett-10(oz36)
+
mett-10(+)
phenotype
n
Not Tum
>100
Not Tum
3
Not Tum
3
Not Tum
6
Tum
4
Tum
7

Chapter 3:

A role for dynein in the inhibition of germ cell proliferative fate

INTRODUCTION

C. elegans germ cells proceed through a well-orchestrated developmental program on their way to producing specialized gametes (Hubbard and Greenstein, 2005). The *C. elegans* gonad functions as an assembly line organized with a distal to proximal polarity with respect to the uterus (Figure 1A). Proliferating germ cells, including the germ line stem cells, reside in the distal region of the gonad that forms the stem cell niche. These cells self-renew through mitosis, or at a certain frequency, differentiate by entering meiosis and give rise to gametes after an extended meiotic prophase (Figure 1B). As there is no evidence for asymmetric division of proliferating germ cells, differentiation is likely a consequence of progressive displacement away from the stem cell niche (Lin, 1997; Crittenden *et al*., 2006; Morrison and Kimble, 2006).

The primary signal instructing germ cells to proliferate is activation of the *glp-1/Notch* signaling pathway in the germ cells through interaction with the somatic distal tip cell that expresses the Notch ligand LAG-2, which provides the stem cell niche (Henderson *et al*., 1994; Hansen and Schedl, 2006; Kimble and Crittenden, 2007). Mutations that disrupt *glp-1/Notch* receptor function result in premature differentiation and meiotic entry of germ line stem cells (Austin and Kimble, 1987), while mutations that hyperactivate *glp-1/Notch* cause germ line tumors characterized by germ cell overproliferation (Berry *et al*., 1997; Pepper *et al*., 2003).

Multiple factors act to restrain GLP-1-dependent germ cell proliferation (Hansen and Schedl, 2006; Kimble and Crittenden, 2007). The *C. elegans mett-10*

gene was initially characterized as an inhibitor of germ cell proliferative fate, but was also shown to play a role in promoting progression through mitotic cell division and meiotic development (Chapter 2). *mett-10* encodes a putative methyltransferase that is conserved in higher eukaryotes and a mutation that disrupts the binding pocket for S-adenosylmethionine compromises the balance between proliferative and meiotic fates (Chapter 2; Wu *et al*., To be published.). METT-10 accumulates in nuclei as germ cells enter meiosis, consistent with its role in inhibiting proliferative fate and promoting meiotic progression (Chapter 2). However, it is unclear how METT-10 nuclear accumulation is controlled, or if it is essential for METT-10 activity.

We find that inhibition of proliferative fate is also regulated by Dynein Light Chain-1 and its partner, Dynein Heavy Chain-1; DLC-1 upregulates *mett-10* RNA levels and promotes the nuclear accumulation of METT-10 protein. Cytoplasmic dynein is a large microtubule-associated motor complex that traffics organelles, proteins, and RNAs toward microtubule minus ends (Karki and Holzbaur, 1999; Carson *et al*., 2001; Vale, 2003). Dynein is required for many cellular processes, including execution of mitotic cell division, a process necessary for cell proliferation (Gonczy *et al*., 1999; Karki and Holzbaur, 1999; Schmidt *et al*., 2005). Thus, the unexpected role of dynein in the inhibition of germ cell proliferative fate demonstrates that proliferative fate is genetically separable from the act of mitotic cell division itself, and addresses how cellular machinery can implement developmental programs.

RESULTS

Dynein Light Chain – 1 (DLC-1) inhibits germ cell proliferative fate

To identify proteins that function to inhibit the proliferative fate and may act as functional partners of METT-10, we took advantage of available yeast two-hybrid data for all conserved worm proteins (Li *et al*., 2004), and compiled a list of proteins that interacted directly with METT-10 (primary interactors) and proteins that interacted with the primary interactors (secondary interactors) (Figure 2). We reasoned that if any of these proteins function with METT-10, they may also inhibit proliferative fate. To test this, we depleted each of the interacting proteins by RNAi in a genetic background sensitized to tumor formation by having excessive *glp-1* activity [*glp-1(oz264gf)*] ((Kerins, 2006). We found five interactors that enhance the *glp-1(oz264)* tumorous phenotype, and thus normally act as inhibitors of the proliferative fate (Table 1 and Figure 2). This list of five interactors included *dlc-1*, an LC8-type dynein light chain, and a component of the dynein motor complex that participates in multiple processes, including minus-end directed protein trafficking and mitotic cell division (Karki and Holzbaur, 1999; Giannakakou *et al*., 2000; Vale, 2003; Moseley *et al*., 2007; O'Rourke *et al*., 2007).

Although DLC-1 depletion causes germ line tumors in the *glp-1(gf)* sensitized genetic background, it disrupts mitotic and meiotic processes in wild-type worms. In addition to apparent polyploid nuclei, which are larger and contain more DNA, many oocytes contained unpaired chromosomes (Figure 3, compare B and C). At first

glance, these findings appear paradoxical because the germ line tumors in the *glp-1* gain-of-function background require additional mitotic divisions. However, when we assessed the degree of DLC-1 knockdown using antibody staining, we found that the role of DLC-1 in inhibiting proliferative fate is uncovered in the *glp-1* mutant background because only a slight decrease in DLC-1 is needed to enhance the tumorous phenotype of the *glp-1(oz264)* mutant without causing mitotic defects. In contrast, more severe knockdown affects both cell fate and cell division, leading to polyploidy (Figure 3F-J).

Although dynein light chains function within the context of the dynein motor complex, other functions independent of the motor complex have been described (Benashski *et al*., 1997; Herzig *et al*., 2000; Rayala *et al*., 2005; King, 2008). There are multiple light chains, but inhibition of proliferative fate was unique to DLC-1 among the multiple dynein light chains we tested, including the closest *dlc-1* paralog *dlc-2*, the Roadblock-type light chain *dyrb-1*, and the Tctex-type light chain, *dylt-1* (Figure 3A). Strikingly, RNAi-mediated depletion of Dynein Heavy Chain-1 (DHC-1), the essential motor component of the dynein motor complex activity (Gonczy *et al*., 1999), also increased tumor formation, suggesting that it plays a role in proliferative fate specification (Figure 3A). We conclude, therefore, that DLC-1 affects the proliferative fate decision in the context of the motor complex, although it is unique among the light chains in doing so.

The dynein motor complex promotes normal localization and levels of METT-10

Similarly to *dlc-1*, loss of METT-10 also enhances germ cell proliferation and formation of germ line tumors in the *glp-1(oz264gf)* sensitized genetic background (Chapter 2). METT-10 accumulates in nuclei as cells enter meiosis, in line with its functions in inhibiting proliferative fate and promoting meiotic development (Figure 4A). Our finding that DLC-1 depletion enhances the *glp-1(oz264gf)* tumorous phenotype, coupled with the established role of dynein in trafficking proteins to the nucleus (Karki and Holzbaur, 1999; Giannakakou *et al*., 2000; Moseley *et al*., 2007; O'Rourke *et al*., 2007), suggested that DLC-1 may inhibit germ cell proliferative fate through regulation of METT-10 nuclear accumulation. Using RNAi, we found that DLC-1 knockdown decreases accumulation of a METT-10::GFP fusion protein in the nucleus throughout the germ line, and also in somatic cells (Figure 4A-B, data not shown).

To confirm that DLC-1 functions with the motor complex to promote METT-10 nuclear accumulation, we tested whether reductions in DHC-1 activity also resulted in a decrease in nuclear METT-10. We found that in a genetic background with decreased DHC-1 function [*dhc-1(or195)*] (Schmidt *et al*., 2005), METT-10::GFP nuclear accumulation is delayed, with a strong nuclear signal only in late pachytene, rather than near transition zone as occurs in wild-type germ lines, in more than 50% of germ lines (Figure 4C). This finding indicates that the dynein motor complex promotes METT-10 nuclear accumulation.

In addition to diminished nuclear localization, overall staining intensity for METT-10::GFP is reduced upon DLC-1 depletion, suggesting that DLC-1 also

promotes or maintains the total METT-10 protein level (Figure 4B). Indeed, immunoprecipitation of METT-10::GFP from animals treated with control RNAi or RNAi against *dlc-1*, revealed that total METT-10::GFP levels are reduced by DLC-1 depletion (Figure 4D). This reduction does not reflect a decrease in germ line size, because the levels of a ubiquitous germ line protein, CGH-1, were unchanged (Figure 4D).

DLC-1 regulates *mett-10* RNA levels

We considered two potential mechanisms by which DLC-1 could regulate total METT-10 protein accumulation. LC8-type dynein light chains regulate transcription (Rayala *et al*., 2005; Rayala *et al*., 2006), and interact directly with various proteins to regulate their subcellular localization and/or dimerization status, which could alternatively affect protein stability (Schnorrer *et al*., 2000; Day *et al*., 2004; Navarro *et al*., 2004; Barbar, 2008). To address whether DLC-1 regulates METT-10 at the RNA level, we tested the effect of DLC-1 depletion on levels of METT-10 mRNA using quantitative RT-PCR, and found that knockdown of DLC-1 results in a 4 to 5-fold reduction in *mett-10* mRNA relative to the germ line ubiquitous gene, *cgh-1* (Figure 4E). Thus, DLC-1 promotes overall METT-10 RNA levels, potentially through a transcriptional mechanism.

DLC-1 binds METT-10 *in vitro*

We tested if DLC-1 directly interacts with METT-10 using GST pulldown affinity chromatography, and found that 6XHis-tagged METT-10 binds GST-DLC-1, but not other dynein light chains that show no effect on proliferative fate specification (Figure 5A). We used a series of amino acid substitutions mutations in DLC-1 to see if its interaction with METT-10 requires the same amino acid domain shown to mediate LC8-type dynein light chain interaction with potential "cargo" proteins and dynein intermediate chain (Navarro *et al*., 2004). Indeed, disruption of amino acid residues F62, T67, and F73 in this motif greatly reduced binding to METT-10, while mutation of H68 did not (Figure 5B), showing that the interaction between DLC-1 and METT-10 is similar to previously characterized interactions (Day *et al*., 2004).

In the course of analyzing the physical interaction between METT-10 and DLC-1, we discovered that METT-10 strongly interacts with itself. We noticed an SDS-stable supershifted band in the gel electrophoresis of some METT-10 proteins equivalent to the expected size of a dimer (Figure 6A), in line with previous reports that some methyltransferases require multimerization for function (Mallam and Jackson, 2007; Tomikawa *et al*., 2008). The stable self-interaction domain of METT-10 maps to the C-terminal region (aa 272-479), and a supershift was never seen with a METT-10 N-terminal fragment that mimics the METT-10(oz36) truncation mutant (aa 1- 271) alone (Figure 6A). To confirm that METT-10 binds to itself, we carried out GST pulldown analysis between various METT-10 fragments and discovered that while the METT-10(oz36) truncated protein does not exhibit the SDS-stable self-interaction, it binds to both itself and to the METT-10 C-terminus in GST-pulldown

analysis (Figure 6B). We also observed the supershifted band for 6XHIS-tagged METT-10 proteins pulled down by GST-tagged METT-10 (Figure 5C, 6B), suggesting that METT-10 may exist in an oligomeric form. Interestingly, the putative METT-10 dimer is pulled-down by DLC-1, indicating that the C-terminal interface by which METT-10 interacts with itself is independent of the interface used to bind DLC-1 (Figure 5C).

DLC-1 and the METT-10 nuclear localization signal (NLS) act redundantly to ensure METT-10 nuclear accumulation

The finding that DLC-1 interacts with METT-10 raised the possibility that DLC-1 directly participates in METT-10 nuclear accumulation. Although the two proteins did not colocalize *in vivo* (Figure 7), it is possible that a transient interaction is sufficient to mediate the effect of DLC-1 on METT-10 localization. To address whether DLC-1 promotes METT-10 localization through direct binding, we needed to specifically test the contribution of DLC-1-interaction to METT-10 nuclear accumulation *in vivo*. To this end, we mapped the residues in METT-10 that interact with DLC-1. Previous work showed that LC8-type light chains interact with a short peptide sequence in their target proteins, usually conforming to either a (S/K)XTQT or GIQVD sequence motif (Benison *et al*., 2007; Barbar, 2008), but METT-10 does not have either of these motifs. We thus tested a series of METT-10 C-terminal truncations (data not shown), followed by individual amino acid replacements in an eight amino acid region for their ability to interact with DLC-1 in GST pulldown

experiments. Mutation of METT-10 amino acid residues D420, N421, S423, and Q424 to alanine severely compromised binding to DLC-1, thus defining the METT-10 motif that interacts with DLC-1 as "DNASQ" (Figure 5D).

To determine the effect of DLC-1-binding on METT-10 localization *in vivo*, we constructed a transgenic version of METT-10::GFP in which the "DNASQ" motif was mutated to "AAAAA" (5A mutant, Figure 8A), and compared the localization of METT-10::GFP constructs within gonadal sheath cells, which are large cells that express METT-10 at high levels and thus are easy to visualize. Wild type METT-10::GFP is concentrated in the nucleus (Figure 4A, 8B), and disruption of the DNASQ motif that interacts with DLC-1 reduces, but does not eliminate, nuclear METT-10::GFP (Figures 4F, 8C).

In addition to the DLC-1 binding motif, METT-10 also contains a potential nuclear localization sequence (ARKRAKA), raising the possibility that this may act redundantly with the DLC-1 binding site to enable METT-10 nuclear accumulation. Supporting this idea, deletion of the putative METT-10 nuclear localization signal (NLS) alone does not block nuclear entry (Figure 7D), but simultaneous disruption of both the NLS and the DLC-1 binding site makes METT-10 predominantly cytoplasmic (Figure 8E).

Cytoplasmic METT-10 rescues most *mett-10* mutant phenotypes

Identification of at least two pathways promoting METT-10 nuclear accumulation enabled us to address if METT-10 nuclear accumulation is essential *in*

vivo, and whether the METT-10:DLC-1 physical interaction is vital to METT-10 function. To this end, we compared the abilities of the integrated transgenes expressing various mutant forms of METT-10 to rescue *mett-10* mutant phenotypes. These included METT-10 with a mutant DLC-1 binding site (*mett-10(5A)::gfp*), a mutant DLC-1 binding motif *and* deletion of the NLS (*mett-10(-NLS, 5A)::gfp*), and METT-10 with a mutant DLC-1 binding site and a mutation in the catalytic core that should reduce the methyltransferase activity (*mett-10(G110R,5A)::gfp)* (see Methods). We compared expression of RNA and protein by the various transgenes using qRT-PCR and western blots (Figure 9, Methods). The RNA and protein levels of wild type and mutant transgenes are similarly correlated, agreeing with the finding described above that DLC-1 promotes METT-10 levels primarily by regulating *mett-10* RNA levels.

Each *mett-10* transgene was tested for its ability to suppress several *mett-10* mutant phenotypes, including abnormalities in somatic and germ cell development observed in the *mett-10* null background, defective proliferative fate specification caused by loss-of-function *mett-10* mutations, and germ line RNAi resistance (Chapter 2).

Loss of *mett-10* function causes protrusion of the vulva, irregular gonadal shape, and defects in germ cell development leading to a sterile phenotype when animals are raised at 25˚C (Chapter 2). While a methyltransferase-defective transgene failed to suppress any defects, *mett-10(5A)::gfp* and *mett-10(-NLS, 5A)::gfp* transgenes fully suppressed the protruding vulva phenotype and partially suppressed

abnormalities in gonad shape and germ cell development (Table 2A). This partial suppression suggests that the degree of METT-10 nuclear accumulation, promoted by both DLC-1-interaction and the NLS, facilitates METT-10 functions, but is not essential. Moreover, even in the absence of both the DLC-1 interaction site and the NLS, some residual METT-10 may still enter the nucleus (some nuclear puncta can be seen for *mett-10(-NLS;5A)::gfp*, Figure 8E), causing partial suppression. The fact that methyltransferase-defective transgene does not rescue any of these phenotypes demonstrates that that enzymatic activity is required for METT-10 function, and it is possible that even if the critical METT-10 targets are nuclear proteins, METT-10 may also modify them in the cytoplasm before they enter the nucleus.

Loss of *mett-10* function compromises the balance between germ cell proliferation and differentiation that, similarly to *dlc-1* and *dhc-1*, are revealed in a *glp-1* hyperactivation mutant background (Chapter 2). Thus, to evaluate the role of METT-10 nuclear accumulation in proliferative fate specification, we tested for rescue of the tumorous phenotype of *glp-1(oz264gf) mett-10(g38)* double mutants. Expression of METT-10(5A)::GFP and METT-10(-NLS,5A)::GFP rescued the tumorous phenotype of *glp-1(oz264) mett-10(g38)* animals, but a methyltransferase-defective version of METT-10 did not (Table 2B). Thus, METT-10 inhibition of proliferative fate, similarly to other METT-10 developmental functions, requires enzymatic activity, but not the full extent of nuclear accumulation that is mediated by its NLS and DLC-1.

Mutation of *mett-10* causes germ line RNAi resistance. To assess whether the mutant transgenes rescue the RNAi pathway defect of *mett-10* mutants, we asked whether expression of METT-10(5A)::GFP or METT-10(-NLS;5A)::GFP could restore *mett-10(ok2204)* susceptibility to dsRNA directed against the germ line gene, *gld-1*. We found that, similarly to other *mett-10* phenotypes, expression of the mutant proteins could at least partially rescue RNAi resistance (Figure 10).

Cytoplasmic retention does not underlie the poisonous nature of METT-10(oz36)

The role of METT-10 in proliferative fate specification was initially revealed by the antimorphic *mett-10(oz36)* truncation mutant, which exhibits germ line tumors even in the presence of wild type *glp-1* (Chapter 2). The dose-dependence of the tumorigenic effect of METT-10(oz36) suggested that it is a "poisonous" protein that disrupts the function of at least one other unknown factor that normally inhibits proliferative fate (Chapter 2). Interestingly, METT-10(oz36) lacks both an NLS and a DLC-1 binding site, and thus is predominantly cytoplasmic (Figure 8A,F), suggesting that this change in localization may contribute, in part, to its poisonous nature.

We tested the hypothesis that cytoplasmic retention of METT-10(oz36) plays a causal role in tumor formation by testing our cytoplasmically-retained METT-10 transgene (*mett-10(-NLS,5A)::gfp)* for the ability to suppress METT-10(oz36)-induced tumors. In addition, we tested whether driving METT-10(oz36) into the nucleus by fusing it to the SV40 NLS could also suppress the tumorous phenotype.

We found that expression of cytoplasmic METT-10 could completely suppress METT-10(oz36) overproliferation. Moreover, the nuclear version of METT-10(oz36), METT-10(oz36::SV40NLS)::GFP, *enhanced* the tumorous phenotype of METT-10(oz36) (Figure 8G, Table 2). Together, these data reinforce the idea that METT-10(oz36) has a dose-dependent effect on tumor formation, and further suggest that this effect is independent of the cytoplasmic localization of the mutant protein.

Interestingly, we also found that a methyltransferase-defective version of METT-10 could suppress METT-10(oz36) induced tumor formation, suggesting that METT-10(oz36) acts as a poison by binding to and interfering with the function of another protein and/or molecule; a methyltransferase-defective version of METT-10 could compete with METT-10(oz36) for binding and relieve this effect. Alternatively, since METT-10(oz36) can bind full-length METT-10 (Figure 6B), a methyltransferase-defective METT-10 could bind METT-10(oz36) itself and neutralize its poisonous activity.

Dynein regulates proliferative fate independently of METT-10

Based on the above observations, one possible explanation for the enhancement of *glp-1(oz264gf)* tumor formation by DLC-1 depletion is the reduced METT-10 accumulation caused by decreased *mett-10* RNA, combined with decreased transport of METT-10 to the nucleus. However, genetic interactions between *mett-10, dlc-1* and *dhc-1* indicate that dynein also plays roles in proliferative fate specification independent of its effects on METT-10 protein accumulation.

RNAi knockdown of DLC-1 enhances tumor formation in the *mett-10(oz36)* genetic background (Table 3A). Two different weak loss-of-function heavy chain alleles, *dhc-1(or195)* (Schmidt *et al*., 2005) and *dhc-1(js319*) (Koushika *et al*., 2004; Schmidt *et al*., 2005), also specifically enhanced the *mett-10(oz36)* tumorous phenotype, although the *dhc-1(js121)* allele did not (Table 3B). Because METT-10(oz36) cannot detectably interact directly with DLC-1, the ability of DLC-1 knockdown and *dhc-1* reduction-of-function mutants to further enhance tumor formation indicates that DLC-1 also regulates proliferative fate independently of its effects on METT-10.

METT-10 and dynein may function together in multiple contexts

The *dhc-1(js319)* dynein heavy chain mutation did not cause tumors when combined with loss-of-function *mett-10* alleles, but the double mutant animals had a fully penetrant sterility not seen in either mutant alone. On closer examination, *dhc-1(js319); mett-10(-)* germ lines exhibited two primary defects reminiscent of the phenotypes caused by RNAi knockdown of DLC-1: polyploidy in the distal region and unpaired chromosomes in diakinesis (Figure 11 and Table 4). We also saw these phenotypes at low penetrance in *dhc-1(js319)* animals, but they are distinct from the cell cycle progression defects observed in *mett-10* single mutants (Chapter 2). Thus, loss of *mett-10* function enhances a hypomorphic *dhc-1* allele, causing phenotypes typical of *dynein* loss of function mutations. This indicates that METT-10 also facilitates the function of the dynein motor complex in cell division and meiosis.

Complete loss of *mett-10* function alone does not cause these phenotypes, indicating that *mett-10* function in cell division and meiotic events is not essential unless dynein function is partially compromised.

Reduction in *glp-1* activity suppresses germ line overproliferation, but not the polyploidy and unpaired chromosome phenotypes of *dhc-1*; *mett-10(oz36)* double mutants (Tables 3 & 4). Thus the roles of *mett-10* and dynein in cell division and meiotic events can be separated from their roles in regulation of the proliferative fate decision. We conclude, therefore, that regulation of proliferative fate, perhaps through negative regulation of *glp-1* signaling, is only one cellular function in which dynein and METT-10 cooperate.

Interestingly, we also found that expression of a METT-10 protein unable to directly interact with DLC-1, METT-10(5A)::GFP, results in polyploidy in the distal region of the germ line, a phenotype reminiscent of loss of *dlc-1* function (Figure 4F, compare with Figure 3C). The penetrance of this phenotype correlated with the level of transgene expression and was suppressible by RNAi directed against GFP (data not shown). This dominant phenotype suggests that METT-10(5A)::GFP acts as a dominant negative with respect to some *dlc-1* functions, potentially through disruption of a complex made up of METT-10, DLC-1, and other proteins.

dhc-1(js121), dhc-1(jor195), and *dhc-1(js319)* each affect a different functional domain of Dynein Heavy Chain-1

The differential genetic interactions between *dynein heavy chain-1* and *mett-10* alleles with respect to proliferative fate specification, cell division, and meiotic pairing/recombination, may be due to the nature of the *dhc-1* mutations, which affect different parts of the heavy chain locus (Figure 12). The mutant with the strongest effect on tumor formation but no effect on the polyploidy/univalent phenotype, *dhc-1(or195)*, was previously shown to carry a missense mutation in the microtubule stalk domain (Figure 12 and O'Rourke *et al*., 2007), which mediates the interaction of the motor complex with microtubules and plays a key role in determining the direction of motility (Carter *et al*., 2008). Sequencing of *dhc-1(js319)*, which has strong genetic interactions with *mett-10* affecting tumor formation, polyploidy, and chromosome pairing, reveals a AG>AA mutation in the splice acceptor for exon 13. If we assume that this mutation results in exon skipping, this would result in a truncation C-terminal to the 5th and 6th "ATP-ase-like" domains; this region has no known function. Finally, *dhc-1(js121)* is predicted to have the most severe effect on dynein function, as it is an AG>>AA mutation in the splice acceptor for exon 6, which encodes the linker domain immediately preceeding the first ATPase domain (Figure 12). The linker domain is thought to play an essential role in dynein motility (Burgess *et al*., 2003). Both *dhc-1(or195)* and *dhc-1(js319)* behave as temperature-sensitive, weak *dynein heavy chain* alleles, especially at the permissive temperature of 20˚C and in the presence of maternal gene product. On the other hand, *dhc-1(js121)*, which is predicted to have the most severe effect on dynein function, behaves as a stronger loss-of-function [*dhc-1(js121)* homozygotes are sterile]. Thus, *dhc-1(js121)* may fail

to enhance *mett-10(oz36)* because of pleiotropic effects that mask any role in proliferative fate specification.

DISCUSSION

Dynein inhibits specification of proliferative fate in the *C. elegans* germ line

The genetic and molecular studies presented here demonstrate that the dynein motor protein complex inhibits the decision of germ cells to proliferate in the *C. elegans* germ line, despite being necessary for the execution of mitotic cell division in those cells that do proliferate. The evidence further indicates that Dynein regulates this cell fate decision in part by promoting expression and function of the METT-10 putative methyltransferase that inhibits proliferative fate, and in part through a METT-10-independent pathway.

DLC-1 regulates METT-10 RNA levels and protein subcellular localization

DLC-1 knockdown reduces both METT-10 RNA and protein levels. The mammalian LC8-type dynein light chain, DLC1, localizes to chromatin and acts in a transcriptional transactivation complex with estrogen receptor (Rayala *et al*., 2005), raising the possibility that DLC-1 could directly regulate *mett-10* transcription. It is also possible that DLC-1 normally promotes *mett-10* RNA stability, or enables the nuclear localization of other proteins that ensure adequate *mett-10* transcription.

The direct physical interaction between DLC-1 and METT-10 reported here appears to play a redundant, non-essential role in METT-10 function. We showed that nuclear localization signal (NLS)-mediated and dynein-mediated pathways act redundantly to ensure normal METT-10 nuclear accumulation. The role of dynein and the microtubule network, and specifically LC8-type light chains, in facilitating the nuclear import of proteins is well documented (Giannakakou *et al*., 2000; Trostel *et al*., 2006; Moseley *et al*., 2007; Roth *et al*., 2007; Desfarges *et al*., 2009; Shrum *et al*., 2009). However, in cases where it has been examined, dynein mediates nuclear accumulation by enhancing the efficiency of NLS-dependent nuclear import (Moseley *et al*., 2007; Roth *et al*., 2007). In these cases, unlike the example of METT-10, nuclear accumulation still requires an intact NLS. Thus, our work reveals a qualitatively different role for dynein, and LC8/DLC-1 interaction, in mediating nuclear accumulation. We cannot rule out the possibility, however, that DLC-1 specifically promotes the function of a secondary, non-canonical NLS in METT-10.

When we specifically disrupted NLS- and DLC-1- mediated METT-10 nuclear accumulation *in vivo*, we found that it plays a non-essential role in most *mett-10* developmental functions. Because our double mutants still retain some residual nuclear METT-10, a small nuclear pool may be sufficient to carry out its function as a methyltransferase. It is also possible that METT-10 association with dynein is transient, and promotes modification of target molecules on their way to the nucleus, with METT-10 nuclear accumulation as a byproduct. In this scenario, cytoplasmic

METT-10 would be able to modify targets in the cytoplasm before their transport to the nucleus.

While DLC-1 may inhibit proliferative fate in part through promotion of normal METT-10 activity, it is clear that DLC-1 (and dynein) inhibit proliferative fate by other means as well, since disruptions in dynein function enhance germ line tumor formation of the *mett-10(oz36)* cytoplasmic mutant. Interestingly, disruptions of dynein function do not cause germ line tumors in other *mett-10* mutant backgrounds, including the null. Since METT-10(oz36) is proposed to "poison" the function of another gene product through an unproductive physical association (Chapter 2), it is possible that dynein promotes the normal function of the gene product(s) poisoned by METT-10(oz36), thus sensitizing *mett-10(oz36)* to perturbations in dynein function. Moreover, it is likely that METT-10, dynein, and this "poisoned factor" function to negatively regulate the pro-proliferative functions *glp-1/Notch* signaling, as the *mett-10(oz36); dhc-1(or195)* tumors are exquisitely sensitive to the levels of *glp-1* activity.

METT-10 and dynein function together in cell division and meiosis

While METT-10 and the dynein motor complex function together to inhibit germ cell proliferative fate, we also uncovered a role for METT-10 in other dynein-dependent processes. Specifically, decreases in METT-10 activity enhance the mitotic and meiotic defects of a weak dynein heavy chain loss-of-function allele, leading to highly penetrant sterility, polyploidy, and unpaired chromosomes in diakinesis.

Interestingly, O'Connell and colleagues identified a phenotype in *mett-10(oj32)* loss-of-function mutants similar to those seen in dynein loss of function mutants (O'Connell *et al*., 1998). Specifically, *mett-10(oj32)* embryos have a visible defect in the flattening of the posterior centrosome during the first asymmetric division (O'Connell *et al*., 1998). The function of centrosome flattening is unclear, but may be caused by the dynein-dependent force that pulls the posterior centrosome towards the posterior pole, thus ensuring asymmetric division (Severson and Bowerman, 2003; Nguyen-Ngoc *et al*., 2007). Importantly, defects in centrosome flattening are also observed for perturbations in dynein and dynactin function (Severson and Bowerman, 2003; Schmidt *et al*., 2005; Couwenbergs *et al*., 2007). Together these data suggest that METT-10, perhaps through its interaction with DLC-1, functions to promote multiple dynein-dependent events, although the mechanisms remain unclear. Moreover, if METT-10 and dynein jointly function in proliferative fate specification, cell division, and meiotic pairing and/or recombination, then the normal function of METT-10 in all these processes may be to promote dynein activity, which in turn promotes METT-10 function in a positive feedback loop.

Proliferative and anti-proliferative roles of dynein

The dynein motor complex participates in a diversity of processes, including nuclear movements, spindle assembly and orientation, mitotic checkpoint inactivation, organelle movement, and endocytosis (Henderson *et al*., 1994; Karki and Holzbaur, 1999). Here we show that dynein inhibits the specification of germ cell

proliferative fate, despite also being necessary for mitotic cell division in proliferating cells. These "anti-proliferative" (cell fate) and "pro-proliferative" (cell fate execution/cell division) functions of dynein are not unique to the maintenance of the balance between proliferation and differentiation in the *C. elegans* germ line. The essential roles of dynein in the execution of cell division are well known (Karki and Holzbaur, 1999), as is its role in promoting the activity of tumor suppressors, including p53, by facilitating their nuclear transport (Giannakakou *et al*., 2000; Fabbro and Henderson, 2003; Trostel *et al*., 2006; Roth *et al*., 2007). Moreover, in keeping with its many cellular functions, the dynein motor complex influences multiple cell fate decisions by a diversity of mechanisms. These include the trafficking of cell fate determinants, such as egalitarian and its associated *oskar* mRNA (Navarro *et al*., 2004), spindle positioning during asymmetric division (Couwenbergs *et al*., 2007), ensuring the normal timing of mitotic cell division (Fan and Ready, 1997), and now by promoting RNA levels and protein nuclear accumulation of a factor influencing cell fate. Thus dynein acts as a "handyman", performing many of the jobs necessary to execute a developmental program.

MATERIALS AND METHODS

General worm culture and genetics

Standard procedures for culture and genetic manipulation of *C. elegans* strains were followed (Brenner, 1974). Strain constructions were verified by single worm PCR and sequencing of alleles.

Alleles used in this study by chromosome:

I: *rrf-1(pk1417), dhc-1(js319), dhc-1(or195), dhc-1(js121)*

III: *mett-10(oz36)*[antimorph], *mett-10(g38)* [hypomorph], *mett-10(tm2697)* [hypomorph], *mett-10(oj32)*[hypomorph], *mett-10(ok2204)*[null], *glp-1(oz264gf), glp-1(bn18ts)*

Integrated Transgenes:

ozIs7[pmett-10:mett-10::gfp; unc-119(+)]

ozIs9[pmett-10:mett-10(5A)::gfp; unc-119(+)] (LOW)

ozIs11[pmett-10:mett-10(5A)::gfp; unc-119(+)] (HIGH)

ozIs15[pmett-10:mett-10(oj32,5A)::gfp; unc-119(+)] (line1)

ozIs16[pmett-10:mett-10(oj32,5A)::gfp; unc-119(+)] (line2)

ozIs20[pmett-10:mett-10(-NLS, 5A)::gfp; unc-119(+)](line 1)

ozIs21[pmett-10:mett-10(-NLS, 5A)::gfp; unc-119(+)](line 2)

ozIs19 [pmett-10::mett-10(oz36)::gfp; unc-119(+)]

ozIs25[pmett-10::mett-10(oz36::SV40NLS)::gfp; unc-119(+)]

Extrachromosomal arrays:

ozEx66 [pmett-10:mett-10::gfp; unc-119(+)]

ozEx69 [pmett-10:mett-10(-NLS)::gfp; unc-119(+)]

ozEx67 [pmett-10:mett-10(5A)::gfp; unc-119(+)]

ozEx72 [pmett-10:mett-10(-NLS, 5A)::gfp; unc-119(+)]

ozEx73 [pmett-10:mett-10(oz36)::gfp; unc-119(+)]

ozEx74[[pmett-10:mett-10(oz36::SV40NLS)::gfp; unc-119(+); pmyo-2::mcherry]

Sequencing of *dhc-1* alleles

To sequence the entirety of the *dhc-1* locus, including introns and exons, primers amplifying 1kb regions and containing 200 bp overlap on either side were used to amplify fragments that spanned the entire *dhc-1* locus, including approximately 200bp upstream and downstream of transcriptional start and stop, and all introns from the *dhc-1(js319)* and *dhc-1(js121)* mutants. These were then cleaned and sequenced, assembled using SeqMan (DNAstar), and aligned to the N2 *dhc-1* sequence from wormbase to identify mutations.

Immunohistochemistry

Germ line dissection, fixation, and staining was carried out as previously described (Lee *et al*., 2007). Antibodies used were: monoclonal mouse ant-GFP (mAb3E6) from Invitrogen (Cat# A-11120) at 1/100, Rabbit anti-DLC-1 at 1/10 (see below) and donkey anti-mouse Alexa 594, goat anti-rabbit Alexa 488, goat anti-rabbit Alexa 594 at 1/400, obtained from Molecular Probes (Invitrogen, CA). EdU labeling and co-staining with antibodies was carried out as described in (Chapter 2).

Generation of anti-DLC-1 antibody and quantification of DLC-1 levels

To generate the GST:DLC-1 fusion protein, full length DLC-1 was cloned into the pGEX-5x-3 vector (GE Healthcare Life Sciences, Cat# 27-4586-01). Inductions were carried out in the *E. coli* strain BL21(DE3) (Sigma, MO). From an overnight starter culture grown at 30˚C, cultures were diluted and grown at 37˚C until they reached an OD of 0.5. Cells were induced with 1mM IPTG for 3 hours at 37˚C. Cells were harvested and GST-DLC-1 was then extracted essentially as described in (Sambrook and Russell, 2001) and injected into rabbits by Pocono Rabbit Farm & Laboratory (Canadensis, PA). Sera were affinity purified against a 6XHIS:DLC-1 fusion protein. To make 6XHIS:DLC-1, DLC-1 was amplified from pGEX (DLC-1), and cloned into pTRCHIS (Invitrogen, Cat # K4410-01, K4410-40). pTRCHIS(DLC-1) was transformed into BL21(DE3) cells, and cultures were induced similarly to GST-DLC-1. 6XHIS-DLC-1 was extracted under native conditions using Ni-NTA agarose (Qiagen, Cat# 30210). 6XHIS-DLC-1 was subsequently coupled to Cyanogen-Bromide activated Sepharose (Sigma, MO, Cat# C9142) and antibody purification was carried out essentially as previously described (Jones *et al*., 1996). Specificity was determined both by Western (where antibody recognizes a single 10kDa band) and by antibody staining of germ lines and intestines from animals treated with and without *dlc-1 RNAi*.

For quantification of DLC-1 levels (in Figure 2J), raw images of DLC-1 staining were imported into Image J, germ lines were traced, and average pixel

intensity was calculated. All pixel intensities were then normalized to represent % knockdown by dividing the pixel intensity for the sample by the average DLC-1 pixel intensity for *glp-1(oz264)* germ lines fed control RNAi and multiplying by 100.

Image capture and processing

Fluorescence micrographs were taken on a Zeiss compound microscope using AxioPlan 2.0 imaging software and Hamamatsu camera. Each dissected and stained gonad was captured as a montage, with overlapping cell boundaries. The montages were then assembled in Adobe Photoshop CS3 and processed identically. The boundary of each montage was processed using a feather tool of 20 pixels for each image. Confocal images were captured on a Perkin Elmer Ultraview Confocal Microscope using a z-step of 0.3 microns.

RNAi screen of METT-10 interactors

RNAi clones were either purchased from Open Biosystems or generated by PCR amplification and cloning of 1kb exonic sequences into the pPD128.36 double T7 promoter vector, sequenced to verify identity, and transformed into the *E. coli* host HT115(DE3). Feeding RNAi was performed as previously described (Lee *et al*., 2007), in *rrf-1(pk1417), rrf-1(pk1417); glp-1(oz264gf)*, and *rrf-1(pk1417); mett-10(oz36)* backgrounds at the permissive temperature (20ºC). F1 L4 hermaphrodites were transferred onto fresh RNAi plates and scored quantitatively for germ line

tumors 48 hrs later by DIC microscopy. In the course of the screen, it came to our attention that *mett-10* mutants are relatively resistant to germ line RNAi.

Construction of transgenes and generation of transgenics

The initial *mett-10::gfp* construct includes 1.6 kb upstream and 1.9 kb downstream of the METT-10 coding region with GFP(ivs):FLAG inserted immediately before the translational stop cloned into the pMM016 vector containing the transformation marker, *unc-119(+)* (Chapter 2). Mutations of the *mett-10* coding region, including NLS deletion, DNASQ>AAAAA, methyltransferase-mutation (G110R), and deletion of coding sequences downstream to the *mett-10(oz36)* premature stop codon, were done with sewing PCR (Lee and Schedl, 2001). To create *mett-10(oz36::SV40NLS)::gfp*, the sequence "CAAAATCGTCTGCCAAAGAAGAAGCGTAAGGTA" encoding the SV40NLS was inserted immediately prior to GFP using sewing PCR and the *mett-10(oz36)::gfp* construct as a template. To create low-copy integrated transgenic lines, the microparticle bombardment method was used (Praitis *et al*., 2001). Generation of extrachromosomal arrays was done by injection *pMM016(mett-10)* plasmids at a concentration of 40ng/ul into *unc-119(ed3)* worms.

GST-pulldowns

Full length METT-10 (*C. elegans* coding region ZK1128.2a), METT-10(oz36) (aa 1-271), or METT-10(Cterm) (aa 272-479) were amplified from N2

Bristol cDNA and cloned into pTRCHIS (Invitrogen, Cat # K4410-01, K4410-40), sequenced, and transformed into BL21(DE3) (Sigma, MO) cells for expression. Proteins were expressed under the same conditions as GST-DLC-1 (above). For GST pulldowns, bacterial extracts were resuspended in PBS + protease inhibitors and sonicated. Cleared cell extracts were added directly to 5ug of GST-DLC-1 already bound to Glutathione-sepharose in 20mM Tris pH 7.5, 500mM NaCl, 0.5% NP40, and 1X protease inhibitors. Binding reactions were carried out overnight at 4˚C, washed 4X with 10mM Tris pH 7.5, 150mM NaCl, and 0.1% NP40. Western blot analysis using an anti-6XHIS antibody (Amersham Biosciences, Cat# 27-4710-01) was performed from beads boiled in SDS-sample buffer with BME. Point mutations in METT-10 and DLC-1 were generated using sewing PCR or site-directed mutagenesis.

Immunoprecipitation and Western Analysis

To generate enough worms for IP-Western of METT-10:GFP (flag), we resuspended worms from ten 60mm overgrown plates of each transgenic line in 5% lactose and 10X OP50 or 1X bacterial expressing dsRNA and plated these onto ten 100mm plates, which were shifted to 25˚C to maximize transgene expression. After two days, worms were washed off in PBS and extracts and IPs were carried out essentially as described in (Guang *et al*., 2008). Immunoprecipitated proteins were analyzed using Western blots with both mouse monoclonal anti-FLAG M2 (Sigma, Cat# F1804) and Rabbit anti-GFP (Invitrogen, Cat#A11122) antibodies. For loading

controls, we used mouse anti-alpha-tubulin (Sigma, Cat#T9026) and anti-CGH-1 (gift of David Greenstein).

RNA quantification

To measure *mett-10:gfp* transgene expression relative to endogenous, each *mett-10::gfp* transgene was crossed into the *mett-10(ok2204)* background, which contains a large deletion of the *mett-10* 5' region. Total RNA was isolated using Trizol (Invitrogen), treated with DNase I (Epicentre), chloroform extracted, ethanol precipitated and dissolved in water. cDNA was synthesized using random hexamer primers and SuperScript VILO reverse transcriptase (Invitrogen). Transcripts were quantified using Sybr green real-time PCR (Clontech) and gene-specific primers (see below) calibrated with genomic DNA. RNA levels were calculated adjusting for amplification efficiency (Pfaffl, 2001) and normalizing to internal *cgh-1* or *act-3* transcripts and external genomic DNA standards. Standard deviations were calculated using all PCR replicates from all biological replicates.

Primers used for quantitative RT-PCR:

Gene	Forward Primer	Reverse Primer
mett-10	TGATATTGGCACCGGAACATCGTG	CATCTCCGTCAGTGGCAATGAACT
dlc-1	TGGCATTGCATCGTCGGAAGAAAC	AGACTTGAATAGCAGGATGGCGAC
act-3	TCTTGACTTGGCTGGACGTGATCT	TGATGTCACGGACGATTTCACGCT
cgh-1	ATCAACTTCCTCCCAAAGGAGCG	TCATACGGCTTGTGCATGTGCTTC

ACKNOWLEDGEMENTS

We thank the *Caenorhabditis* Genetics Center, the Japanese National Bioresource Project, the *C. elegans* gene knockout consortium, and Mike Nonet for strains. We thank Ziva Misulovin for assistance with the quantitative RT-PCR shown in Figures 4E and S2 and Siqun Xu for technical assistance in generating *mett-10::gfp* arrays. We extend our sincerest thanks to Dale Dorsett, Swathi Arur, Yair Dorsett, Justin Fay, Kevin O'Connell, Jim Skeath, Paul Fox, Doug Chalker, Mike Nonet, Jim Havranek, and John Cooper for experimental suggestions, provisions of reagents, or comments on the manuscript. This work was supported by GM63310 awarded to T.S.

REFERENCES

Austin, J., and Kimble, J. (1987). glp-1 is required in the germ line for regulation of the decision between mitosis and meiosis in C. elegans. Cell *51*, 589-599.

Barbar, E. (2008). Dynein light chain LC8 is a dimerization hub essential in diverse protein networks. Biochemistry *47*, 503-508.

Benashski, S.E., Harrison, A., Patel-King, R.S., and King, S.M. (1997). Dimerization of the highly conserved light chain shared by dynein and myosin V. J Biol Chem *272*, 20929-20935.

Benison, G., Karplus, P.A., and Barbar, E. (2007). Structure and dynamics of LC8 complexes with KXTQT-motif peptides: swallow and dynein intermediate chain compete for a common site. J Mol Biol *371*, 457-468.

Berry, L.W., Westlund, B., and Schedl, T. (1997). Germ-line tumor formation caused by activation of glp-1, a Caenorhabditis elegans member of the Notch family of receptors. Development *124*, 925-936.

Brenner, S. (1974). The genetics of Caenorhabditis elegans. Genetics *77*, 71-94.

Burgess, S.A., Walker, M.L., Sakakibara, H., Knight, P.J., and Oiwa, K. (2003). Dynein structure and power stroke. Nature *421*, 715-718.

Carson, J.H., Cui, H., and Barbarese, E. (2001). The balance of power in RNA trafficking. Curr Opin Neurobiol *11*, 558-563.

Carter, A.P., Garbarino, J.E., Wilson-Kubalek, E.M., Shipley, W.E., Cho, C., Milligan, R.A., Vale, R.D., and Gibbons, I.R. (2008). Structure and functional role of dynein's microtubule-binding domain. Science *322*, 1691-1695.

Couwenbergs, C., Labbe, J.C., Goulding, M., Marty, T., Bowerman, B., and Gotta, M. (2007). Heterotrimeric G protein signaling functions with dynein to promote spindle positioning in C. elegans. J Cell Biol *179*, 15-22.

Crittenden, S.L., Leonhard, K.A., Byrd, D.T., and Kimble, J. (2006). Cellular analyses of the mitotic region in the Caenorhabditis elegans adult germ line. Mol Biol Cell *17*, 3051-3061.

Day, C.L., Puthalakath, H., Skea, G., Strasser, A., Barsukov, I., Lian, L., Huang, D., and Hinds, M.G. (2004). Localization of dynein light chains 1 and 2 and their pro-apoptotic ligands. Biochem. J. *377*, 595-605.

Desfarges, S., Salin, B., Calmels, C., Andreola, M.L., Parissi, V., and Fournier, M. (2009). HIV-1 integrase trafficking in S. cerevisiae: a useful model to dissect the microtubule network involvement of viral protein nuclear import. Yeast *26*, 39-54.

Dorsett, M., Westlund, B., and Schedl, T. (submitted.). METT-10, a putative methyltransferase, inhibits germ cell proliferative fate in *Caenorhabditis elegans.*

Fabbro, M., and Henderson, B.R. (2003). Regulation of tumor suppressors by nuclear-cytoplasmic shuttling. Exp Cell Res *282*, 59-69.

Fan, S.S., and Ready, D.F. (1997). Glued participates in distinct microtubule-based activities in Drosophila eye development. Development *124*, 1497-1507.

Giannakakou, P., Sackett, D.L., Ward, Y., Webster, K.R., Blagosklonny, M.V., and Fojo, T. (2000). p53 is associated with cellular microtubules and is transported to the nucleus by dynein. Nat Cell Biol *2*, 709-717.

Gonczy, P., Pichler, S., Kirkham, M., and Hyman, A.A. (1999). Cytoplasmic dynein is required for distinct aspects of MTOC positioning, including centrosome separation, in the one cell stage Caenorhabditis elegans embryo. J Cell Biol *147*, 135-150.

Guang, S., Bochner, A.F., Pavelec, D.M., Burkhart, K.B., Harding, S., Lachowiec, J., and Kennedy, S. (2008). An Argonaute transports siRNAs from the cytoplasm to the nucleus. Science *321*, 537-541.

Hansen, D., and Schedl, T. (2006). The regulatory network controlling the proliferation-meiotic entry decision in the Caenorhabditis elegans germ line. Curr Top Dev Biol *76*, 185-215.

Henderson, S.T., Gao, D., Lambie, E.J., and Kimble, J. (1994). lag-2 may encode a signaling ligand for the GLP-1 and LIN-12 receptors of C. elegans. Development *120*, 2913-2924.

Herzig, R.P., Andersson, U., and Scarpulla, R.C. (2000). Dynein light chain interacts with NRF-1 and EWG, structurally and functionally related transcription factors from humans and drosophila. J Cell Sci *113 Pt 23*, 4263-4273.

Hubbard, E.J., and Greenstein, D. (2005). Introduction to the germ line. WormBook, 1-4.

Jones, A.R., Francis, R., and Schedl, T. (1996). GLD-1, a cytoplasmic protein essential for oocyte differentiation, shows stage- and sex-specific expression during Caenorhabditis elegans germ line development. Dev Biol *180*, 165-183.

Karki, S., and Holzbaur, E.L. (1999). Cytoplasmic dynein and dynactin in cell division and intracellular transport. Curr Opin Cell Biol *11*, 45-53.

Kerins, J. (2006). PRP-17 and the pre-mRNA splicing pathway are preferentially required for the proliferation versus meiotic development decision and germ line sex determination in *Caenorhabditis elegans.*, Washington University Saint Louis, MO.

Kimble, J., and Crittenden, S.L. (2007). Controls of germ line stem cells, entry into meiosis, and the sperm/oocyte decision in Caenorhabditis elegans. Annu Rev Cell Dev Biol *23*, 405-433.

King, S.M. (2008). Dynein-independent functions of DYNLL1/LC8: redox state sensing and transcriptional control. Sci Signal *1*, pe51.

Koonce, M.P., and Tikhonenko, I. (2000). Functional elements within the dynein microtubule-binding domain. Mol Biol Cell *11*, 523-529.

Koushika, S.P., Schaefer, A.M., Vincent, R., Willis, J.H., Bowerman, B., and Nonet, M.L. (2004). Mutations in Caenorhabditis elegans cytoplasmic dynein components reveal specificity of neuronal retrograde cargo. J Neurosci *24*, 3907-3916.

Lee, M.H., Ohmachi, M., Arur, S., Nayak, S., Francis, R., Church, D., Lambie, E., and Schedl, T. (2007). Multiple functions and dynamic activation of MPK-1 extracellular signal-regulated kinase signaling in Caenorhabditis elegans germ line development. Genetics *177*, 2039-2062.

Lee, M.H., and Schedl, T. (2001). Identification of in vivo mRNA targets of GLD-1, a maxi-KH motif containing protein required for C. elegans germ cell development. Genes Dev *15*, 2408-2420.

Li, S., Armstrong, C.M., Bertin, N., Ge, H., Milstein, S., Boxem, M., Vidalain, P.O., Han, J.D., Chesneau, A., Hao, T., Goldberg, D.S., Li, N., Martinez, M., Rual, J.F., Lamesch, P., Xu, L., Tewari, M., Wong, S.L., Zhang, L.V., Berriz, G.F., Jacotot, L., Vaglio, P., Reboul, J., Hirozane-Kishikawa, T., Li, Q., Gabel, H.W., Elewa, A., Baumgartner, B., Rose, D.J., Yu, H., Bosak, S., Sequerra, R., Fraser, A., Mango, S.E., Saxton, W.M., Strome, S., Van Den Heuvel, S., Piano, F., Vandenhaute, J., Sardet, C., Gerstein, M., Doucette-Stamm, L., Gunsalus, K.C., Harper, J.W., Cusick, M.E., Roth, F.P., Hill, D.E., and Vidal, M. (2004). A map of the interactome network of the metazoan C. elegans. Science *303*, 540-543.

Lin, H. (1997). The tao of stem cells in the germ line. Annu Rev Genet *31*, 455-491.

Mallam, A.L., and Jackson, S.E. (2007). The dimerization of an alpha/beta-knotted protein is essential for structure and function. Structure *15*, 111-122.

Morrison, S.J., and Kimble, J. (2006). Asymmetric and symmetric stem-cell divisions in development and cancer. Nature *441*, 1068-1074.

Moseley, G.W., Roth, D.M., DeJesus, M.A., Leyton, D.L., Filmer, R.P., Pouton, C.W., and Jans, D.A. (2007). Dynein light chain association sequences can facilitate nuclear protein import. Mol Biol Cell *18*, 3204-3213.

Navarro, C., Puthalakath, H., Adams, J.M., Strasser, A., and Lehmann, R. (2004). Egalitarian binds dynein light chain to establish oocyte polarity and maintain oocyte fate. Nat Cell Biol *6*, 427-435.

Nguyen-Ngoc, T., Afshar, K., and Gonczy, P. (2007). Coupling of cortical dynein and G alpha proteins mediates spindle positioning in Caenorhabditis elegans. Nat Cell Biol *9*, 1294-1302.

O'Connell, K.F., Leys, C.M., and White, J.G. (1998). A genetic screen for temperature-sensitive cell-division mutants of Caenorhabditis elegans. Genetics *149*, 1303-1321.

O'Rourke, S.M., Dorfman, M.D., Carter, J.C., and Bowerman, B. (2007). Dynein modifiers in C. elegans: light chains suppress conditional heavy chain mutants. PLoS Genet *3*, e128.

Pepper, A.S., Killian, D.J., and Hubbard, E.J. (2003). Genetic analysis of Caenorhabditis elegans glp-1 mutants suggests receptor interaction or competition. Genetics *163*, 115-132.

Pfaffl, M.W. (2001). A new mathematical model for relative quantification in real-time RT-PCR. Nucleic Acids Res *29*, e45.

Praitis, V., Casey, E., Collar, D., and Austin, J. (2001). Creation of low-copy integrated transgenic lines in Caenorhabditis elegans. Genetics *157*, 1217-1226.

Rayala, S.K., den Hollander, P., Balasenthil, S., Yang, Z., Broaddus, R.R., and Kumar, R. (2005). Functional regulation of oestrogen receptor pathway by the dynein light chain 1. EMBO Rep *6*, 538-544.

Rayala, S.K., den Hollander, P., Manavathi, B., Talukder, A.H., Song, C., Peng, S., Barnekow, A., Kremerskothen, J., and Kumar, R. (2006). Essential role of KIBRA in

co-activator function of dynein light chain 1 in mammalian cells. J Biol Chem *281*, 19092-19099.

Roth, D.M., Moseley, G.W., Glover, D., Pouton, C.W., and Jans, D.A. (2007). A microtubule-facilitated nuclear import pathway for cancer regulatory proteins. Traffic *8*, 673-686.

Sambrook, J., and Russell, D. (2001). Molecular Cloning A Laboratory Manual, vol. 3, Cold Spring Harbor, New York: Cold Spring Harbor Laboratory Press, 15.36-15.39.

Schmidt, D.J., Rose, D.J., Saxton, W.M., and Strome, S. (2005). Functional analysis of cytoplasmic dynein heavy chain in Caenorhabditis elegans with fast-acting temperature-sensitive mutations. Mol Biol Cell *16*, 1200-1212.

Schnorrer, F., Bohmann, K., and Nusslein-Volhard, C. (2000). The molecular motor dynein is involved in targeting swallow and bicoid RNA to the anterior pole of Drosophila oocytes. Nat Cell Biol *2*, 185-190.

Severson, A.F., and Bowerman, B. (2003). Myosin and the PAR proteins polarize microfilament-dependent forces that shape and position mitotic spindles in Caenorhabditis elegans. J Cell Biol *161*, 21-26.

Shrum, C.K., Defrancisco, D., and Meffert, M.K. (2009). Stimulated nuclear translocation of NF-kappaB and shuttling differentially depend on dynein and the dynactin complex. Proc Natl Acad Sci U S A *106*, 2647-2652.

Tomikawa, C., Ochi, A., and Hori, H. (2008). The C-terminal region of thermophilic tRNA (m7G46) methyltransferase (TrmB) stabilizes the dimer structure and enhances fidelity of methylation. Proteins *71*, 1400-1408.

Trostel, S.Y., Sackett, D.L., and Fojo, T. (2006). Oligomerization of p53 precedes its association with dynein and nuclear accumulation. Cell Cycle *5*, 2253-2259.

Tynan, S.H., Gee, M.A., and Vallee, R.B. (2000). Distinct but overlapping sites within the cytoplasmic dynein heavy chain for dimerization and for intermediate chain and light intermediate chain binding. J Biol Chem *275*, 32769-32774.

Vale, R.D. (2003). The molecular motor toolbox for intracellular transport. Cell *112*, 467-480.

Wu, H., Min, J., Zeng, H., Loppnau, P., Weigelt, J., Sundstrom, M., Arrowsmith, C.H., Edwards, A.M., Bochkarev, A., and Plotnikov, A.N. (To be published.). The Crystal Structure of Human methyltransferase 10 domain containing protein. http://www.rcsb.org/pdb/explore.do?structureId=2H00.

Table 1: An RNAi screen of METT-10 yeast two-hybrid interactors reveals multiple inhibitors of proliferative fate

gene name	COSMID	%Tum (*rrf-1(pk1417); glp-1(oz264)* (n)	%Tum *GFP(RNAi)* control (n)	two-tailed p-value
	R07B7.2	16.9(130)	14.6(96)	0.71
dlc-1	T26A5.9	87.5(88)	11.8(76)	<0.0001*
pqn-59	R119.4	58.8(216)	14.9(262)	<0.0001*
plk-1	C14B9.4	22.5(80)	26.9 (26)	0.79
vab-3[#]	F14F3.1	7.9(68)	13.8(50)	0.26
eya-1[#]	C49A1.4	18.8(154)	12.3(138)	0.15
npp-9	F59A2.1	16.7(66)	10.0 (70)	0.31
mpk-1	F43C1.2	0(70)	18(50)	0.0002**
pmk-1	B0218.3	12.8 (86)	11.8 (76)	1
	W03D8.3	6.8(88)	9.6 (94)	0.59
ran-1	K01G5.4	6.9(58)	20.8(96)	0.02**
hrd-1	F55A11.3	51.6(192)	16.7(192)	<0.0001*
scrm-8	K08D10.7	9.7(72)	9.6(94)	1
cks-1	C09G4.3	25.0 (144)	13.1(130)	0.006*
tag-332	Y119C1B.8	62.5(152)	12.3(154)	<0.0001*

All genes are organized by "interactome" branch, with the first row after each division occupied by the gene predicted to be a primary interactor of METT-10.

[#]*vab-3* and *eya-1* are found in two separate interactome branches, and are predicted to directly interact with both *pqn-59* and *npp-9*.

*RNAi treatments that led to significant enhancement of the *glp-1(oz264)* tumorous phenotype.

**RNAi treatments that significantly suppressed *glp-1(oz264)* overproliferation. All animals were scored at 2 days past the L4 stage at 20˚C. p-values were calculated by Fisher's exact test, using simultaneous GFP RNAi treatments to calculate expected values.

Table 2 : transgenic rescue of *mett-10* phenotypes

A. transgene	*mett-10(ok2204)* @ 25˚C % Pvl	% Ste	n	% abnormal gonad shape (n)*
no transgene	98	99	82	30(44)
met-10(wt)::gfp	5	0	38	0(35)
mett-10(5A)::gfp LOW	65	19**	43	n.d.
mett-10(5A)::gfp HIGH	1	0	137	3(32)**
mett-10 (enzymatic-defective,5A)::gfp, line 1	92	98	46	30(43)
mett-10 (enzymatic-defective,5A)::gfp, line 2	97	99	97	n.d.
mett-10(-NLS,5A)::gfp line 1	0	19	42	10(31)**
mett-10(-NLS,5A)::gfp line 2	0	14	36	12(25)

*gonads with one or more ectopic distal protrusions.
**two-tailed p-value, Fisher's exact test < .05
Pvl = protruding vulva, Ste = sterile

B.	% Tumorous germ lines (n)		
transgene	*mett-10(ok2204) (m-z-, 15˚C)*	*mett-10(oz36) (m+z-, 20˚C)*	*glp-1(oz264) mett-10(g38)* (m+z-)
no transgene	0(96)	41(66)	89(47)
met-10(wt)::gfp	0(136)	0(80)	0(56)
mett-10(5A)::gfp LOW	0(86)	0(86)	0(54)
mett-10(5A)::gfp HIGH	0(36)	n.d.	n.d.
mett-10 (enzymatic-defective,5A)::gfp, line 1	0(36)	n.d.	91(84)
mett-10 (enzymatic-defective,5A)::gfp, line 2	0(48)	2(107)	94(83)
mett-10(-NLS, 5A)::gfp, line 1	0(37)	0 (128)	4.3 (94)
mett-10(oz36)::gfp	n.d.	94(90)	n.d.
mett-10(oz36:SV40NLS)::gfp	n.d.	97(74)	n.d.

Table 3: compromising dynein function enhances the tumorous phenotype of the *mett-10(oz36)* mutant

genotype	%Tum	n
A. *dlc-1*[#]		
rrf-1(pk1417); mett-10(oz36); gfp(RNAi)	3	117
rrf-1(pk1417); dlc-1(RNAi)	0	122
rrf-1(pk1417); mett-10(oz36); dlc-1(RNAi)	62	130
B. *dynein heavy chain*[$]		
dhc-1(or195)	0	37
mett-10(oz36)	43	65
dhc-1(or195); glp-1(oz264)	9	22
dhc-1(or195); mett-10(tm2697)	0	35
dhc-1(or195); mett-10(g38)	0	18
dhc-1(or195); mett-10(oj32)	0	26
dhc-1(or195); mett-10(ok2204)	0	65
dhc-1(or195); mett-10(oz36)	100**	46
dhc-1(or195); glp-1(bn18) mett-10(oz36)	0	38
dhc-1(js319)	0	26
dhc-1(js319); glp-1(oz264)	6	17
dhc-1(js319); mett-10(tm2697)	0	59
dhc-1(js319); mett-10(g38)	0	40
dhc-1(js319); mett-10(oj32)	0	30
dhc-1(js319); mett-10(ok2204)	0	24
dhc-1(js319); mett-10(oz36)	76**	42
dhc-1(js319); glp-1(bn18) mett-10(oz36)	0	52
dhc-1(js121); mett-10(oz36)	3	35

[#] Animals were m-z-, i.e. came from homozygous mutant mothers. The *rrf-1(pk1417)* enables germ line restricted RNAi. All RNAi and scoring was carried out at 20˚C.

[$]All animals were m+, i.e. came from mothers carrying a wild type copy of mett-10 and were scored at 2 days past L4 at 20˚C by dissection and DAPI staining.

** indicates significance calculated by Fisher's exact test, using *mett-10(oz36)* alone for expected values.

Table 4: *mett-10* loss-of-function alleles enhance mitotic and meiotic defects of a *dhc-1* allele.

	% Germ lines		
genotype	with polyploid nuclei	with univalents in diakinesis	n
dhc-1(js319)	4	4	26
dhc-1(js319); glp-1(oz264)	5	0	19
dhc-1(js319); mett-10(tm2697)	100	42	59
dhc-1(js319); mett-10(g38)	100	30	40
dhc-1(js319); mett-10(ok2204)	92	8	24
dhc-1(js319); mett-10(oj32)	97	3	30
dhc-1(js319); mett-10(oz36)	100	-	42
dhc-1(js319); glp-1(bn18) mett-10(oz36)	100	12	52

Polyploid nuclei are large and DAPI dense. These are distinct from the enlarged, diffusely staining nuclei indicative of cell cycle arrest observed in *mett-10(-)* mutants.

All animals were m+, i.e. came from mothers carrying a wild type copy of mett-10 and were scored at 2 days past L4.

Figure I

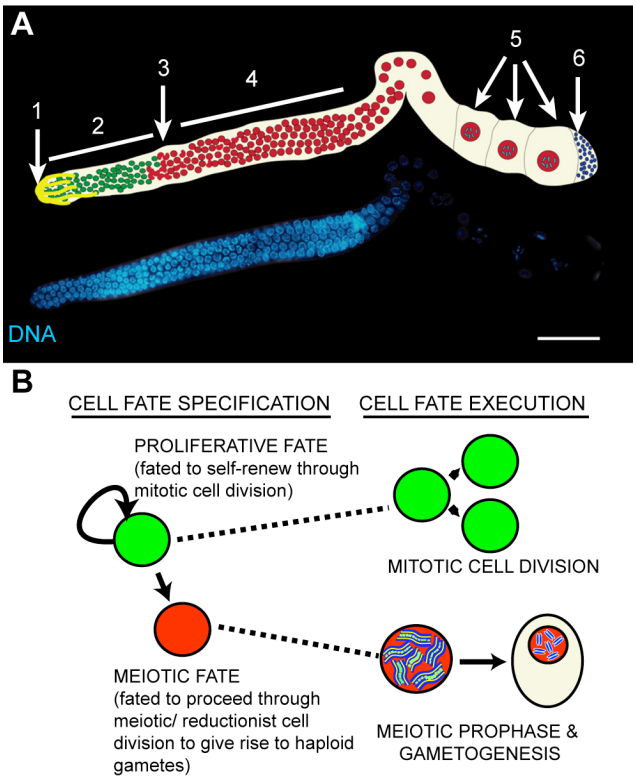

Figure 1. Organization of the *C. elegans* germ line. (A) A fluorescence micrograph of a dissected, DAPI-stained adult *C. elegans* hermaphrodite germ line with schematic. In the distal region proliferating germ cells (2) reside in close contact with the somatic distal tip cell (1). At the transition zone (3), germ cells enter meiosis, and proceed through meiotic prophase (4) to give rise to sperm (6) and oocytes (5). (B) Scheme depicting the decision that *C. elegans* germ line stem cells have to make between maintaining a proliferative fate (green) versus differentiation (red), to produce gametes.

Figure 2

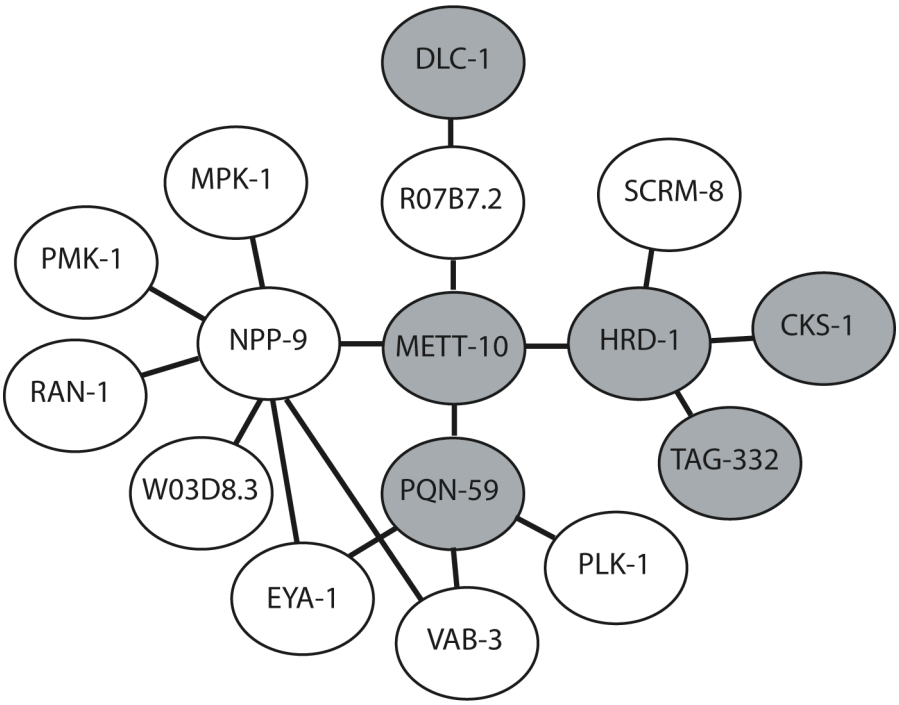

Figure 2. Schematic of yeast two-hybrid interactome for METT-10. Each individual line indicates a direct interaction identified in a genome-wide yeast two-hybrid screen (Li *et al*., 2004). Ovals represent an individual gene. Shaded ovals represent genes whose disruption by either mutation RNAi enhances *glp-1(oz264gf)* overproliferation.

Figure 3. *dlc-1* inhibits proliferative fate in the *C. elegans* germ line. (A) RNAi against *dlc-1* and *dhc-1* enhances tumor formation in the *glp-1(oz264gf)* background at 20˚C, while RNAi against other light chains does not; *dlc-2:* paralog of *dlc-1*; *dylt-1:* Tctex-type dynein light chain; *dyrb-1:* Roadblock-type light chain. Two-tailed p-values determined using Fisher's Exact Test. In wild type germ lines (B) as well as in *dlc-1* RNAi of control animals (C), a 3 hr pulse of the nucleotide analog EdU, which incorporates during DNA synthesis, labels (green) only the very distal end (left) of the germ line, although *dlc-1* RNAi causes polyploid nuclei containing large, dense DNA bodies (white arrow) and unpaired chromosomes in diakinesis. Insets show chromosomal morphology of diakinetic oocytes, with 6 sets of bivalents in oocytes from control germ lines (B), but 12 univalents for *dlc-1* RNAi (C). (D-E) *dlc-1* RNAi causes tumor formation and EdU incorporation throughout the germ line in *glp-1(oz264gf)* (E), while *glp-1(oz264gf)* mutant on its own has only a marginal increase in EdU-incorporation (D). (F-H) Staining against DLC-1 in *glp-1(oz264gf)* animals treated with dsRNA targeting either *gfp* as a control (F) or *dlc-1* (G-H). (G) a tumorous germ line with partial DLC-1 knockdown and unaffected nuclear morphology and (H) a tumorous germ line with strong DLC-1 knockdown and abnormal nuclear morphology. (I) Inset from (H) highlights the large size of abnormal nuclei. Solid arrows indicate large, DNA dense (abnormal) nuclei, and feather arrows indicate nuclei of relatively normal size. (J) Quantification of DLC-1 levels by pixel intensity for *glp-1(oz264gf); gfp(RNAi)* germ lines (white bar), *glp-1(oz264gf);dlc-1(RNAi)* tumorous germ lines with normal nuclear morphology (black

bar), and *glp-1(oz264gf);dlc-1(RNAi)* tumorous germ lines with abnormal nuclear morphology (grey bar). Error bars indicate the SEM. All scale bars = 20 microns.

Figure 3

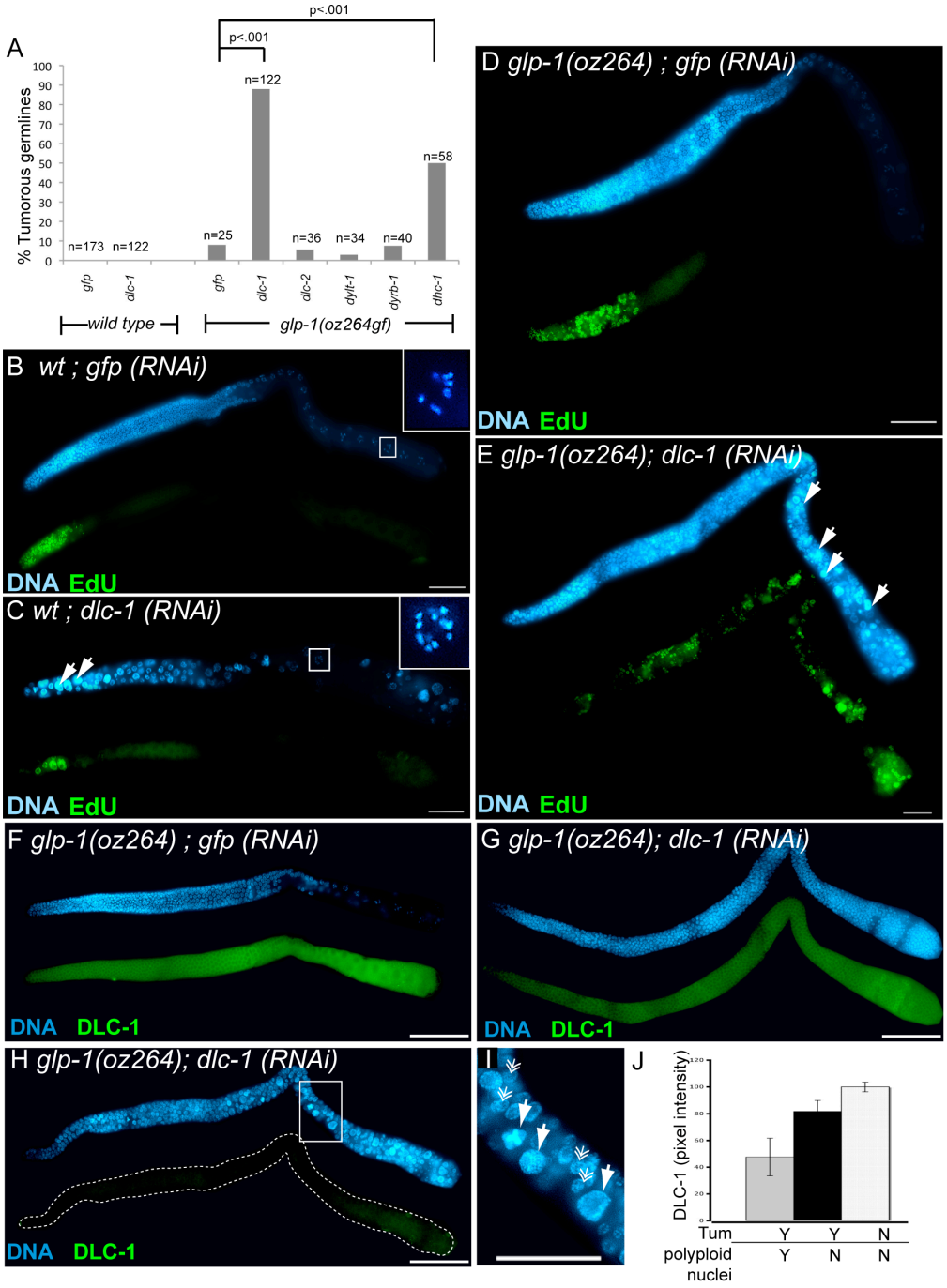
A
p<.001
p<.001
% Tumorous germlines
n=173
n=122
n=25
n=122
n=36
n=34
n=40
n=58
gfp
dlc-1
gfp
dlc-1
dlc-2
dylt-1
dynb-1
dhc-1
wild type
glp-1(oz264gf)
B wt ; gfp (RNAi)
DNA EdU
C wt ; dlc-1 (RNAi)
DNA EdU
D glp-1(oz264) ; gfp (RNAi)
DNA EdU
E glp-1(oz264); dlc-1 (RNAi)
DNA EdU
F glp-1(oz264) ; gfp (RNAi)
DNA DLC-1
G glp-1(oz264); dlc-1 (RNAi)
DNA DLC-1
H glp-1(oz264); dlc-1 (RNAi)
DNA DLC-1
I
J
DLC-1 (pixel intensity)
Tum
polyploid nuclei
Y Y N
Y N N

Figure 4. DLC-1 promotes METT-10 nuclear accumulation. (A) METT-10::GFP expression in a wild type germ line. (B) *dlc-1* RNAi causes a decrease in METT-10::GFP accumulation, abnormal nuclear morphology (left panel), and unpaired chromosomes in diakinesis (right panel, yellow arrows). (C) METT-10::GFP nuclear accumulation is delayed in the *dhc-1(or195)* mutant background, with nuclear accumulation observed only in late pachytene. Solid and feather arrows indicate nuclei positive and negative for METT-10::GFP, respectively (D) IP-westerns for METT-10:GFP levels in whole animals subject to both control (empty vector) RNAi as well as *dlc-1(RNAi)*. CGH-1 is a germ line ubiquitous protein. (E) qRT-PCR for *dlc-1* and *mett-10* normalized to *cgh-1* mRNA levels. RNAi was carried out in the *rrf-1(pk1417)* background, which retains RNAi only in the germ line. (F) METT-10(5A)::GFP protein is reduced in germ line nuclei, although some nuclear METT-10 (5A):GFP is observed in nuclei of the somatic gonad (see circled sheath cell nucleus). At variable penetrance, abnormal, DNA-dense nuclei similar to those observed for *dlc-1 (RNAi)* are seen at the distal end. Germ line shown is more severe than most.

Figure 4

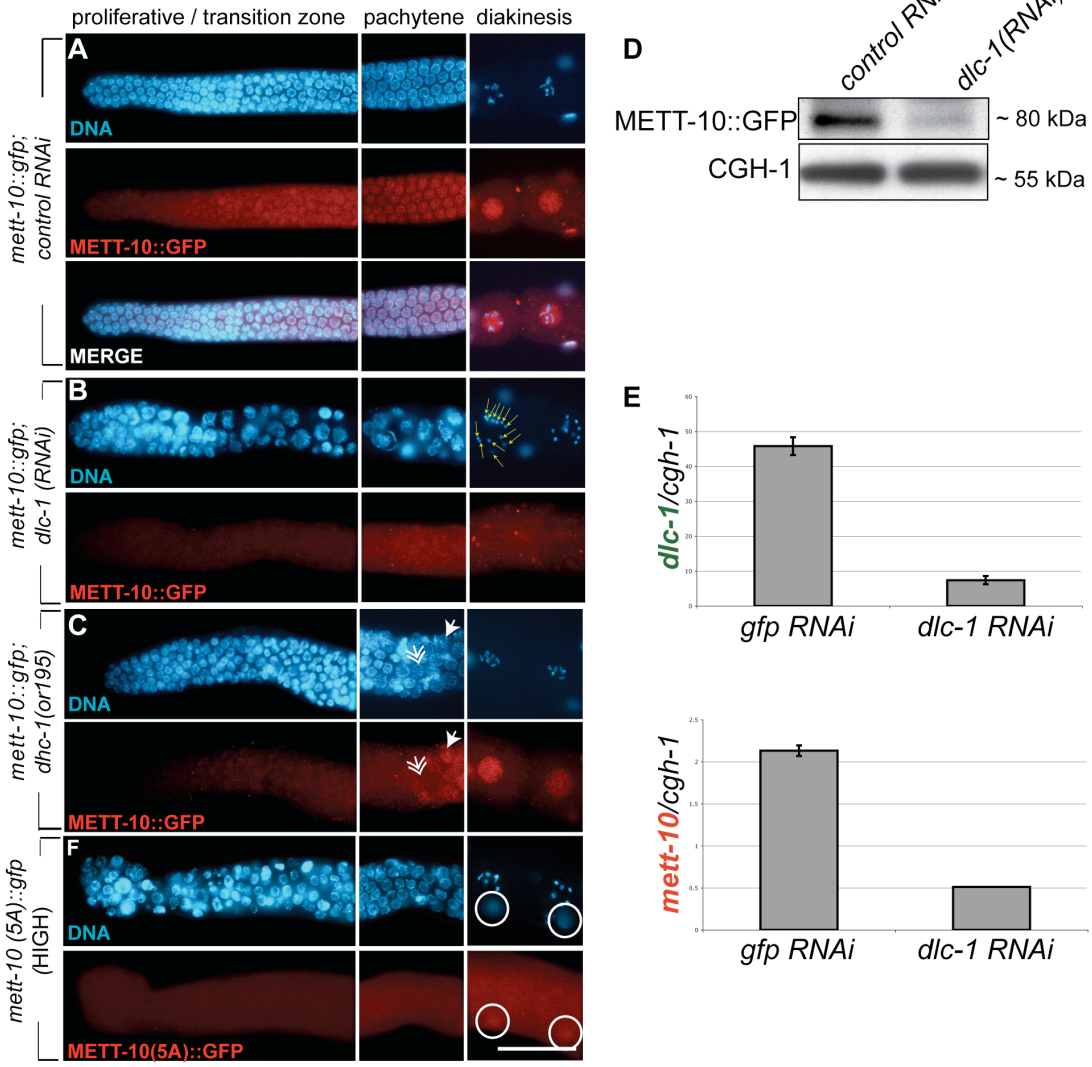
proliferative / transition zone
pachytene
diakinesis
A
DNA
METT-10::GFP
MERGE
mett-10::gfp; control RNAi
B
DNA
METT-10::GFP
mett-10::gfp; dlc-1 (RNAi)
C
DNA
METT-10::GFP
mett-10::gfp; dhc-1(or195)
F
DNA
METT-10(5A)::GFP
mett-10 (5A)::gfp (HIGH)
D
control RNAi
dlc-1(RNAi)
METT-10::GFP
~ 80 kDa
CGH-1
~ 55 kDa
E
dlc-1/cgh-1
gfp RNAi
dlc-1 RNAi
mett-10/cgh-1
gfp RNAi
dlc-1 RNAi

Figure 5. METT-10 binds DLC-1 *in vitro*. (A) Full length 6X-HIS METT-10 is pulled down by GST-DLC-1, weakly pulled down by GST-DLC-2, and not by GST-DYLT-1 or GST-DYRB-1. (B) GST-DLC-1 point mutants (Coomassie) were assayed for binding to full length 6XHIS-METT-10 proteins. (C) A dimeric band (feathered arrow) is observed when full length 6X-HIS-METT-10 is pulled down with GST-DLC-1 and full length GST-METT-10. (D) Fine mapping of the DLC-1 binding domain of METT-10 using GST-pulldown analysis analogous to that shown in (A). The identity of individually-mutated METT-10 residues are labeled on the left.

Figure 5

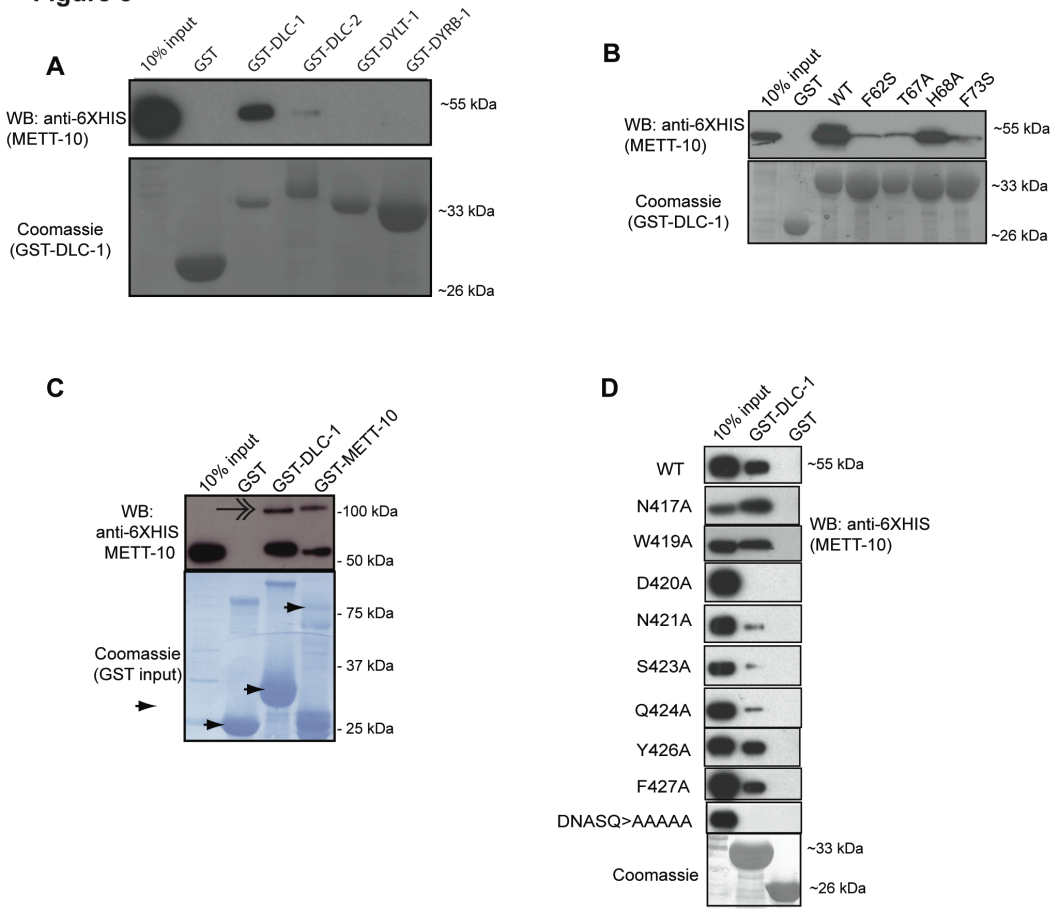
A
10% input
GST
GST-DLC-1
GST-DLC-2
GST-DYLT-1
GST-DYRB-1
WB: anti-6XHIS
(METT-10)
~55 kDa
Coomassie
(GST-DLC-1)
~33 kDa
~26 kDa
B
10% input
GST
WT
F62S
T67A
H68A
F73S
WB: anti-6XHIS
(METT-10)
~55 kDa
Coomassie
(GST-DLC-1)
~33 kDa
~26 kDa
C
10% input
GST
GST-DLC-1
GST-METT-10
WB:
anti-6XHIS
METT-10
-100 kDa
- 50 kDa
- 75 kDa
Coomassie
(GST input)
- 37 kDa
- 25 kDa
D
10% input
GST-DLC-1
GST
WT
N417A
W419A
D420A
N421A
S423A
Q424A
Y426A
F427A
DNASQ>AAAAA
~55 kDa
WB: anti-6XHIS
(METT-10)
Coomassie
~33 kDa
~26 kDa

Figure 6. METT-10 can form multimers. (A) Western blot analysis on bacterially expressed 6XHIS-METT-10 fusion proteins reveals bands that run at the size of monomers (*) and dimers ($). (B) GST pulldown analysis between METT-10 protein fragments. The C-terminal METT-10 protein fragment (aa 272-479) binds full length and METT-10(oz36) (aa 1-271) protein fragments (gel on left). Feathered arrow indicates that 6XHIS-METT-10(C-term) runs at the size of a dimer. 6XHIS-METT-10(oz36) protein fragment can bind a GST-tagged METT-10(oz36) fragment, but no dimeric band is observed (gel on right).

Figure 6

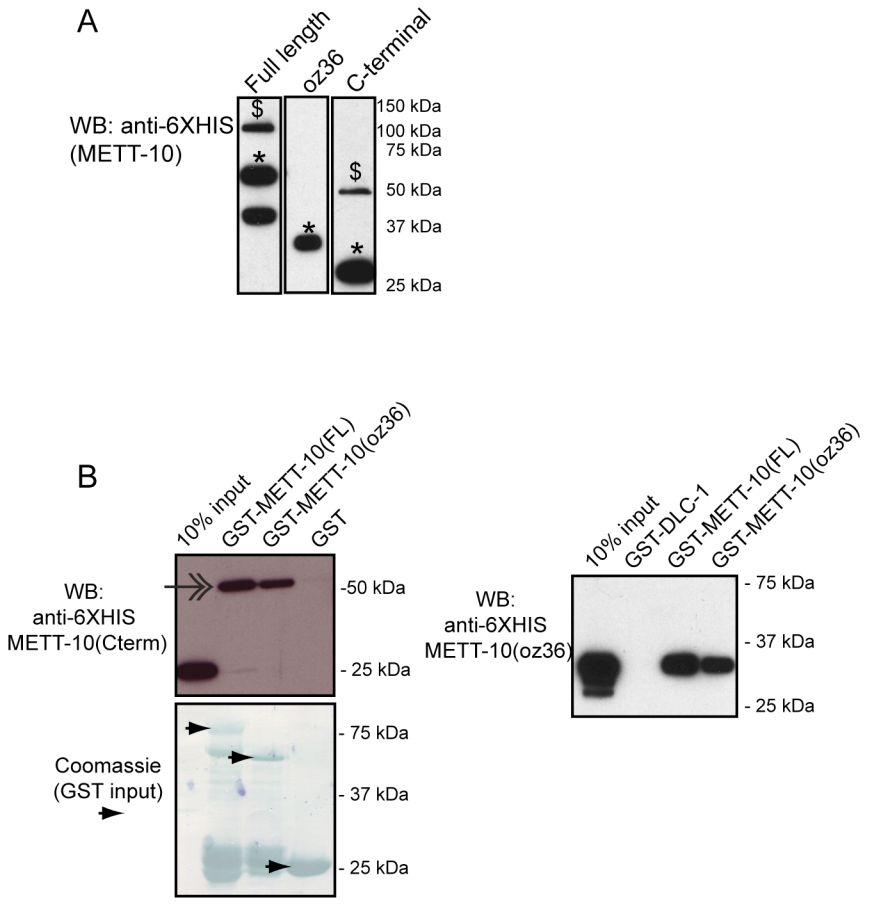
A
Full length
oz36
C-terminal
WB: anti-6XHIS
(METT-10)
$
*
$
*
*
150 kDa
100 kDa
75 kDa
50 kDa
37 kDa
25 kDa
B
10% input
GST-METT-10(FL)
GST-METT-10(oz36)
GST
WB:
anti-6XHIS
METT-10(Cterm)
-50 kDa
- 25 kDa
Coomassie
(GST input)
- 75 kDa
- 37 kDa
- 25 kDa
10% input
GST-DLC-1
GST-METT-10(FL)
GST-METT-10(oz36)
WB:
anti-6XHIS
METT-10(oz36)
- 75 kDa
- 37 kDa
- 25 kDa

Figure 7. METT-10 and DLC-1 do not co-localize *in vivo*. Scanning-Laser Confocal images of germ cells in meiotic pachytene co-stained with an antibodies against METT-10::GFP (green) DLC-1 (red), and DAPI to visualize DNA (blue). (A) DLC-1 is a predominantly cytoplasmic protein, although some nuclear puncta are observed, agreeing with previous findings in mammalian cells (Rayala *et al*., 2005). (B) METT-10::GFP is predominantly nucleocytoplasmic in pachytene germ cells, although there appears to be some punctate staining within the nucleus as well. (C) Merge of (A) and (B). METT-10::GFP and DLC-1 do not colocalize; rather, nuclear puncta appear to be adjacent to one another. (D) Neither DLC-1 nor METT-10::GFP puncta extensively co-localize with DNA.

Figure 7

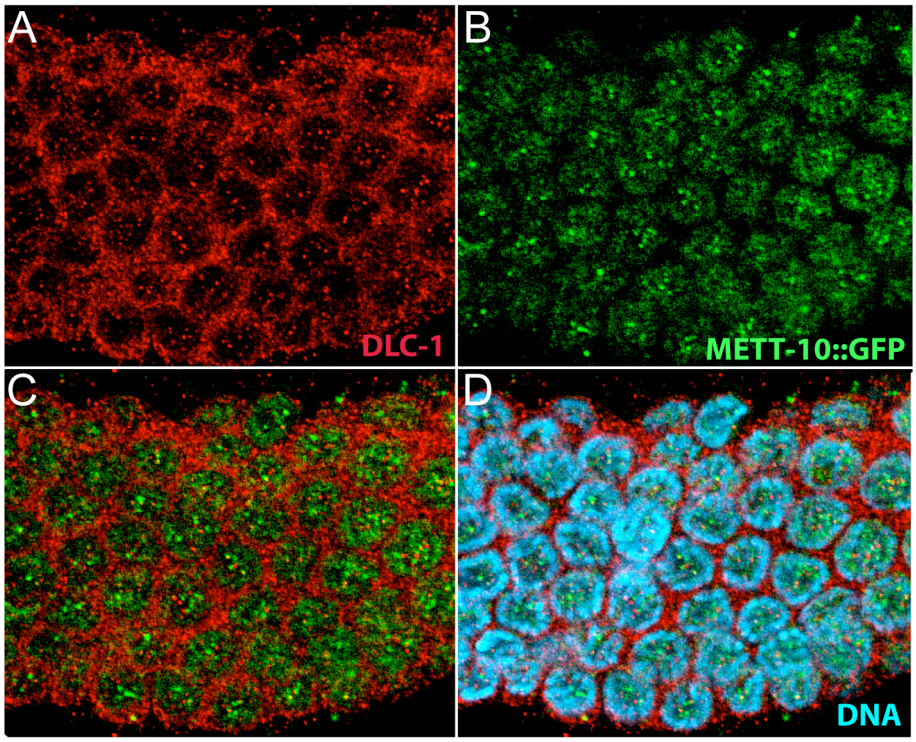

Figure 8. A dual mechanism ensures METT-10 nuclear accumulation. (A) Domain architecture of METT-10 marked with protein sequence change caused by *mett-10(oz36)* and location of the DLC-1 binding motif. Gray shading highlights the conserved methyltransferase-10 domain, and purple indicates the nuclear localization consensus sequence. (B-G) Confocal images (0.3 microns) of wild type and mutant METT-10::GFP expression in gonadal sheath cells stained with antibodies against GFP and lamin to visualize nuclear membrane.

Figure 8

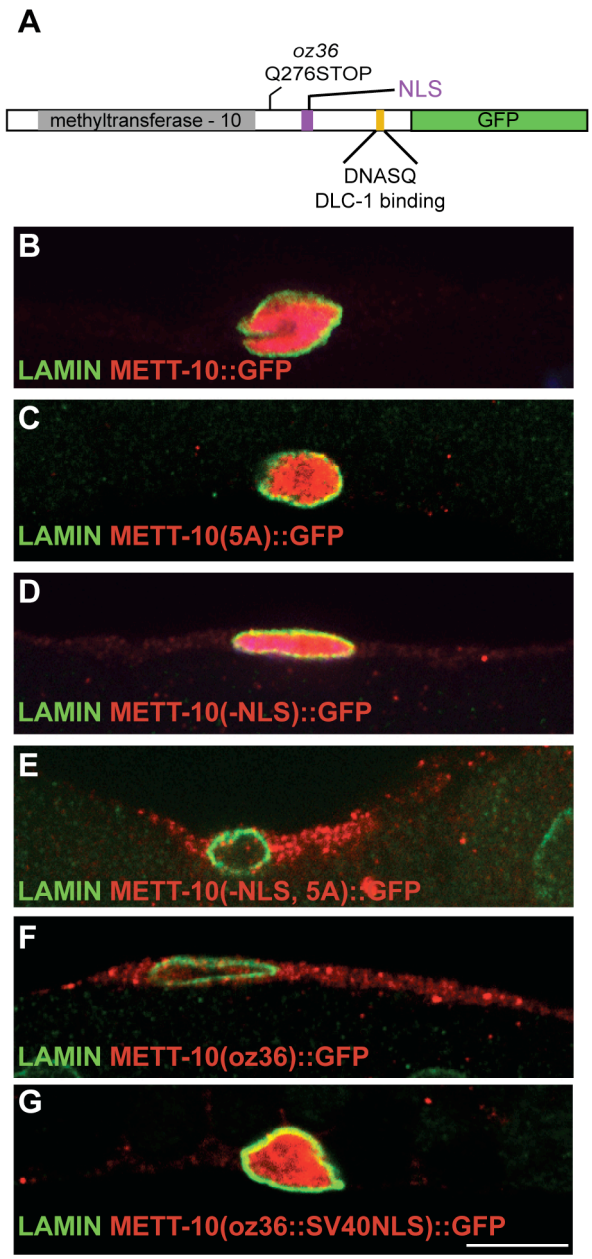
A
oz36
Q276STOP
NLS
methyltransferase - 10
GFP
DNASQ
DLC-1 binding
B
LAMIN METT-10::GFP
C
LAMIN METT-10(5A)::GFP
D
LAMIN METT-10(-NLS)::GFP
E
LAMIN METT-10(-NLS, 5A)::GFP
F
LAMIN METT-10(oz36)::GFP
G
LAMIN METT-10(oz36::SV40NLS)::GFP

Figure 9. Measurements of *mett-10* transgenic and endogenous expression. (A) qRT-PCR analysis for levels of endogenous and transgenic *mett-10* expression. All transgenes were crossed into the *mett-10(ok2204)* background, which contains a large deletion of the N-terminal portion of the gene. Primers corresponding to this deleted region were used to measure gene expression (see Methods). These primers amplify the endogenous gene in a wild type genetic background, and only the transgene in the *mett-10(ok2204); mett-10::gfp* genetic background. Expression values shown correspond to a calculated ratio of *mett-10* to *actin* expression, with endogenous gene expression normalized to a value of 1 (see Methods). (B) IP-Westerns of wild type and *mett-10(5A)::gfp* transgenes.

Figure 9

A

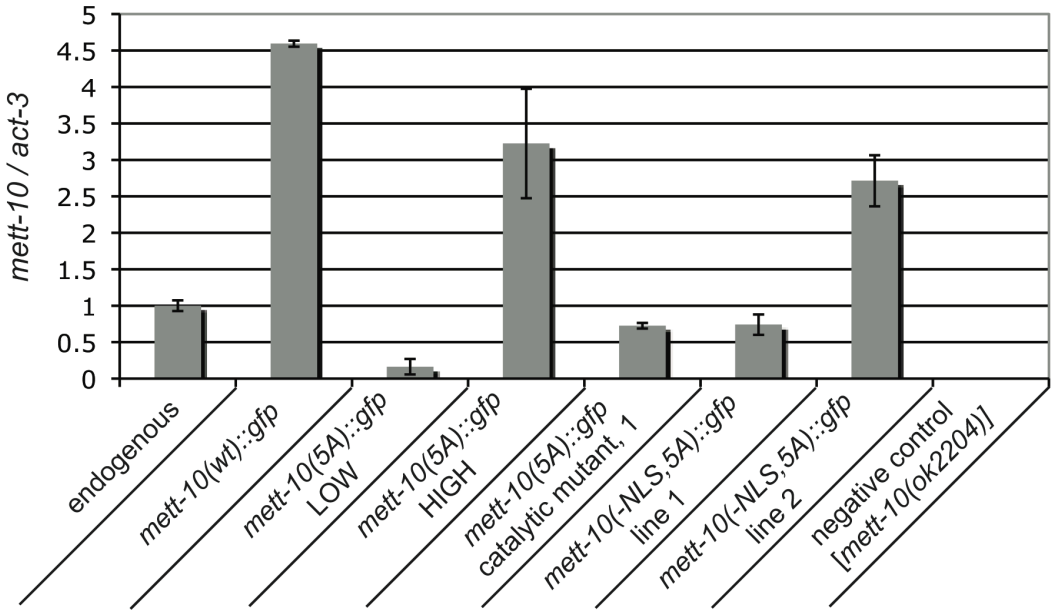
mett-10 / act-3
5
4.5
4
3.5
3
2.5
2
1.5
1
0.5
0
endogenous
mett-10(wt)::gfp
mett-10(5A)::gfp LOW
mett-10(5A)::gfp HIGH
mett-10(5A)::gfp catalytic mutant, 1
mett-10(-NLS,5A)::gfp line 1
mett-10(-NLS,5A)::gfp line 2
negative control [mett-10(ok2204)]

B

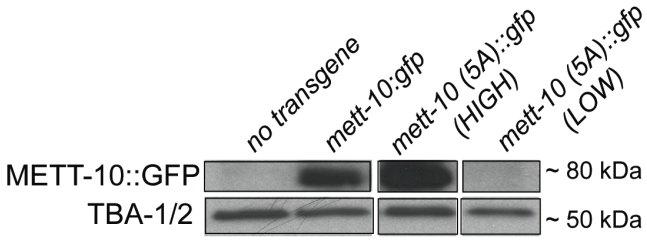
no transgene
mett-10:gfp
mett-10 (5A)::gfp (HIGH)
mett-10 (5A)::gfp (LOW)
METT-10::GFP
TBA-1/2
~ 80 kDa
~ 50 kDa

Figure 10

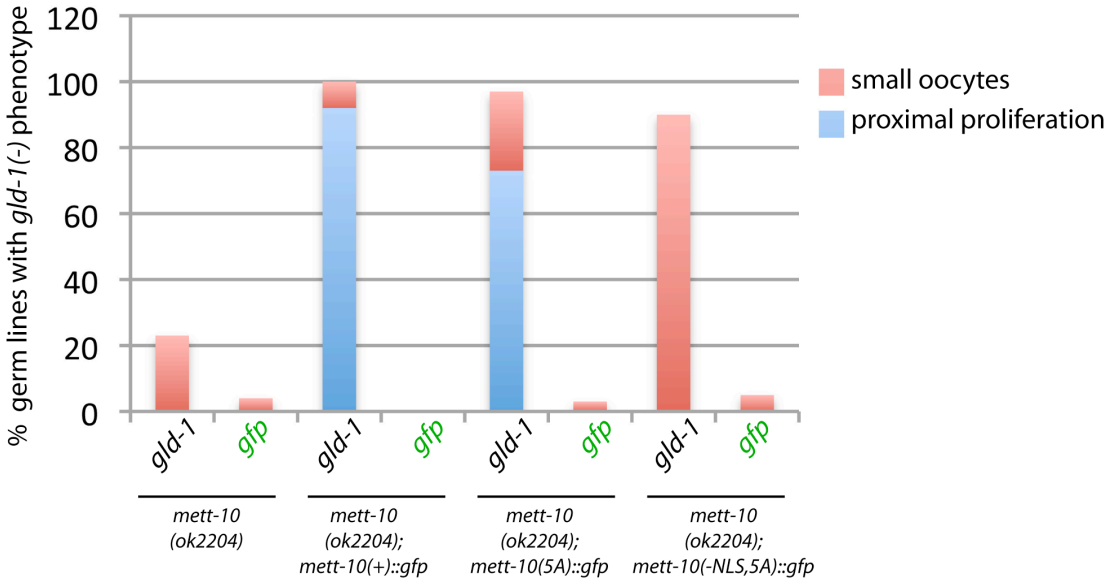

Figure 10. A cytoplasmic version of METT-10 can partially suppress the *mett-10(ok2204)* RNAi-resistance phenotype. *mett-10(ok2204)* animals carrying either wild type *mett-10::gfp*, *mett-10(5A)::gfp*, or *mett-10(-NLS, 5A)::gfp* were fed dsRNA directed against the germ line –expressed gene, *gld-1*. F1 animals were scored for two phenotypes associated with *gld-1* disruption: small oocytes (less severe) and ectopic proximal proliferation (more severe).

Figure 11

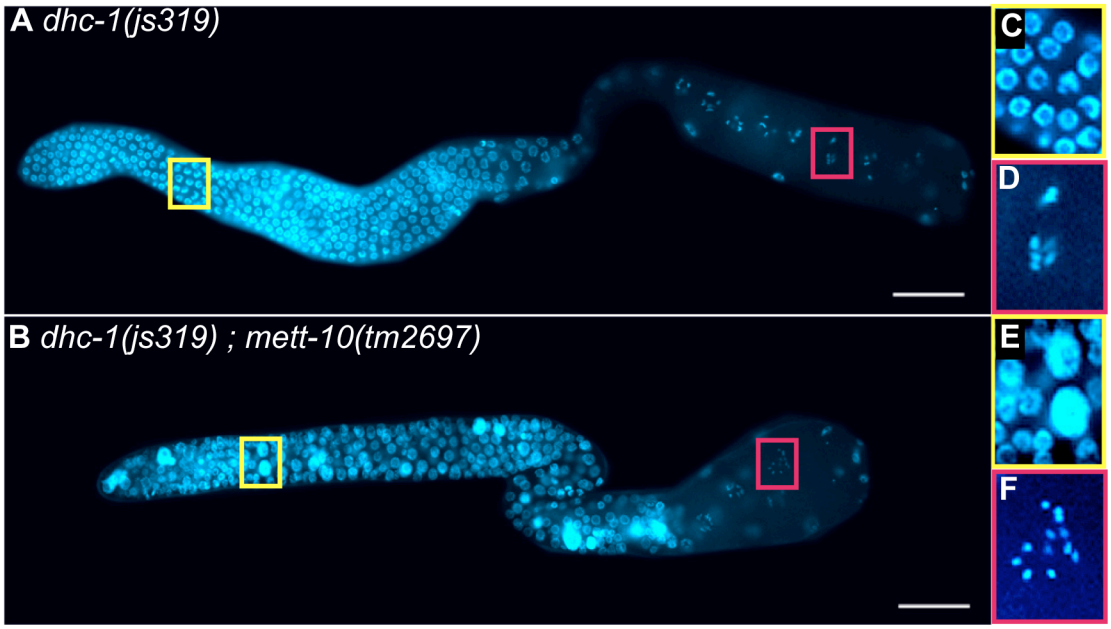

Figure 11. *mett-10* mutants enhance dynein loss-of-function phenotypes of the *dhc-1(js319)* allele. (A, C-D) Most *dhc-1(js319)*mutant germ lines are relatively normal at both 20 and 25˚C, although they exhibit polyploidy (large DNA-dense nuclei) and univalent (unpaired chromosomes in diakinesis) at very low penetrance. (B, E-F) Double mutants between *dhc-1(js319)* and any *mett-10* allele leads to significant enhancement of both these phenotypes, and all double mutant animals are sterile. This set of phenotypes closely phenocopies loss of *dlc-1* function in the germ line.

Figure 12. Schematic of *dynein heavy chain-1* mutations. (A) Diagram of intron/exon structure of the *dhc-1* locus, with encoded protein domains. The N-terminal tail region contains that binding sites for Dynein Intermediate Chain (DIC) and Dynein Light Intermediate Chain (LIC) (blue) (Tynan *et al*., 2000). These are followed by the first four ATPase domains containing consensus P-loop sequences (yellow), followed by the microtubule stalk and globular microtubule binding domain (red) (Koonce and Tikhonenko, 2000). Locations of the nucleotide changes in *dhc-1(js121)*, *dhc-1(or195)*, and *dhc-1(js319)* are shown. (B) Model of Dynein Heavy Chain with location of mutant alleles. If we assume that the splice acceptor mutations lead to exon skipping, *dhc-1(js121)* would lead to a deletion within the linker domain, while *dhc-1(js319)* would truncate DHC-1 C-terminal to the 5th and 6th ATPase-like domains.

Figure 12

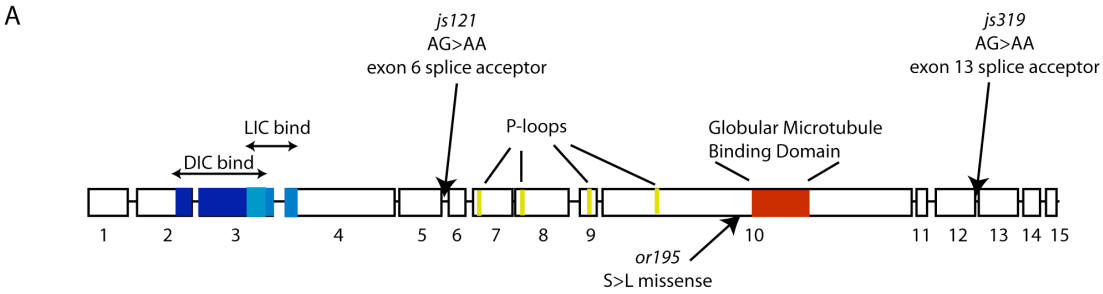
A
js121
AG>AA
exon 6 splice acceptor
js319
AG>AA
exon 13 splice acceptor
LIC bind
DIC bind
P-loops
Globular Microtubule
Binding Domain
1 2 3 4 5 6 7 8 9 10 11 12 13 14 15
or195
S>L missense

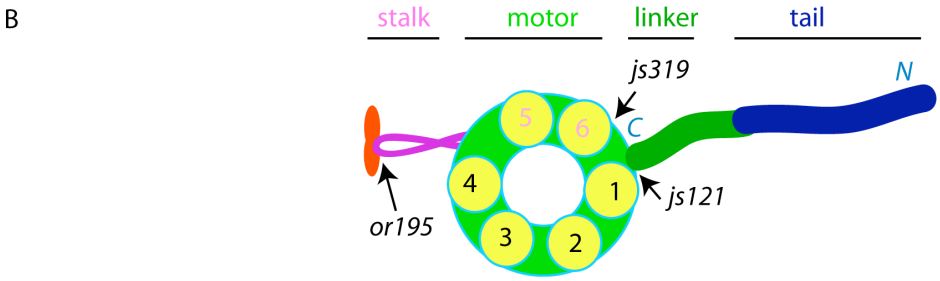
B
stalk
motor
linker
tail
js319
N
C
5
6
4
1
3
2
or195
js121

Chapter 4 (Discussion):

The Pleiotropic Consequences of *mett-10* Disruption

"Always the beautiful answer who asks a more beautiful question."

-e.e. cummings, 1938

The goal of development is to build and maintain an organism. METT-10 is an interesting protein in that it plays roles in both the construction and maintenance of *C.elegans*. In addition to an essential role in development of the embryo, vulva, and somatic gonad, METT-10 regulates germ cell proliferation and promotes the production of gametes by ensuring normal mitotic cell cycle progression and meiotic development. These essential functions of METT-10 in germ cells maintain the gamete population in adult life and the species in general.

Although our initial interest in *mett-10* centered on its function in proliferative fate specification, the studies presented here uncovered additional cellular roles in RNA interference, dynein function in mitosis and meiosis, cell cycle progression, and meiotic development. A central question that arises from these findings is whether a single cellular function underlies the diversity of *mett-10* phenotypes and whether some phenotypes are the downstream consequences of another. Alternatively, these cellular functions and their associated phenotypes might be separable and independent. Understanding the causal relationship between underlying cellular function and phenotype will enhance our understanding of the construction and maintenance of the organism as a functioning whole, and the imbalance that underlies disease.

Methyltransferase activity likely underlies all cellular functions of METT-10

METT-10 most likely functions as a methyltransferase. It contains a full SAM-dependent methyltransferase fold and the human homolog binds SAM (Wu *et*

al., To be published.). Significantly, the *oj32* allele mutates a highly conserved glycine that forms the core of the SAM-binding pocket, and is predicted to reduce methyltransferase activity. The *mett-10(oj32)* mutant exhibits defects in proliferative fate specification, RNA interference, cell cycle progression, and promotion of dynein function, suggesting that methyltransferase activity underlies all METT-10 cellular functions (Figure 1). We do not know what METT-10 methylates, or the functional consequence of methylation, but it is likely that METT-10 has multiple targets. This is supported by the phenotype of the tumorous *mett-10(oz36)* mutant, which preferentially affects proliferative fate specification under lower temperature conditions.

Joint functions of METT-10 and dynein in the *C. elegans* germ line

DLC-1 and METT-10 cooperatively inhibit proliferative cell fate (Figure 1). DLC-1 interacts physically with METT-10, promotes *mett-10* RNA levels, and, in the context of the motor complex, promotes METT-10 nuclear localization. Moreover, the role of dynein in regulation of proliferative fate is not limited to regulation of METT-10 alone, as genetic disruption of either *dlc-1* or *dhc-1* can enhance the tumorous phenotype of the *mett-10(oz36)* mutant that lacks the DLC-1-binding motif.

In addition to a joint function in proliferative fate specification, METT-10 promotes other dynein-dependent processes (Figure 1). Loss of *mett-10* function enhances the mitotic and meiotic defects of a weak dynein heavy chain loss-of-function allele, leading to polyploidy and unpaired diakinetic chromosomes.

Expression of a METT-10 protein that is unable to bind DLC-1 acts as a dominant negative and causes germ cell polyploidy, suggesting that it may disrupt a DLC-1-containing complex. Finally, the *mett-10(oj32)* loss-of-function allele has a defect in centrosome flattening, a dynein-dependent process, during the first embryonic division (O'Connell *et al*., 1998).

The genetic interactions between *mett-10* and *dlc-1* in proliferative fate specification, mitotic cell division, and meiosis suggest that these different cellular functions may have a common underlying mechanism. However, the experiments presented here delineate a role for DLC-1 in promoting METT-10 activity during proliferative fate specification, and a role for METT-10 in promoting DLC-1 activity during cell division and meiotic pairing and/or recombination. The most parsimonious interpretation of these findings is that METT-10 promotes DLC-1 activity, which, in turn, promotes METT-10 function in a positive feedback loop (Figure 2).

How could METT-10 affect DLC-1 function? DLC-1 is an LC8-type dynein light chain, which exists as a dimer when associated with the dynein motor complex (Vale, 2003). Two models have been proposed for the role of the LC8 dynein light chain with respect to the dynein motor complex. One model suggests that LC8 dimers act as dimerization hubs, binding to regions of intrinsic disorder in a diverse set of proteins, leading to increased structural organization and dimerization (Wang *et al*., 2004; Barbar, 2008). This model proposes that LC8 promotes normal dynein function by promoting dimerization of the dynein intermediate chain (Barbar, 2008; King,

2008). Indeed, since METT-10 can simultaneously bind to itself and to DLC-1, it is possible that DLC-1 promotes METT-10 dimerization *in vivo*. A second model proposes that DLC-1/LC8 functions as a cargo adaptor molecule, enabling the association of the dynein motor complex with a wide spectrum of proteins (Karki and Holzbaur, 1999; Navarro *et al*., 2004; Lee *et al*., 2006). The unifying theme of both models is that DLC-1 carries out multiple cellular functions by binding to and regulating the function of a diverse set of target proteins. It is possible that METT-10 methylates targets of the dynein motor complex, and that this methylation event promotes their association with DLC-1 or the motor complex. Alternatively, METT-10 and DLC-1 could coordinately regulate target proteins by coupling multiple modes of regulation, such as post-translational modification and subcellular localization. In both cases, association with dynein would enhance METT-10 function, but may not be essential.

The relationship of RNA interference to other METT-10 cellular functions

Small RNAs play broad roles in development, and given their roles in regulation of gene expression and chromatin structure, it is no surprise that defects in RNA-mediated silencing lead to widespread alterations in development (Zamore and Haley, 2005) . Indeed, the microRNA pathway was first characterized for its role in developmental timing, and many RNAi genes, particularly the Argonaute family of proteins, play essential and conserved roles in germ line maintenance and function (Lee *et al*., 1993; Deng and Lin, 2002; Yigit *et al*., 2006). Moreover, multiple RNAi

mutants exhibit cell division defects that are thought to arise from function of RNA-mediated silencing in regulation of chromatin structure (Zamore and Haley, 2005; Yigit *et al*., 2006). Thus, while the role of METT-10 in RNAi is unlikely to completely account for its function in proliferative fate specification (see Discussion, Chapter 2), it probably contributes to the gross morphological defects observed in *mett-10* mutants (Figure 1).

Could there be any functional overlap between the roles of METT-10 in RNAi and in dynein function? While we did not detect an RNAi defect for multiple alleles of *dynein heavy chain-1* (data not shown), several emerging lines of evidence point to a functional connection between RNAi-related processes and the cytoskeleton. In *Drosophila* germ cells, defects in the piRNA pathway lead to the formation of large aggregates of dynein heavy chain in the cytoplasm (Navarro *et al*., 2009). Moreover, two different RNAi screens have identified roles for cytoskeletal factors in promoting RNA-mediated silencing pathways. For example, a group of genes that act in the dynein–dependent pathway mediating asymmetric division and centrosome flattening (*lin-5* and *gpr-1/2*) can promote transgene silencing (Kim *et al*., 2005), while roles for tubulin, dynactin, and various dynein subunits are proposed to mediate *lin-14* silencing via the microRNA pathway (Parry *et al*., 2007). Thus, it is possible that the dual roles of METT-10 in dynein function and RNAi are not coincidental, and further investigation may illuminate a mechanism underlying the functional connections between the cytoskeleton and RNA-mediated silencing.

A complete picture?

An organism is less the sum of its component parts than it is the sum of their connections. Homeostasis and survival require not just that individual organs or tissues are connected, but that all cellular pathways are connected to each other in a network. Genome-wide studies of gene expression and physical association of proteins can drive our ideas of how such vast networks are organized, but in depth studies of genes like *mett-10* whose roles span seemingly disparate cellular functions may eventually make concrete contributions to our understanding of the complex interactions between cellular machinery, gene regulatory mechanisms, and the phenotypic consequences of their disruption.

REFERENCES

Barbar, E. (2008). Dynein light chain LC8 is a dimerization hub essential in diverse protein networks. Biochemistry *47*, 503-508.

Deng, W., and Lin, H. (2002). miwi, a murine homolog of piwi, encodes a cytoplasmic protein essential for spermatogenesis. Dev Cell *2*, 819-830.

Karki, S., and Holzbaur, E.L. (1999). Cytoplasmic dynein and dynactin in cell division and intracellular transport. Curr Opin Cell Biol *11*, 45-53.

Kim, J.K., Gabel, H.W., Kamath, R.S., Tewari, M., Pasquinelli, A., Rual, J.F., Kennedy, S., Dybbs, M., Bertin, N., Kaplan, J.M., Vidal, M., and Ruvkun, G. (2005). Functional genomic analysis of RNA interference in C. elegans. Science *308*, 1164-1167.

King, S.M. (2008). Dynein-independent functions of DYNLL1/LC8: redox state sensing and transcriptional control. Sci Signal *1*, pe51.

Lee, K.H., Lee, S., Kim, B., Chang, S., Kim, S.W., Paick, J.S., and Rhee, K. (2006). Dazl can bind to dynein motor complex and may play a role in transport of specific mRNAs. EMBO J *25*, 4263-4270.

Lee, R.C., Feinbaum, R.L., and Ambros, V. (1993). The C. elegans heterochronic gene lin-4 encodes small RNAs with antisense complementarity to lin-14. Cell *75*, 843-854.

Navarro, C., Bullock, S., and Lehmann, R. (2009). Altered dynein-dependent transport in piRNA pathway mutants. Proc Natl Acad Sci U S A.

Navarro, C., Puthalakath, H., Adams, J.M., Strasser, A., and Lehmann, R. (2004). Egalitarian binds dynein light chain to establish oocyte polarity and maintain oocyte fate. Nat Cell Biol *6*, 427-435.

O'Connell, K.F., Leys, C.M., and White, J.G. (1998). A genetic screen for temperature-sensitive cell-division mutants of Caenorhabditis elegans. Genetics *149*, 1303-1321.

Parry, D.H., Xu, J., and Ruvkun, G. (2007). A whole-genome RNAi Screen for C. elegans miRNA pathway genes. Curr Biol *17*, 2013-2022.

Vale, R.D. (2003). The molecular motor toolbox for intracellular transport. Cell *112*, 467-480.

Wang, L., Hare, M., Hays, T.S., and Barbar, E. (2004). Dynein light chain LC8 promotes assembly of the coiled-coil domain of swallow protein. Biochemistry *43*, 4611-4620.

Wu, H., Min, J., Zeng, H., Loppnau, P., Weigelt, J., Sundstrom, M., Arrowsmith, C.H., Edwards, A.M., Bochkarev, A., and Plotnikov, A.N. (To be published.). The Crystal Structure of Human methyltransferase 10 domain containing protein. http://www.rcsb.org/pdb/explore.do?structureId=2H00.

Yigit, E., Batista, P.J., Bei, Y., Pang, K.M., Chen, C.C., Tolia, N.H., Joshua-Tor, L., Mitani, S., Simard, M.J., and Mello, C.C. (2006). Analysis of the C. elegans Argonaute family reveals that distinct Argonautes act sequentially during RNAi. Cell *127*, 747-757.

Zamore, P.D., and Haley, B. (2005). Ribo-gnome: the big world of small RNAs. Science *309*, 1519-1524.

Figure 1. A model for the pleiotropic consequences of *mett-10* disruption.

METT-10 plays roles in multiple cellular processes, but the relationship between these processes (yellow), their underlying mechanisms (orange), and the phenotypic consequences of their disruption (green) are not well understood. It is likely that METT-10 methyltransferase activity (red) is essential for all METT-10 functions, that METT-10 has multiple targets, that there is significant interplay between these functions, and that the phenotypic effects of *mett-10* disruption are the downstream consequence of multiple underlying cellular defects. In the diagram, line thickness represents strength of experimental evidence supporting the functional connection, with dotted lines have the least supporting experimental evidence.

Figure 1

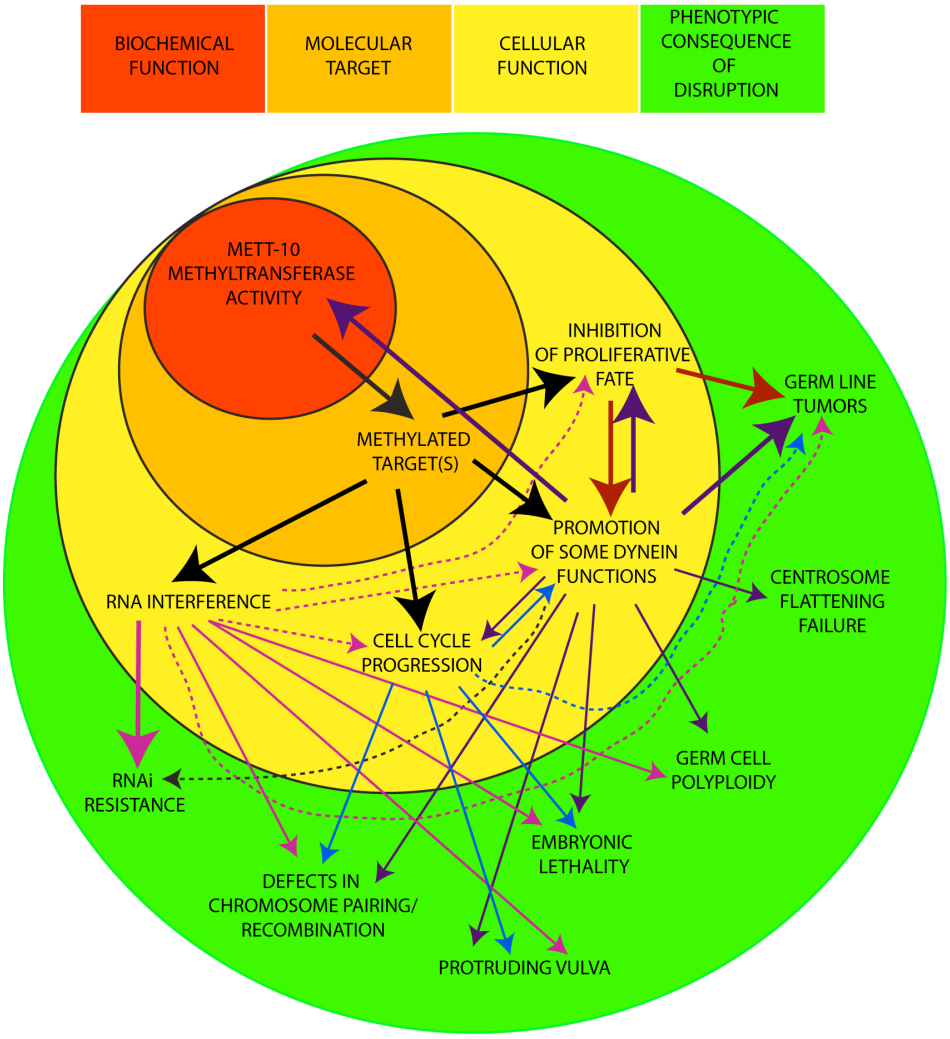
BIOCHEMICAL FUNCTION
MOLECULAR TARGET
CELLULAR FUNCTION
PHENOTYPIC CONSEQUENCE OF DISRUPTION
METT-10 METHYLTRANSFERASE ACTIVITY
METHYLATED TARGET(S)
INHIBITION OF PROLIFERATIVE FATE
GERM LINE TUMORS
PROMOTION OF SOME DYNEIN FUNCTIONS
CENTROSOME FLATTENING FAILURE
RNA INTERFERENCE
CELL CYCLE PROGRESSION
GERM CELL POLYPLOIDY
RNAi RESISTANCE
EMBRYONIC LETHALITY
DEFECTS IN CHROMOSOME PAIRING/ RECOMBINATION
PROTRUDING VULVA

Figure 2

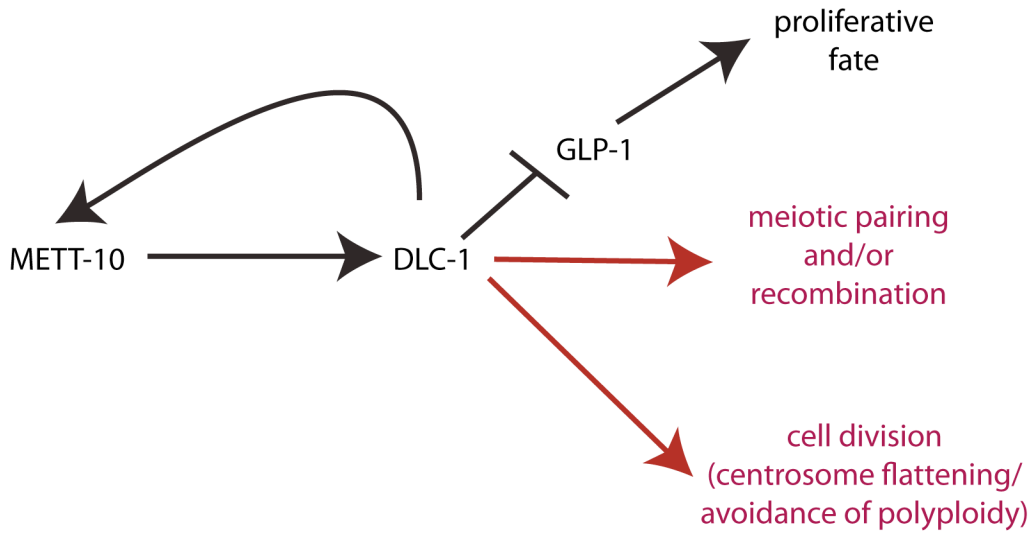

Figure 2. A genetic model for joint functions of METT-10 and DLC-1. METT-10 and DLC-1 both function in *glp-1*-dependent inhibition of proliferative fate, the avoidance of polyploidy, centrosome flattening (O'Connell *et al*., 1998), and in meiotic pairing and/or recombination. In the inhibition of proliferative fate, DLC-1 promotes METT-10 levels and localization. However, *dlc-1* activity is essential for other functions (red), while METT-10 function is not. The most parsimonious explanation is that METT-10 normally promotes DLC-1 function, and DLC-1 in turn promotes METT-10 activity in a positive feedback loop.